

THESIS FOR THE DEGREE OF DOCTOR OF PHILOSOPHY

Development of Aerobic Oxidative *N*-Heterocyclic Carbene Catalysis
via Multistep Electron Transfer and its Application

Anton Axelsson

Department of Chemistry and Chemical Engineering

CHALMERS UNIVERSITY OF TECHNOLOGY

Gothenburg, Sweden 2019

Development of Aerobic Oxidative *N*-Heterocyclic Carbene Catalysis via Multistep Electron Transfer and its Application

ANTON AXELSSON

ISBN: 978-91-7905-231-7

©Anton Axelsson, 2019.

Doktorsavhandlingar vid Chalmers tekniska högskola

Ny serie nr 4698

ISSN0346-718X

Department of Chemistry and Chemical Engineering

Chalmers University of Technology

SE-412 96 Gothenburg

Sweden

Telephone + 46 (0)31-772 1000

Cover:

[Schematisk representation av målet att möjliggöra aerobisk NHC-katalys med en naturbild som bakgrund.]

Printed by Chalmers Reproservice

Gothenburg, Sweden 2019

Development of Aerobic Oxidative *N*-Heterocyclic Carbene Catalysis via Multistep Electron Transfer and its Application

Anton Axelsson

Department of Chemistry and Chemical Engineering
Chalmers University of Technology

Abstract

Oxidation reactions are ubiquitous in synthetic chemistry, but generally suffer from formation of large amounts of potentially toxic byproducts. Aerial oxygen represents an ideal oxidant since it is inexpensive, non-toxic and only forms water as a byproduct. However, aerobic oxidations are characterized by high activation barriers leading to formation of kinetic side products. A common way to circumvent this is by introducing electron transfer mediators (ETMs) to achieve kinetically useful reactions.

N-heterocyclic carbenes (NHCs) are an important group of organocatalysts that have been used in a wide range of both redox neutral and oxidative transformations. In this thesis, an ETM strategy is used to enable aerobic NHC catalysis. The developed protocol has been employed in aerobic acylations of a wide range of alcohols and oxazolidinones. A method for telescoped carbonation and acylation of the biobased feedstock glycerol has also been developed. The aerobic system was also extended to both the racemic and asymmetric synthesis of dihydropyranones.

Lastly, the obtained dihydropyranones were used to achieve the formal addition of acetone to unactivated Michael acceptors. The method furnishes 5-oxohexanoates and 5-oxohexanamides in good to excellent yields and proceeds through a ring-opening and retro-Claisen fragmentation sequence. The mechanism has been investigated using both kinetic and density functional theory methods, and a dual role of the catalyst is proposed.

To summarize, the combination of ETMs and NHC catalysis enable the use of aerial oxygen as the terminal oxidant in distinct reaction pathways, with water as the only byproduct.

Keywords: Organocatalysis, *N*-heterocyclic carbene, aerobic oxidation, electron transfer mediator, green chemistry, asymmetric synthesis, acylation, dihydropyranone, Michael addition, kinetics.

*Hur väldig är ej rymden,
hur mäktig ej dess gåta,
hur liten inte jag.*

Harry Martinson

List of Publications

This thesis is based on the following publications that will be referred to by their Roman numerals in the text. Reprints were made with kind permission from the publishers.

- I. Attractive aerobic access to the α,β -unsaturated acyl azolium intermediate: oxidative NHC catalysis via multistep electron transfer
L. Ta,* A. Axelsson,* H. Sundén.
Green Chem., 2016, *18* (3), 686–690
- II. Organocatalytic valorisation of glycerol via a dual NHC-catalysed telescoped reaction
A. Axelsson, A. Antoine-Michard, H. Sundén.
Green Chem., 2017, *19* (11), 2477–2481.
- III. N-acylation of oxazolidinones via aerobic NHC-catalysis
L. Ta,* A. Axelsson,* H. Sundén.
J. Org. Chem. **2018**, *83*, 19, 12261–12268.
- IV. Asymmetric aerobic oxidative NHC-catalysed synthesis of dihydropyranones utilising a system of electron transfer mediators
A. Axelsson, E. Hammarvid, L. Ta, H. Sundén.
Chem. Commun., 2016, *52* (77), 11571–11574.
- V. Formal addition of acetone to unactivated Michael acceptors via ring-opening and retro-Claisen fragmentation of dihydropyranones
A. Axelsson, E. Hammarvid, M. Rahm, H. Sundén.
Manuscript. ChemRxiv. Preprint. <https://doi.org/10.26434/chemrxiv.9822575.v1>

*These authors contributed equally.

Contribution report

Paper I

Contributed to the outline of the study. Performed half of the experimental work. Wrote parts of the manuscript. Analyzed the results together with L.T and H.S.

Paper II

Formulated the research problem, designed the study together with H.S. Coordinated the experimental work and performed most of the experimental work. Wrote the majority of the manuscript. Analyzed the results together with H.S.

Paper III

Performed half of the experimental work. Wrote parts of the manuscript. Analyzed the results together with L.T and H.S

Paper IV

Formulated the research problem, designed the study together with H.S. Coordinated the experimental work and performed a third of the experimental work. Wrote parts of the manuscript. Analyzed the results together with H.S and L.T.

Paper V

Formulated the research problem, designed the study together with H.S and M.R. Performed most of the experimental work. Designed the kinetic experiments. Performed the quantum chemical investigation under supervision of M.R. Wrote the majority of the manuscript. Analyzed the results together with H.S and M.R.

Related publications not included in the thesis:

1. Biomimetic Oxidative Carbene Catalysis: Enabling Aerial Oxygen as a Terminal Oxidant
A. Axelsson, L. Ta, H. Sundén.
Synlett, 2017, 28 (08), 873-878
2. Direct Highly Regioselective Functionalization of Carbohydrates: A Three-Component Reaction Combining the Dissolving and Catalytic Efficiency of Ionic Liquids
A. Axelsson, L. Ta, H. Sundén.
Eur. J. Org. Chem., 2016, 2016 (20), 3339-3343.
3. Ionic Liquids as Carbene Catalyst Precursors in the One-Pot Four-Component Assembly of Oxo Triphenylhexanoates (OTHOs)
A. Axelsson,* L. Ta,* H. Sundén.
Catalysts, 2015, 5 (4), 2052-2067.
4. Highly Stereoselective Synthesis of 1,6-Ketoesters Mediated by Ionic Liquids: A Three-component Reaction Enabling Rapid Access to a New Class of Low Molecular Weight Gelators.
H. Sundén, L. Ta , A. Axelsson.
J. Vis. exp., 2015, 105, e53213.
5. Ionic Liquids as Precatalysts in the Highly Stereoselective Conjugate Addition of α,β -Unsaturated Aldehydes to Chalcones
L. Ta,* A. Axelsson,* J. Bijl, M. Haukka, H. Sundén.
Chem. Eur. J., 2014, 20 (43), 13889-13893.

*These authors contributed equally.

List of Abbreviations

DBU	1,8-Diazabicyclo[5.4.0]undec-7-ene
cf.	Confer (Latin), compare
DCM	Dichloromethane
DFT	Density functional theory
DMC	Dimethyl carbonate
DMSO	Dimethyl sulfoxide
EDG	Electron donating group
ee	Enantiomeric excess
<i>Et al.</i>	<i>Et alii</i> (Latin), and others
Eq.	Equivalents
ETM	Electron transfer mediator
EWG	Electron withdrawing group
FePc	Iron(II) phthalocyanine
GC-FID	Gas chromatography flame ionization detector
GC-MS	Gas chromatography mass spectrometry
HOMO	Highest occupied molecular orbital
HAT	Hydrogen atom transfer
IR	Infrared
IUPAC	International Union of Pure and Applied Chemistry
KIE	Kinetic isotope effect
LUMO	Lowest unoccupied molecular orbital
mRNA	Messenger ribonucleic acid
N.D	Not determined

NHC	<i>N</i> -heterocyclic carbene
NMR	Nuclear magnetic resonance
OCIF	Osteoclastogenesis inhibitory factor
PEBPL α A	Polyoma enhancer binding protein 2 α A
PCET	Proton coupled electron transfer
PET	polyethylene terephthalate
RDS	Rate determining step
r.r	Regioisomeric ratio
SCE	Saturated calomel electrode
SET	Single electron transfer
TBD	Triazabicyclo[4.4.0]dec-5-ene
THF	Tetrahydrofuran
<i>p</i> -TsOH	<i>p</i> -Toluenesulfonic acid
UN	United Nations

Table of Contents

1. Introduction and Background	1
1.1 <i>Chemistry and our society</i>	1
1.2 <i>Organocatalysis</i>	3
2. Theory and Methodology	5
2.1 <i>N-Heterocyclic Carbene Structure and Reactivity</i>	5
2.1.1 <i>Oxidative N-Heterocyclic Carbene Catalysis</i>	8
2.2 <i>The α,β-Unsaturated Acyl Azolium Intermediate</i>	11
2.3 <i>Catalytic Aerobic Oxidations</i>	13
3. Hypothesis and Aim	16
4. Aerobic Access to the α,β-Unsaturated Acyl Azolium Intermediate (Paper I)	17
4.1 <i>Aerobic NHC Catalysis</i>	17
4.2 <i>Identification of a Suitable System for Aerobic NHC Catalysis</i>	18
5. Valorization of Glycerol via a Dual NHC-Catalyzed Telescoped Reaction (Paper III)	23
5.1 <i>Chemical Valorization of Biomass</i>	23
6.2 <i>Design of a Telescoped Reaction for Dual Glycerol Functionalization</i>	24
6. N-Acylation of Oxazolidinones via Aerobic NHC Catalysis (paper III)	28
6.1 <i>The Difficulty of Developing NHC-Catalyzed N-acylations</i>	28
6.2 <i>Optimization and Scope</i>	29
7. Summary of NHC-Catalyzed Aerobic Acylations	33
8. Aerobic Oxidative NHC-Catalyzed Synthesis of Dihydropyranones (Paper I and IV)	34
8.1 <i>Natural Occurrence of Dihydropyranones</i>	34
8.1 <i>Racemic synthesis of dihydropyranones (paper I)</i>	35
8.2 <i>Development of an asymmetric synthesis of dihydropyranones (paper IV)</i>	35
9. Formal Addition of Acetone to Unactivated Michael Acceptors via Ring-opening and Retro-Claisen Fragmentation of Dihydropyranones (Paper V)	40
9.2 <i>Mechanistic inquires</i>	44
9.3 <i>Quantum Chemical investigation of the Reaction Mechanism</i>	52
10. Summary of Aerobic Synthesis of Dihydropyranones and Their Organocatalytic Ring-Opening and Fragmentation (Paper I, IV and V)	55
11. Conclusion and Outlook	56
12. Acknowledgement	58
13. References	59

1. Introduction and Background

1.1 Chemistry and our society

Modern chemistry has revolutionized our society. Today, chemistry is essential for our production of food, water, fuels, medicine and materials. The structure of three remarkable chemicals that have played a large role in this development can be seen in Figure 1. For instance, Flemings discovery of penicillin, exemplified by the first orally available penicillin phenoxymethylpenicillin, and its use as antibiotics have transformed modern healthcare.^[1] The Haber-Bosh process, used to produce ammonia, has enabled us to access large amounts of fertilizers that uphold our current food production.^[2] Lastly, the plastic polyethylene terephthalate (PET), one of the most commonly used plastic in the world.^[3] As a testament to chemistry's contributions to mankind, the International Union of Pure and Applied Chemistry (IUPAC) and the United Nations (UN) declared 2011 the international year of chemistry, with the banner *Chemistry—our life, our future*.^[4]

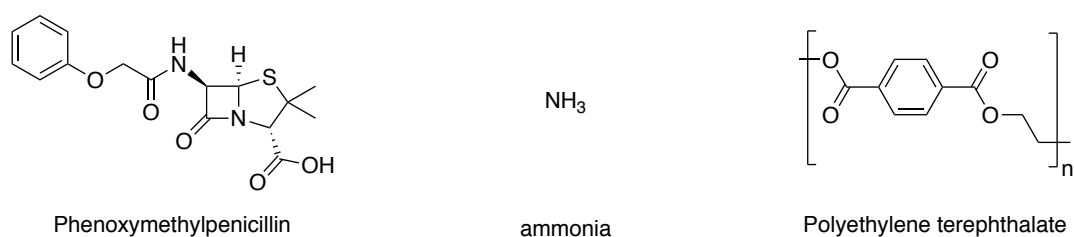


Figure 1. The structure of phenoxymethylpenicillin, ammonia and polyethylene terephthalate.

However, the rapid growth of the chemical industry during the last century has not been without cost. Rapid consumption of finite resources, disastrous cases of pollution and increased demands for improved efficiency has created a pressure to develop a more sustainable chemical industry.^[5] Within the field of chemistry, work related to sustainable development is often referred to as green chemistry. The term was coined by Anastas and Warner who initially defined it as the “Design of chemical products and processes to reduce or eliminate the use of hazardous substances”.^[6] Today, green chemistry is concerned with much more, such as energy conservation, life cycle consideration, waste reduction and the use of renewable feedstock. Anastas and Warner developed a set of twelve principles meant to serve as guidelines to construct a greener chemical process (Figure 2). The principles that are of particular relevance for the work presented in this thesis will be described more thoroughly below.

- | | |
|--------------------------------------|--|
| 1. Waste Prevention | 7. Use of Renewable Feedstocks |
| 2. Atom Economy | 8. Reduce Derivatives |
| 3. Less Hazardous Chemical Syntheses | 9. Catalysis |
| 4. Designing Safer Chemicals | 10. Design for Degradation |
| 5. Safer Solvents and Auxiliaries | 11. Real-time analysis for Pollution Prevention |
| 6. Design for Energy Efficiency | 12. Inherently Safer Chemistry for Accident Prevention |

Figure 2. The twelve principles of green chemistry.

The first principle states that it is better to prevent the formation of waste than to manage it after it has been produced. This especially holds true for the fine chemical and pharmaceutical industry, which generate large amounts of waste. A recent survey on 21 compounds, either in phase three clinical trials or commercially available drugs, showed that every kilogram of product generates on average 76 kg of waste excluding water (range 24–239 kg).^[7] Solvents represent the majority of the waste produced, typically ranging between 80–90% for the pharmaceutical industry. Solvent choice is therefore the fifth principle of green chemistry.^[8] Several guides for sustainable solvent selection are available.^[9]

Waste prevention is also connected to principle two, the design of reactions with high atom economy and to principle nine, the promotion of catalysis over stoichiometric methods. Atom economy is one of many green chemistry metrics and was introduced by Trost in 1991. It measures the mass efficiency of the transformation of starting materials into products assuming total conversion.^[10] It should be noted that atom economy does not take solvent usage in consideration, but other metrics that do so exist, such as the E-factor.^[11]

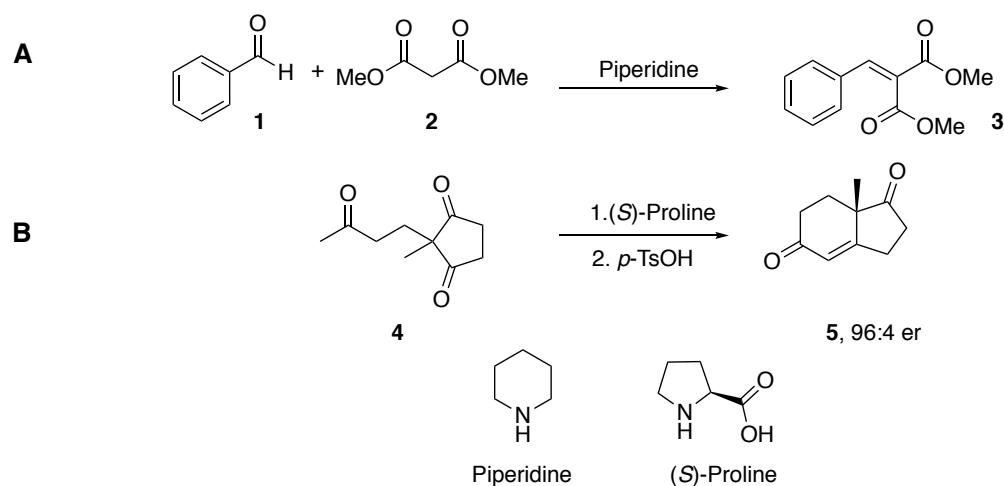
A catalyst is a compound that increases the rate of a reaction without being consumed in the process, so using catalysis is a common way to increase the atom economy of a reaction.^[12] Catalysis also enables the reaction to be performed under milder and often more energy efficient conditions, for instance by running the reaction at ambient rather than elevated temperature. Sometimes it is also possible to recover and recycle the catalyst, since it is not consumed in the reaction.

Principle seven deals with the use of renewable feedstock. It has been estimated that 95% of all the carbon containing molecules needed to sustain daily life are derived from petrochemical resources, the majority of which are used as fuels.^[13] The building blocks available for the synthetic chemical industry are to a large extent petroleum-based, and roughly 10% of the world production of crude oil is used in the manufacturing of industrial chemicals.^[14] Since oil is a depleting and non-sustainable resource, the chemical industry must eventually switch from petroleum based to biobased building blocks. The two largest classes of biomass used as renewable feedstocks are lignocellulosic materials and plant oils.^[15]

1.2 Organocatalysis

A catalyst is a compound that increases the rate, but not the overall standard Gibbs free energy change, of a chemical reaction without being consumed.^[12] Catalysis is of fundamental importance to modern society and can be found in numerous aspects of daily life. A famous example is the use of heterogeneous catalysts based on precious metals such as palladium, platinum and rhodium to purify exhaust from combustion engines found in cars and other vehicles, lessening air pollution.^[16]

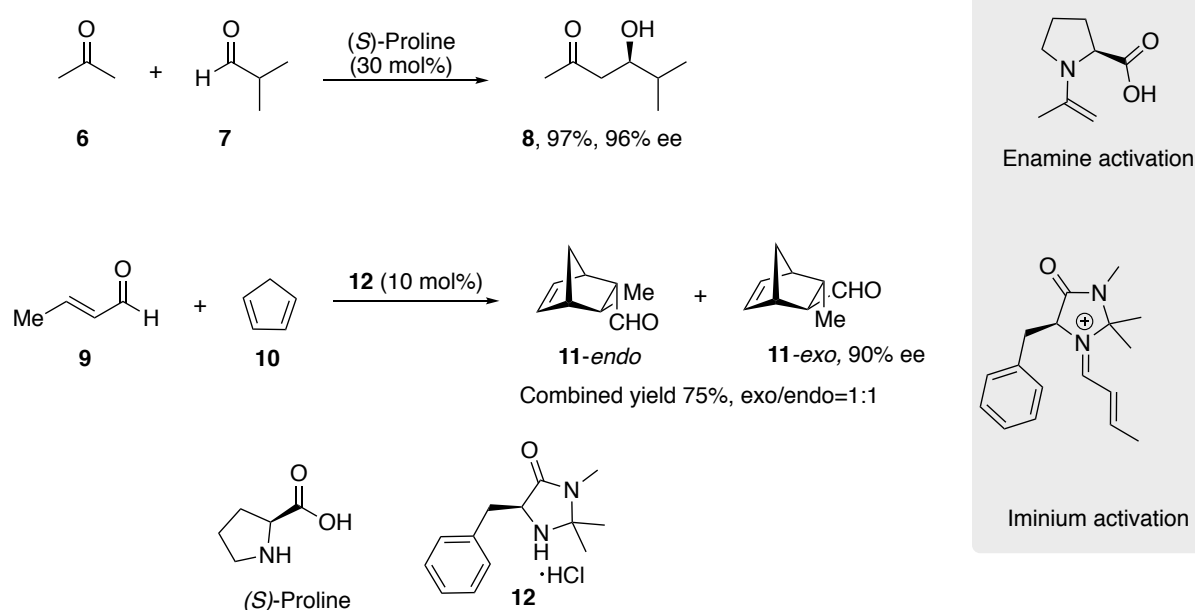
For a long period of time, the field of catalysis was dominated by the use of transition metal catalysts. However, it has been known for more than a century that small organic molecules can act as potent catalysts. Already in 1896, Knoevenagel reported the amino-catalyzed condensation of dimethyl malonate (**2**), and benzaldehyde (**1**) to yield **3** (Scheme 1 A). The reaction is catalyzed by both primary and secondary amines and is nowadays known as the Knoevenagel condensation.^[17] This is one of the first reported organocatalytic reactions. In the early 1900s, it was found that amino acids and secondary ammonium salts catalyzed both the Knoevenagel condensation and the aldol reaction.^[18] While catalysis using amino acids has been known for over a hundred years, it was not until the early 1970s that an asymmetric organocatalytic reaction was reported, namely the Hajos-Parrish-Eder-Sauer-Wiechert reaction (Scheme 1 B).^[19] In this reaction (*S*)-proline was used as a catalyst in an asymmetric intramolecular aldol reaction of triketone **4**, which upon acid catalyzed dehydration using *p*-toluenesulfonic acid (*p*-TsOH) yielded diketone **5** in 96:4 enantiomeric ratio (er).



Scheme 1. An example of a Knoevenagel condensation and the Hajos-Parrish-Eder-Saur-Wiechert reaction.

Although the catalytic abilities of simple amines were well known, the field of organocatalysis was rather dormant during the next 30 years. With some notable exceptions like the use of (*R*)-proline in the total synthesis of erythronolide A reported by Woodward *et al.*^[20] However, in the year 2000 two seminal reports laid the foundation of modern organocatalysis (Scheme 2). List *et al.* reported the use (*S*)-proline in the asymmetric aldol reaction between acetone (**6**) and aldehydes, such as isobutyraldehyde (**7**) yielding hydroxyketone **8**,^[21] using an activation strategy now called enamine catalysis.^[22] Independently, MacMillan *et al.* reported the use of (*S*)-phenylalanine derived catalyst **12** in the asymmetric Diels-Alder reaction between α,β -unsaturated aldehydes such as but-2-enal (**9**) and dienes such as cyclopenta-1,3-diene (**10**), yielding bridged compound **11** in excellent yield and enantioselectivity, however with poor exo/endo selectivity.^[23] The postulated mechanism involves an activation mode now commonly called iminium catalysis.^[24]

Organocatalysis have since then developed tremendously and is nowadays a key part of the synthetic chemistry toolbox.^[25] A wide range of activation modes in addition to enamine and iminium catalysis have been developed such as chiral Brønsted acids,^[26] organic superbases,^[27] hydrogen bond donors^[28] and phase-transfer catalysts.^[29] Organocatalysts are in general cheaper, more durable and less toxic than their transition metal counterparts. However, organocatalysts often require higher loadings to achieve efficient reactions compared to transition metal catalysts. The use of organocatalysis also circumvents the energy demanding and environmentally destructive mining of precious metals. Moreover, organocatalysis avoids the metal-scavenging required to remove traces of metal contaminants where they are not tolerated, as in the pharmaceutical industry.^[30] Taken together, these factors make organocatalysis a more sustainable option than transition metal catalysis. In fact, in 2019 IUPAC declared enantioselective organocatalysis one out of ten chemical innovations that will change our world.^[31]



Scheme 2. The organocatalytic asymmetric aldol and Diels-Alder reactions reported by List and MacMillan respectively

2. Theory and Methodology

2.1 *N*-Heterocyclic Carbene Structure and Reactivity

N-heterocyclic carbenes (NHCs) are a common type of organocatalysts that are characterized by the presence of a neutral bivalent carbon atom with six valence electrons, a so called carbene, within an *N*-heterocycle.^[32] Carbenes are highly reactive compounds with transient lifetimes. However, it is possible to stabilize carbenes by introducing adjacent heteroatoms enabling resonance stabilization *via* the corresponding ylide, as in the first persistent carbene (**13**) reported by Bertrand *et al.* in 1988 (Figure 3).^[33] Three years later Arduengo *et al.* reported the first stable NHC, which was based on an imidazolium scaffold.^[34]

The nitrogen atoms adjacent to the carbene carbon make NHCs more stable than the general carbene. The energy of the highest occupied molecular orbital (HOMO) is decreased while the energy of the lowest unoccupied molecular orbital (LUMO) is increased, hence favoring the singlet state over the triplet state of the carbene. This leads to a thermodynamic stabilization and an increase of the nucleophilicity of the carbene carbon, as seen by the resonance structure (Figure 3 A). The electronic effects of nitrogen atoms in NHCs are sometimes referred to as a *push-pull effect*, as a result of their σ -withdrawing (inductive) and π -donating (mesomeric, lone pair to vacant p-orbital) nature. The incorporation of the carbene in cyclic structures imposes a sp^2 -like hybridization of the carbene carbon further favoring the singlet state of the carbene. Lastly, *N*-substituents stabilize NHCs by disfavoring the reversible dimerization of carbenes, known as the Wanzlick equilibrium (Figure 3 B).^[32, 35] Most NHCs are based on either the imidazolium, triazolium or thiazolium scaffold and are commonly accessed by deprotonation of the corresponding azolium salts.

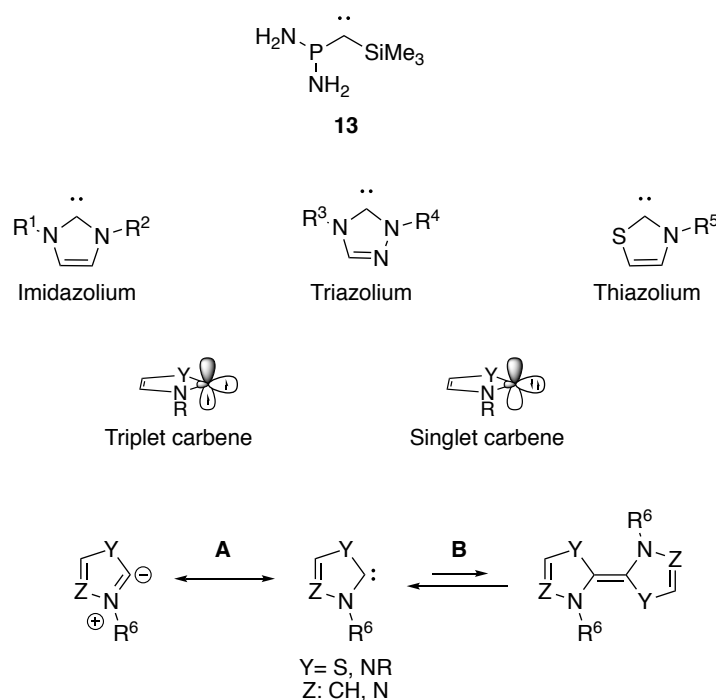


Figure 3. The structure and stabilization of the first persistent carbene and NHCs.

The reactivity of the NHC is highly sensitive towards both the azolium core and the *N*-substituent(s). For instance, the pK_a-value of the most commonly used NHCs spans over almost 12 units (in DMSO, Figure 4). Triazolium based NHCs are generally the most acidic, with pK_a-values ranging from 12–15.5.^[36] The effect of the *N*-substituent can be seen for the two bicyclic triazolium NHCs, where changing from a pentafluorophenyl group (**14**) to a mesityl group (**15**) results in an increased pK_a with almost 3.4 units. The choice of counterion has a negligible effect on the pK_a, as seen for the chiral indanol-based triazoliums **15** and **16**. Thiazolium based NHCs have been investigated to a lesser extent than the triazoliums and imidazolium ones, but in general they are considered to be of intermediate acidity with pK_a-values around 16 (**18**).^[37]

The imidazolium based NHCs (**19–21**) are generally the least acidic ones with pK_a-values ranging from 19–24.^[38] Diarylimidazoliums are generally the most acidic imidazolium based NHCs and introduction of alkyl substituents tend to increase the pK_a-value. 4,5-Dialkylated imidazolium such as **21** are considerably less acidic than the unsubstituted ones, an effect that has been ascribed to the electron donating abilities of the alkyl groups.^[38b] The observation that NHCs are commonly used together with relatively weak bases such as triethylamine, pK_a 9 in DMSO,^[39] has led to the suggestion that no free carbene actually is formed in solution. Instead, computational studies suggest that deprotonation of the azolium occurs simultaneous as addition to the electrophile, via a general base mechanism.^[40]

Besides being Brønsted bases, NHCs are also nucleophilic. Their nucleophilicity has been quantified according to the Mayr-Patz equation, $\log k = S_N(N + E)$, where k is the rate constant, S_N is the nucleophile-specific slope parameter, N is the nucleophilicity parameter and E is the solvent-independent electrophilicity parameter.^[41] In general, NHCs are of moderate nucleophilicity but of high Lewis basicity. Meaning that the kinetic ability of NHCs to add to Lewis acids are moderate, but the thermodynamic drive to do so is very high.^[41b] Triazolium derived carbenes are generally less nucleophilic than their imidazolium counterparts. For instance, the Enders carbene **22** has a N -value of 14.07, which makes it slightly more nucleophilic than triphenylphosphine ($N=13.69$) and less nucleophilic than DMAP ($N=15.90$). The nucleophilicity of imidazolium based NHCs (**19**, **23–25**) ranges from 16–23.^[42] The imidazolium carbene with an 2,6-dimethoxyphenyl substituent (**26**) is the most nucleophilic carbene reported to date. It is worth noting that while exchanging an *N*-aryl substituent to an *N*-alkyl one increases the basicity of the carbene, but the nucleophilicity is decreased (*cf.* **19** *vs.* **20** and **19** *vs.* **23**). When dealing with these comparisons, one must bear in mind that basicity is a thermodynamic property while nucleophilicity is a kinetic one. However, they do often correlate, but evidently, they do not in this instance.

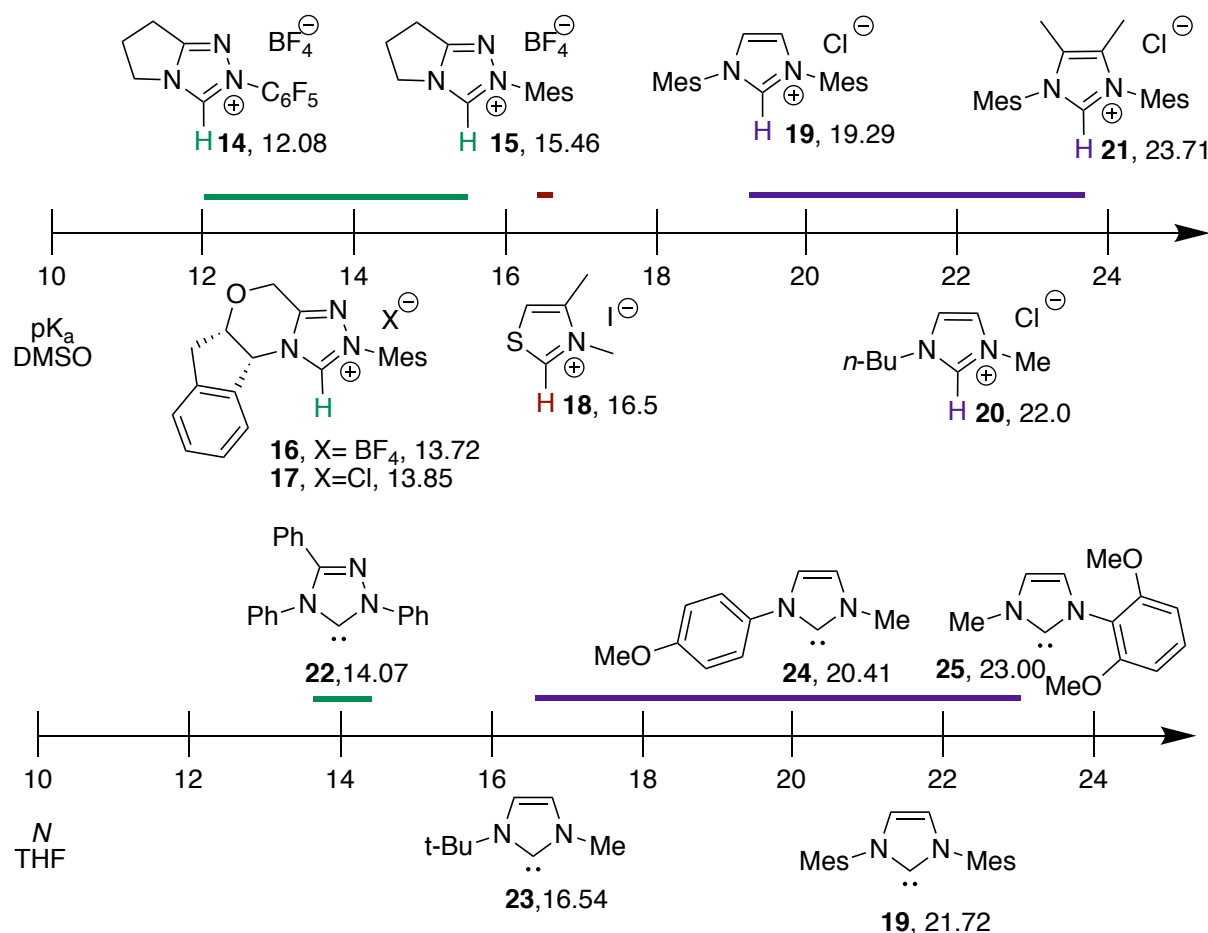
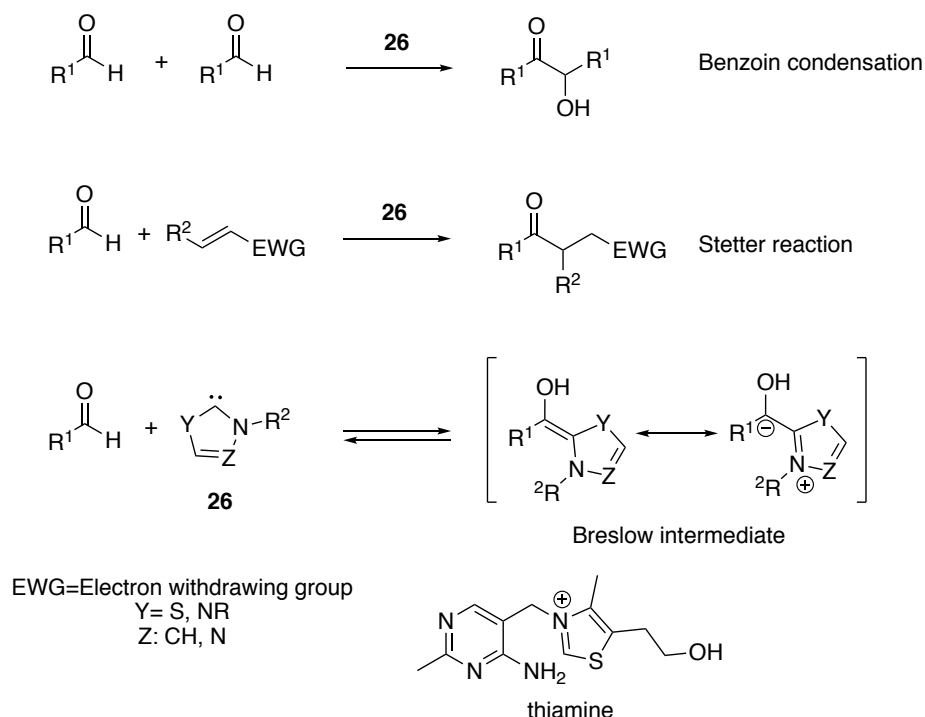


Figure 4. The pK_a and nucleophilicity parameter (N) of commonly used NHCs.

Although persistent carbenes were not reported until 1989, the catalytic ability of NHCs have been known since 1958 when Breslow proposed a carbene mechanism for the thiamine (vitamin B1) catalyzed decarboxylation of pyruvate by pyruvate dehydrogenase.^[43] Fifteen years earlier, Ugai *et al.* had reported that thiamine could replace alkali cyanides as catalysts for the benzoin condensation (Scheme 3).^[44] In 1976, Stetter reported that thiamine also could replace alkali cyanides in the addition of aldehydes to Michael acceptors, the so called Stetter reaction.^[45] In both reactions, umpolung of the aldehyde *via* the Breslow intermediate is followed by nucleophilic addition to the respective electrophile. Umpolung is the German term for inversion and refers to the inversion of polarity. It was first described by Wittig^[46] and later on made popular by Seebach,^[47] and is a valuable strategy in organic synthesis.^[48]

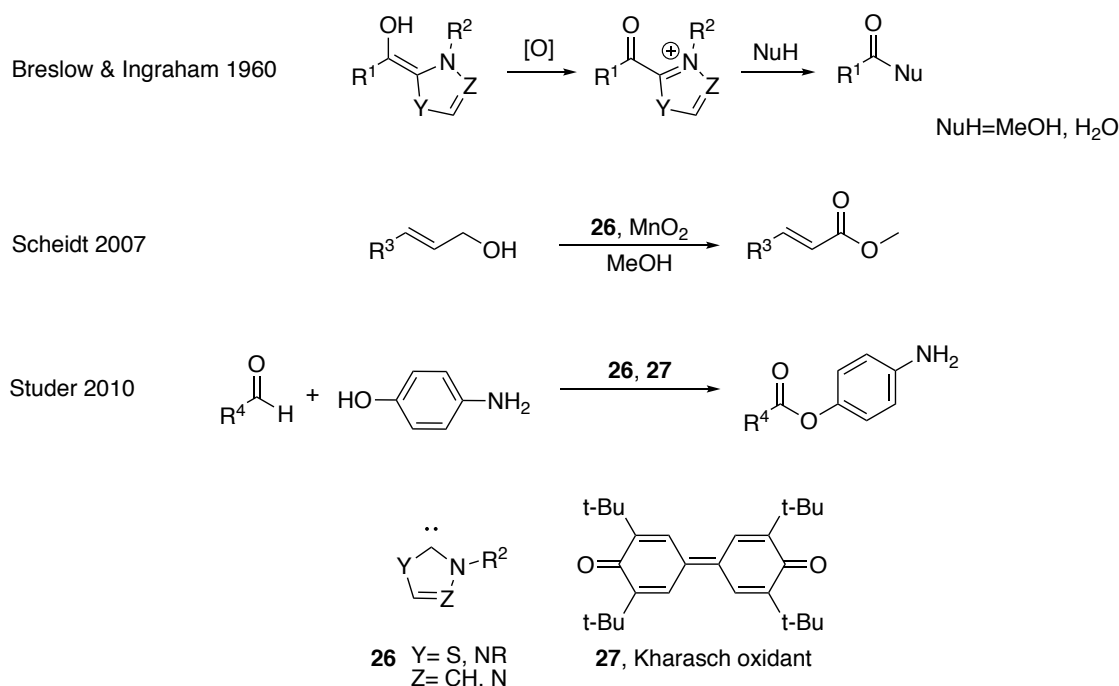


Scheme 3. The benzoin condensation, the Stetter reaction and the NHC-catalyzed umpolung of aldehydes via formation of the Breslow intermediate.

2.1.1 Oxidative *N*-Heterocyclic Carbene Catalysis

The Breslow intermediate is electron-rich, which makes it susceptible for oxidation to the corresponding acyl azolium. As noted by Breslow in 1960, acetyl thiazolium salts behave as *activated acetates* and readily reacts with nucleophiles such as water or methanol (Scheme 4).^[49] Ingraham *et al.* independently reported a similar reactivity of 2-benzoyl thiazolium salts concurrently with Breslow.^[50] These observations laid the foundation of a prototypical NHC-catalyzed reaction, namely the oxidative esterification of aldehydes, as first reported by Castells *et al.*^[51] The original report used nitrobenzene as oxidant, but several inorganic^[52] and organic oxidants may be used.^[53]

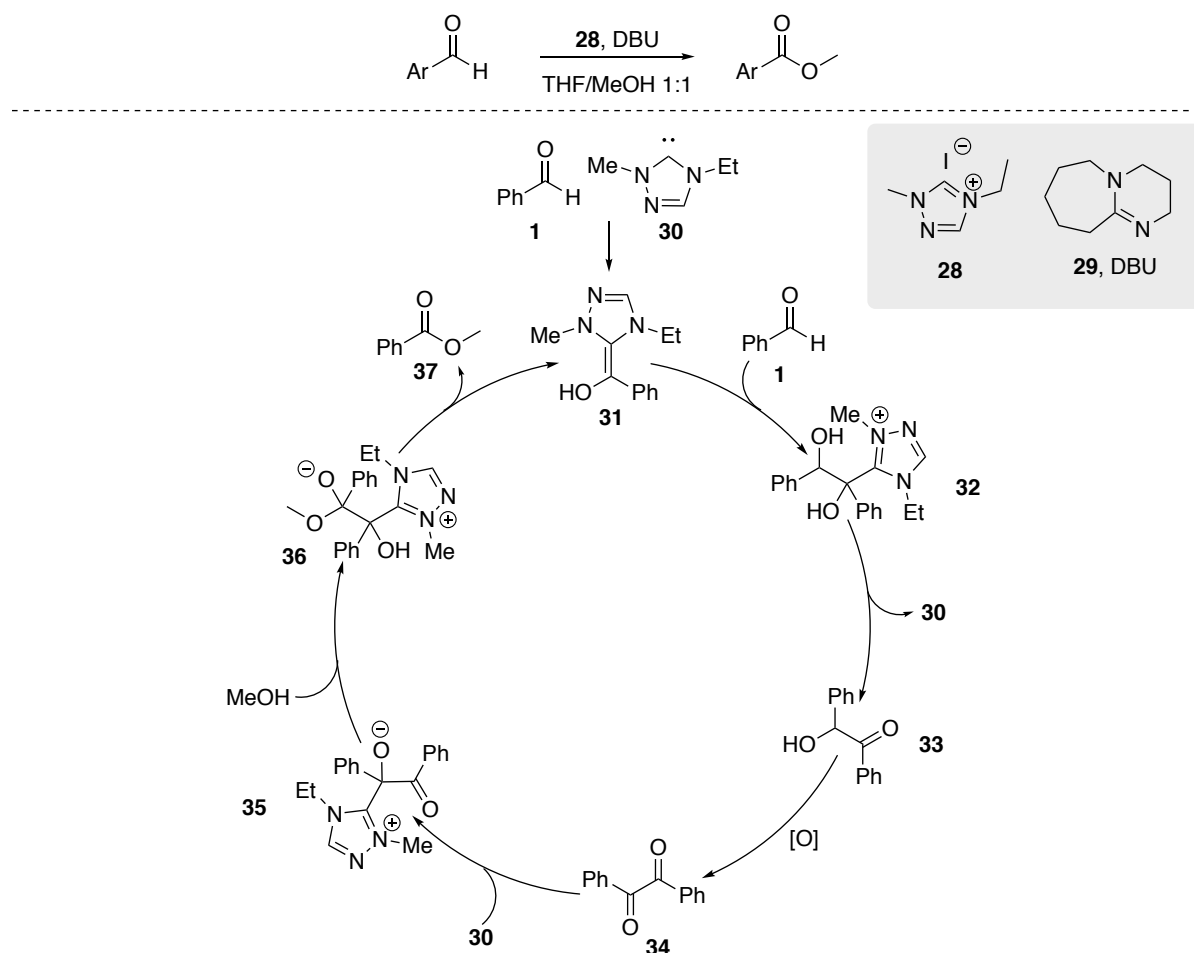
Oxidative esterification gained a lot of interest during the rapid expansion of NHC catalysis in the beginning of the twenty-first century (Scheme 4). In 2005 an oxidative thioesterification of aldehydes was reported.^[54] Soon thereafter, Scheidt reported an NHC-catalyzed oxidation of allylic and benzylic alcohols to esters using MnO_2 as the oxidant.^[55] In 2010, Studer reported the chemoselective *O*-acylation of aminoalcohols using oxidative NHC catalysis.^[56] In this seminal report Studer also introduced the use of 3,3',5,5'-tetra-*tert*-butyldiphenylquinone **27**, also known as the Kharasch oxidant,^[57] which quickly gained widespread use as oxidant in NHC-catalysis. The success of oxidant **27** has been attributed to its sterical encumbrance, which impedes the formation of covalent adducts between the NHC and the quinone.^[58]



Scheme 4. Oxidation of the Breslow intermediate yielding the electrophilic acyl azolium intermediate and some of its uses in synthesis.

Several oxidants are capable of oxidizing the Breslow intermediate, but they all suffer from either poor atom economy or the need of large excess. Initial attempts using oxygen as a sustainable oxidant where met with failure. Instead, the carboxylic acid was obtained as the main product.^[59]

However, in 2013 Cannon *et al.* reported a novel reaction pathway that led to the first aerobic esterification of aromatic aldehydes (Scheme 5).^[60] Based on the required large excess of alcohol, the observed dependence of sterics and pK_a, as well as the identification and isolation of several proposed intermediates, an unconventional mechanism was suggested.^[61] The reaction commences with deprotonation of triazolium salt **28** with 1,8-diazabicyclo[5.4.0]undec-7-ene (**29**, DBU) yielding free carbene **30**. Breslow intermediate **31** is formed through nucleophilic 1,2-addition of carbene **30** to benzaldehyde (**1**) and subsequent proton transfer. Formal acyl anion **31** adds in a 1,2-fashion to another molecule of benzaldehyde and subsequent protonation results in diol **32**. Later, **32** collapses to benzoin **33** *via* elimination of carbene **30**. α -Hydroxyketone **33** is then oxidized by aerial oxygen under base catalysis, yielding benzil (**34**). Nucleophilic addition of the carbene (**30**) to the diketone yields zwitterion **35**, which is rapidly converted to anionic hemiacetal **36** by reacting with methanol. Scission of the C–C-bond in **36** yields methyl benzoate **37** and regenerates Breslow intermediate **31**, which completes the cycle.

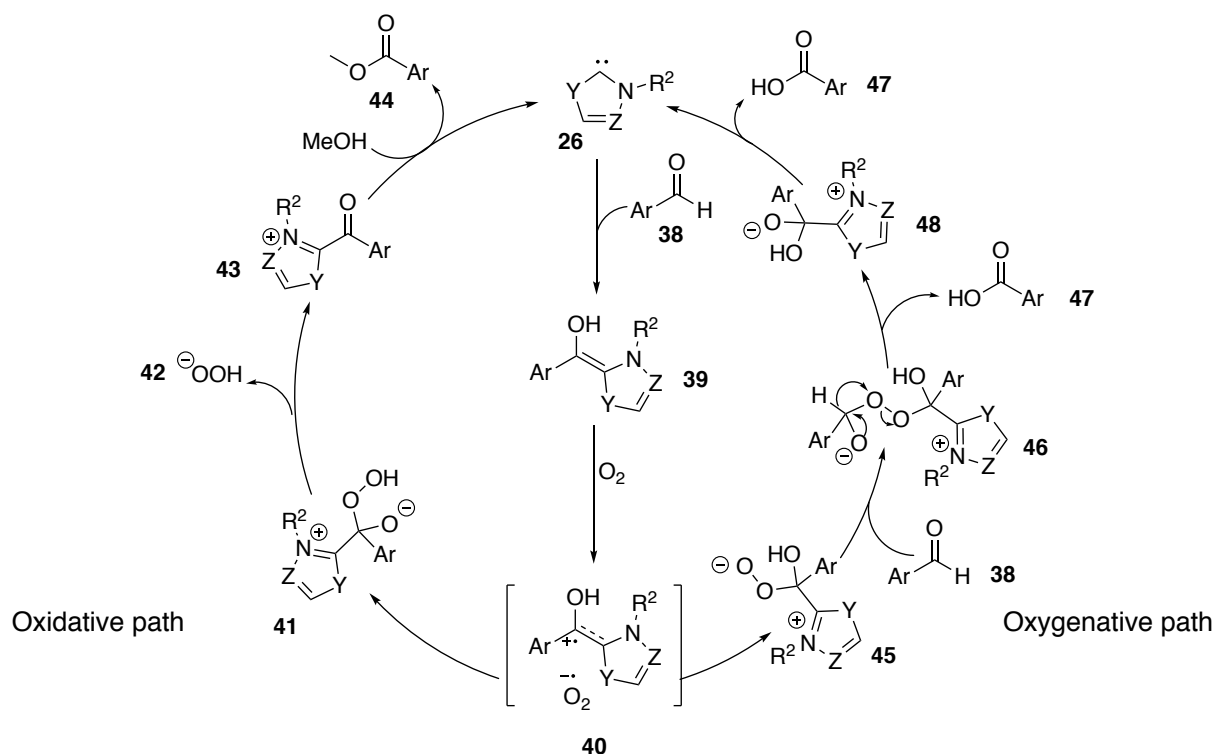


Scheme 5. Aerobic esterification of aromatic aldehydes via oxidation of the benzoin intermediate.

The Canon protocol suffers somewhat from a limited scope and the need of high loadings of alcohol. However, its selectivity gives it a large advantage over conventional aerobic NHC-catalyzed reactions. By circumventing direct oxidation of the Breslow intermediate, formation of carboxylic acid as a side product is prevented.

The poor selectivity is a consequence of the two different paths available for direct aerobic oxidation of the Breslow intermediate, either oxidative or oxygenative (Scheme 6). Both paths begin with the formation of Breslow intermediate **39** *via* nucleophilic 1,2-addition of carbene **26** to aldehyde **38**. Single electron transfer (SET) from electron-rich **39** to dioxygen forms charge-transfer complex **40**, which upon radical recombination may yield two tautomeric peroxides, **41** or **45**. In the oxidative path, tetrahedral intermediate **41** collapses and expels hydrogen peroxide anion (**42**) yielding acyl azolium **43**, which is intercepted by methanol yielding ester **44** and regenerating carbene catalyst **26**. Even if the desired product is formed through the oxidative pathway, the carboxylic acid side product may still be formed by a NHC-catalyzed side reaction between the aldehyde and the formed hydrogen peroxide.^[62]

In the oxygenative pathway, charge-transfer complex **40** recombines to form anionic peroxide **45** that reacts with an additional equivalent of aldehyde yielding intermediate **46**. Peroxide **46** fragments, in a similar manner to the Baeyer–Villiger oxidation, yielding carboxylic acid **47** and anionic hemiacetal **48**, which then forms another equivalent of carboxylic acid **47** by elimination of carbene **26**. Direct formation of the peroxy acid *via* elimination of the carbene from tetrahedral intermediate **45** and subsequent reduction has also been suggested as a route to the carboxylic acid.^[63] Whether the oxygenative or the oxidative path is predominant is highly dependent on the substitution pattern of the aldehyde.^[64] The ambiguity of which path is governing makes the development of a general aerobic esterification by direct oxidation of the Breslow intermediate difficult.



Scheme 6. The oxidative and oxygenative path for aerobic oxidation of the Breslow intermediate.

2.2 The α,β -Unsaturated Acyl Azolium Intermediate

Oxidative NHC catalysis offers several other activation modes besides the use of the acyl azolium as an acylating agent. For instance, *via* enolate azolium reactivity in asymmetric fluorinations^[65] and vinyl enolate azoliums in formal [3+3] cycloadditions yielding benzene derivatives.^[66] However, the most important intermediate in oxidative NHC catalysis is, arguably, the α,β -unsaturated acyl azolium formed by oxidation of the corresponding homoenolate.^[67] The α,β -unsaturated acyl azolium is a 1,3-biselectrophile and has been isolated and thoroughly characterized by several physical organic chemistry techniques (*vide infra*).

The X-ray structure of α,β -unsaturated acyl azolium **50**,^[68] alongside published values for some physical descriptors for key intermediates in organocatalytic LUMO-activation of Michael acceptors are presented in Figure 5.^[69] A comparison of the absorption frequency for the C=O stretch and chemical shift of the β -carbon suggests a similar reactivity of acyl azolium **50** and acyl ammonium **51**, which exhibit similar C=O bond strengths but increased polarization at the β -carbon as compared to electron deficient enone **52**. An assessment of the electrophilicity parameter E ($\log k = S_N(E + N)$),^[41a] shows that iminium ion **49** is the most potent electrophile, followed by acyl azolium **50** and quite far behind enone **52**. The same trend can also be observed in the chemical shift of the β -carbon. The electrophilicity of **50** is comparable to that of highly activated Michael acceptors such as benzyldenemalononitriles and 2-benzylidene-indan-1,3-ones.^[70] In the crystal structure of **50** the C–C double bond and the carbonyl double bond is almost completely coplanar (torsion angle 6.2°), which is the optimal configuration for 1,4-addition. The imidazolium ring of **50** is tilted with respect to the carbonyl group (torsion angle 35.5°) reducing conjugation, which could partly explain the lower electrophilicity compared to **49**.

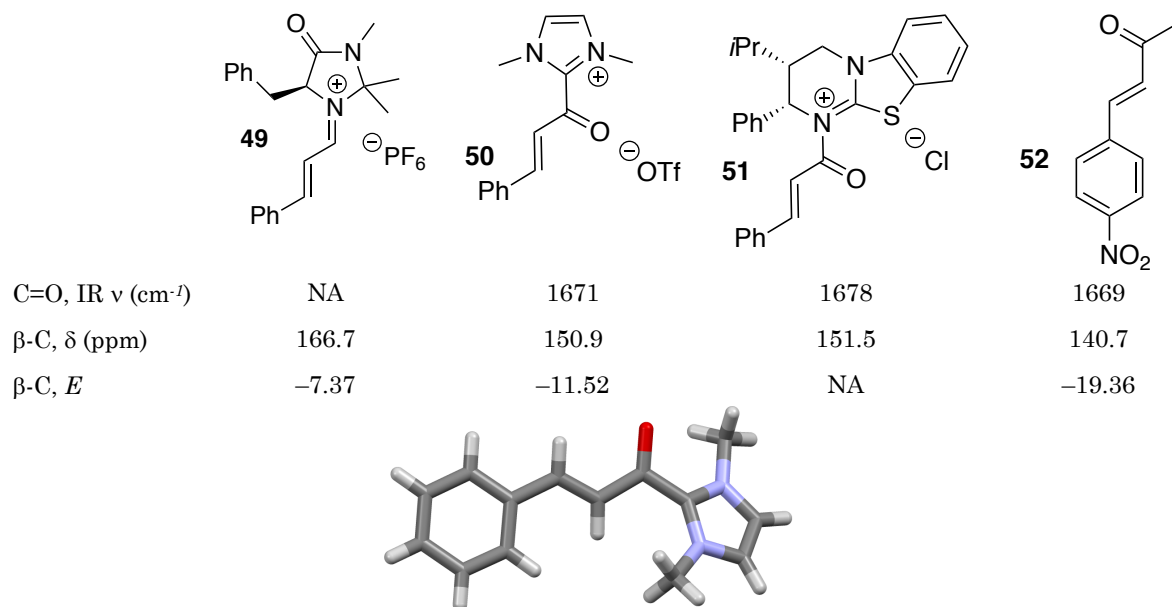
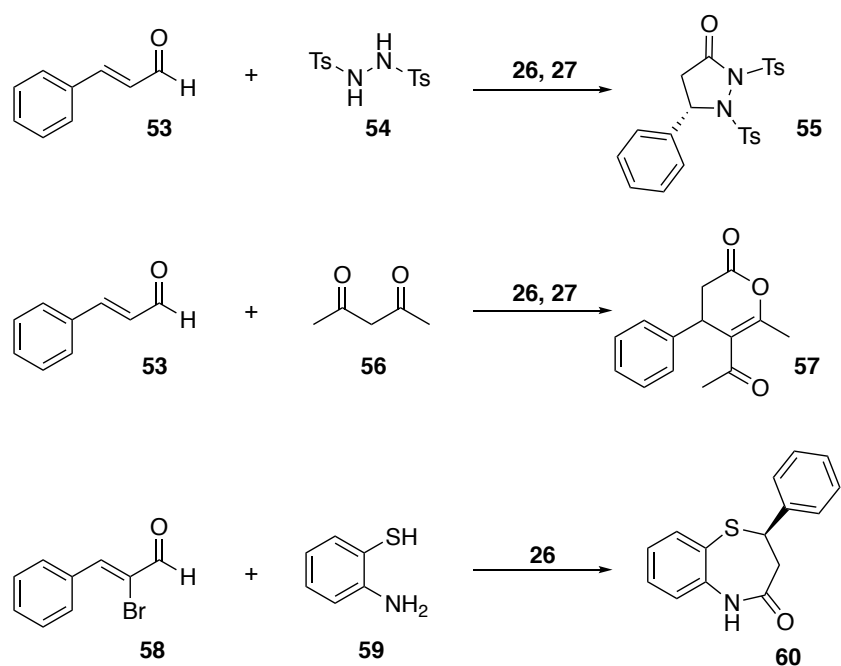


Figure 5. Structure and physical parameters for some important intermediates in organocatalysis and the X-ray structure of **56**, NA: not available.

The most characteristic reaction of the α,β -unsaturated acyl azolium is its reaction with 1,3-dicarbonyl compounds, such as acetylacetone **56**, yielding dihydropyranones (**57**), as first reported by Studer (Scheme 7).^[71] Since then, a wide range of different heterocycles have been synthesized *via* this activation mode.^[67] For instance, reaction with tosylated hydrazine (**54**) yields pyrazolidine **55** as reported by Chi *et al.*^[72] Several different benzothiazepines (**60**), a privileged structure in medicinal chemistry, is available by reaction between α -bromoenal **58** and aminothiols **59**. In this reaction, the α,β -unsaturated acyl azolium is formed by internal, and not external oxidation.^[73]



Scheme 7. Some transformations involving the α,β -unsaturated acyl azolium intermediate.

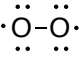
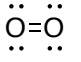



2.3 Catalytic Aerobic Oxidations

Oxidation reactions are ubiquitous in synthetic chemistry. Traditional oxidants are often based on either manganese, chromium or iodine and are often of high molecular weight to gain substrate selectivity in the reaction. As a result, oxidation reactions are usually characterized by the formation of large amounts of byproducts, which is not compatible with the concept of green chemistry.^[74] Therefore the use of sustainable oxidants such as hydrogen peroxide^[75] or molecular oxygen is gaining ground.^[76] Hydrogen peroxide is advantageous as it is a liquid, miscible with water, making it relatively easy to handle even on large scale. However, hydrogen peroxide is prone to degradation through a radical process that can be initiated by the presence of impurities such as metallic particles. Molecular oxygen is, on the other hand, abundant and inexpensive since air can often be used directly. Large scale implementation of aerobic oxidations is linked to safety issues, however risks can be reduced in several ways, for instance by the implementation of flow reactors.^[77] Both oxygen and hydrogen peroxide offers a high efficacy per weight of oxidant and lead to the formation of non-hazardous byproducts (typically water).

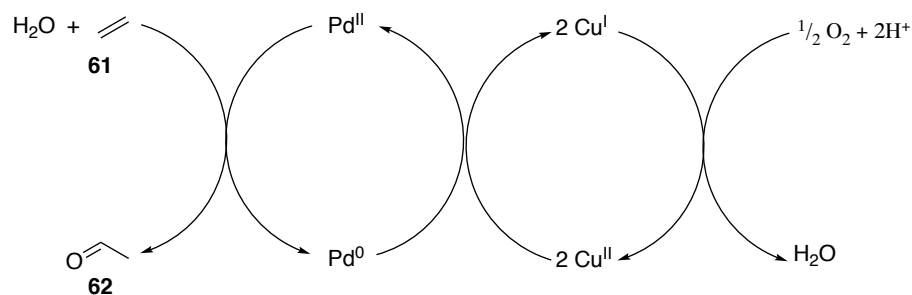
Oxygen (O_2) is a peculiar molecule. It has a triplet ground state making it a diradical,^[78] but somehow oxygen is stable enough to constitute about 21% of the earth's atmosphere.^[79] Radicals are notorious for their reactivity and typically requires stabilization by either sterical or electronical means to be isolatable.^[80] Yet, somehow oxygen persists without sterical encumbrance. Another exotic feature of oxygen's reactivity is that although triplet oxygen is apparently *stable* under atmospheric conditions, singlet oxygen is not.^[81] The observed effect of multiplicity on the reactivity of oxygen is in stark contrast to general trends, as in the stabilization of NHCs discussed in section 2.1. As a reference, the structure of triplet/singlet oxygen and some carbon centered triplet diradicals and their

lifetimes are given in Table 1.^[82] Thermodynamic analysis of aerobic oxidations further complicates the issue, as it shows that oxygen reacts exothermically with every element except gold.^[83] It has even been argued that it is oxygen, and not the hydrocarbon, that should be considered energy-rich in combustion reactions.^[84] The reason for the apparent stability of oxygen is clearly not thermodynamic but kinetic,^[85] and such species are often referred to as persistent, or long-lived, rather than stable. Hence, aerobic oxidations are generally characterized by favorable thermodynamics and high-activation barriers, requiring high temperatures to be efficient.

Table 1. Structure and lifetime of some triplet diradicals and singlet oxygen.

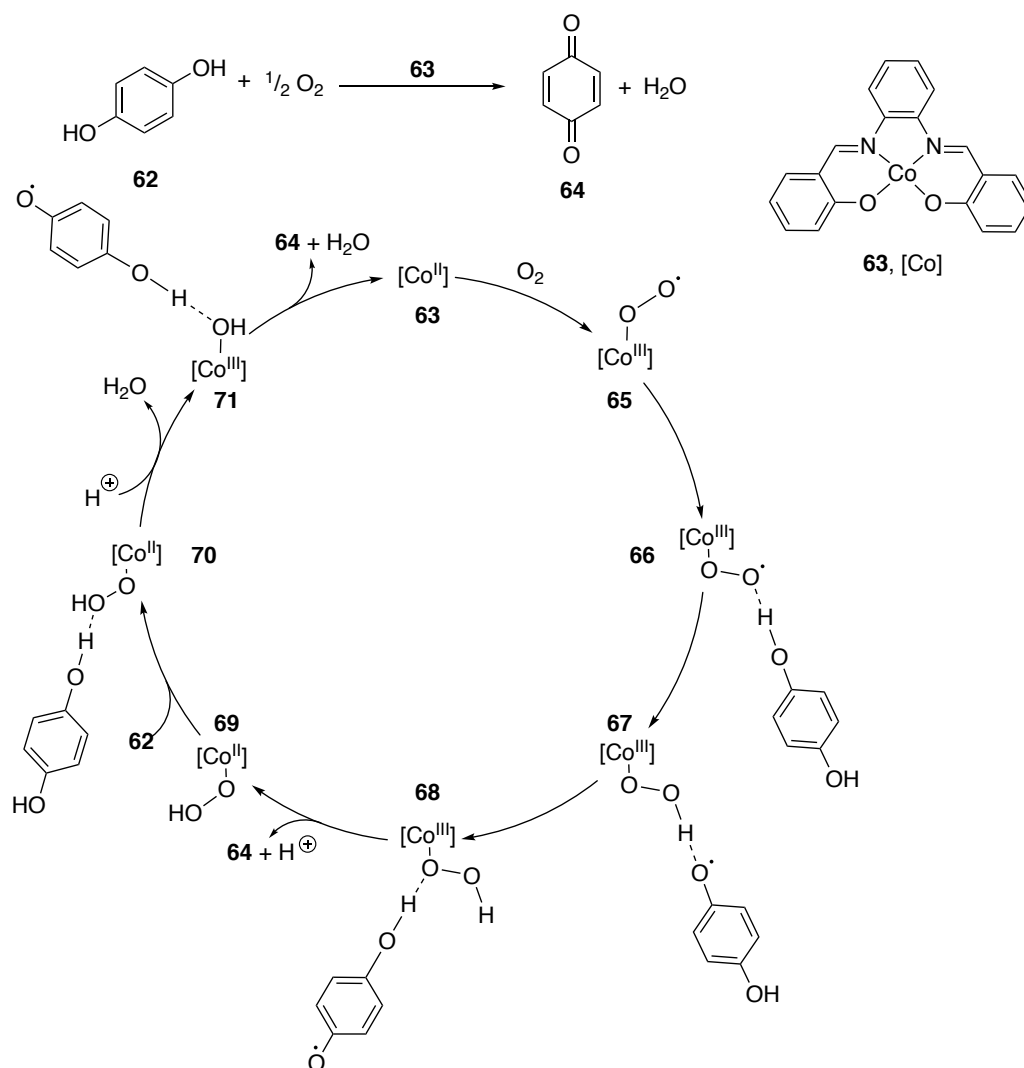
					
	Triplet	Singlet			
Lifetime	Persistent	32 μ s ^a	93 ns ^b	390 ns ^a	365 ns ^a
a) Measured in benzene at room temperature, values given with a \pm 15% interval. b) Measured in benzene at 8 °C, values given with a \pm 18% interval.					

The high activation barrier for aerobic oxidations is a prerequisite for life as we know it, lessening the extent of oxidative damage. Nonetheless, it complicates the use of oxygen in synthetic transformations, often resulting in the formation of kinetic side products. Inspired by the way nature circumvents these high activation barriers in the respiratory chain, synthetic chemists have started to employ electron transfer mediators (ETMs) in aerobic transformations.^[86] The ETMs work in concert, transporting electrons from the substrate to oxygen *via* a low-energy path thereby circumventing unfavorable reaction kinetics. This strategy allows the replacement of one large activation barrier by several smaller ones. An industrial application of ETMs is the aerobic oxidation of ethylene to acetaldehyde in the Wacker process (Scheme 8). In this process, ethylene (**69**) is oxidized by a palladium(II) species, yielding acetaldehyde (**70**) and palladium(0), which is re-oxidized by a copper(II) salt. The obtained Cu(I) is then readily oxidized back to Cu(II) by aerial oxygen, which completes the redox cycle. The direct oxidation of Pd(0) with oxygen is sluggish, with a kinetic preference for the formation of palladium black instead. However, with the addition of Cu(II) as an ETM the reaction proceeds efficiently.^[86]



Scheme 8. The Wacker oxidation of ethylene to acetaldehyde.

The transition metal catalyzed aerobic oxidation of hydroquinones to quinones is a common reaction step in ETM based systems, where the formed quinone later oxidizes either the substrate or another ETM. The cobalt(II) salophen-catalyzed (**63**) aerobic oxidation of hydroquinone **62** to quinone **64** in methanol has been extensively investigated by a series of kinetic, spectroscopic and computational techniques (Scheme 9).^[87] The proposed mechanism begins with the endergonic reaction between oxygen and **63** resulting in production of superoxide **65**. Hydroquinone **62** forms hydrogen bonded complex **66** with the superoxide, which triggers hydrogen atom transfer (HAT) yielding peroxide intermediate **67**. Complex **67** rearranges to hydrogen bonded complex **68** and the hydroquinone radical is further oxidized *via* proton coupled electron transfer (PCEP) to quinone **64** and Co(II) complex **69**. This step has been proposed to be the rate determining step (RDS). The Co(II) complex binds to another molecule of **62** through hydrogen bonding generating peroxide intermediate **70**, which *via* a second HAT reaction gives water and cobalt(III) hydroxide **71**. A second PCET regenerates **63** from **71**, releasing water and a second molecule of quinone **64**.



Scheme 9. The mechanism of the Co(salophen) catalyzed aerobic oxidation of quinone **72**.

3. Hypothesis and Aim

This thesis is based on the hypothesis that it is possible to develop efficient and general protocols for aerobic NHC catalysis using an ETM strategy. From the hypothesis, three specific aims were formulated:

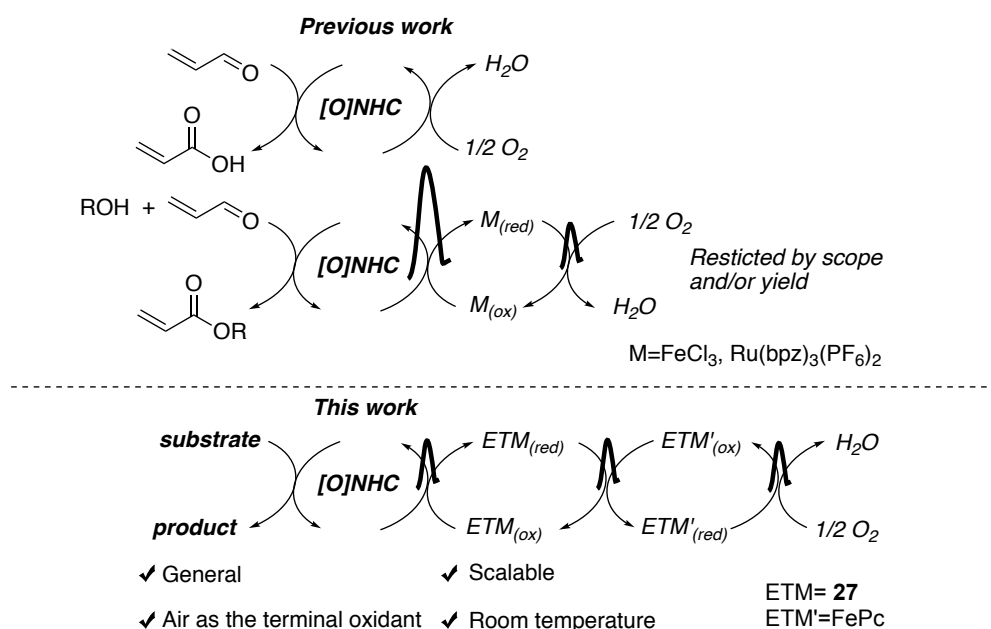
1. Identify a suitable system of ETMs to enable aerobic NHC-catalyzed reactions.
2. Investigate the generality of the developed system compared to traditional oxidative NHC catalysis.
3. Investigate further use of the developed protocol and the obtained products.

4. Aerobic Access to the α,β -Unsaturated Acyl Azolium Intermediate (Paper I)

4.1 Aerobic NHC Catalysis

The use of stoichiometric amounts of high molecular weight oxidants such as **27** hampers large-scale applications of the rich chemistry associated with oxidative NHC catalysis.^[53b, 88] The formation of large amounts of byproducts is accompanied by large costs due to energy demanding separation and disposal, which obstructs industrial applications from both a sustainable and an economic perspective. Aerial oxygen is an appealing oxidant since it is non-toxic, cheap and only forms water as a byproduct. Bäckvall *et al.* pioneered the use of ETMs in aerobic transformations, and the strategy is amenable for several transition metal catalyzed reactions such as 1,4-oxidation of 1,3-dienes,^[89] oxidation of alcohols^[90] and oxidative carbocyclizations.^[91]

Direct aerobic oxidation of the homoenolate is reported to yield the carboxylic acid,^[92] and early reports using either a Fe(III) or Ru(II) based ETM suffered from restricted scope and high reaction temperatures (Scheme 10).^[63, 93] The limitations of the previously reported aerobic oxidations could potentially be attributed to inefficient ETM systems, leading to the formation of kinetic side products such as the carboxylic acid. It was hypothesized that using two ETMs instead of only one would enable a more kinetically potent oxidation of the homoenolate, thereby allowing aerobic access to the α,β -unsaturated acyl azolium.



Scheme 10. Aerobic oxidations of the homoenolate.

4.2 Identification of a Suitable System for Aerobic NHC Catalysis

The aerobic esterification of cinnamaldehyde (**63**) with methanol was chosen as the model reaction (Table 2). α,β -Unsaturated aldehydes are known to undergo several NHC-catalyzed reactions, such as formation of saturated ester **77**, cinnamic acid (**78**) or γ -butyrolactone **79**. Selectivity toward methyl cinnamate **72** would hence be a good indicator of efficiency in the oxidation of the homoenolate. With stoichiometric amounts of Kharasch oxidant **27**, methyl cinnamate was obtained in 74% yield and 78% selectivity, using NHC precatalyst **73** and the base 1,5,7-triazabicyclo[4.4.0]dec-5-ene (TBD) in acetonitrile (entry 1). When the loading of **27** was decreased to 1 mol% both the yield and the selectivity were drastically reduced, even with prolonged reaction time (entry 2). The result indicates that the direct aerobic oxidation of the formed hydroquinone (Scheme 11, **83**) is slow, leading to the formation of kinetic side products.

Iron(II) phthalocyanine, FePc, is known to oxidize several hydroquinones to the corresponding quinones in the presence of air.^[94] In combination with the previously reported selectivity of **27** toward oxidation of the homoenolate, it was theorized that the combination of FePc and Kharasch oxidant would constitute an efficient ETM system. Indeed, by using 1 mol% of **27** and 0.5 mol% of FePc, methyl cinnamate was obtained in 80% yield and 88% selectivity (entry 3). Later on, it was shown that **27** can be replaced with phenol **76**, maintaining both reactivity and selectivity (entry 4). Phenol **76** is used as a precursor in the synthesis of **27**, and under the developed reaction conditions it is rapidly transformed into **27** *in situ*. Moreover, **76** is a bulk chemical that is considerable cheaper than **27** (**76**: 538.2 SEK/kg, **27**: 1261.67 SEK/50 mg).^[95] With an efficient ETM system in hand, different NHC precatalysts were examined. Thiazolium based precatalyst **74** proved inactive (entry 5), while imidazolium **19** and bicyclic triazolium **75** formed methyl cinnamate in lower yield and selectivity as compared to **73** (entry 6 and 7). Lastly, the effect of NHC loading was examined and it was found that higher loading gave lower yield with lower selectivity (entry 8 and 9). This effect may be rationalized as follows: increased concentration of the NHC combined with maintained loading of the ETM system leads to an increased average lifetime of the homoenolate, resulting in the formation of kinetic side products.

Table 2. Screening of reaction conditions.

<div> <div> <p>73</p> </div> <div> <p>74</p> </div> <div> <p>19</p> </div> <div> <p>75</p> </div> <div> <p>76</p> </div> <div> <p>FePc</p> </div> </div>						
<div> <div> <p>Potential side products</p> <p>77</p> </div> <div> <p>78</p> </div> <div> <p>79</p> </div> </div>						
Entry ^a	NHC	ETM (eq.)	ETM' (FePc, eq.)	Time (h)	Yield (%) ^b	Selectivity(%) ^c
1	73	27 (1.0)	-	4	74	78
2	73	27 (0.01)	-	7	24	40
3	73	27 (0.01)	0.005	4	80	88
4	73	76 (0.02)	0.005	4	85	89
5	74	76 (0.02)	0.005	-	-	-
6	19	76 (0.02)	0.005	22	65	65
7	75	76 (0.02)	0.005	4	68	68
8	73 ^d	76 (0.02)	0.005	4	19	19
9	73 ^e	76 (0.02)	0.005	4	67	74

a) **53** (0.5 mmol), TBD (0.5 eq.), MeOH (4.0 eq.), NHC (0.02 eq.), ETM (0.02 eq.), ETM', MeCN (1.0 ml). b) Yield determined by ¹H NMR using durene as internal standard. c) Yield over conversion. d) 0.50 eq. NHC used. e) 0.20 eq. NHC used.

To gain further insight the kinetic profile of the reaction was monitored by gas chromatography equipped with a flame ionization detector (GC-FID) in a series of elimination experiments (Figure 6). In presence of both FePc and **76**, cinnamaldehyde is transformed into methyl cinnamate in >90% yield within 5h. Elimination of either FePc or **76** results in about 40% yield within 3h, while exclusion of both FePc and **76** results in about 30% yield. In all reactions, full conversion of cinnamaldehyde is observed and cinnamic acid is obtained as a major side product, indicating that without both FePc and **76** the oxygenative pathway is dominating.

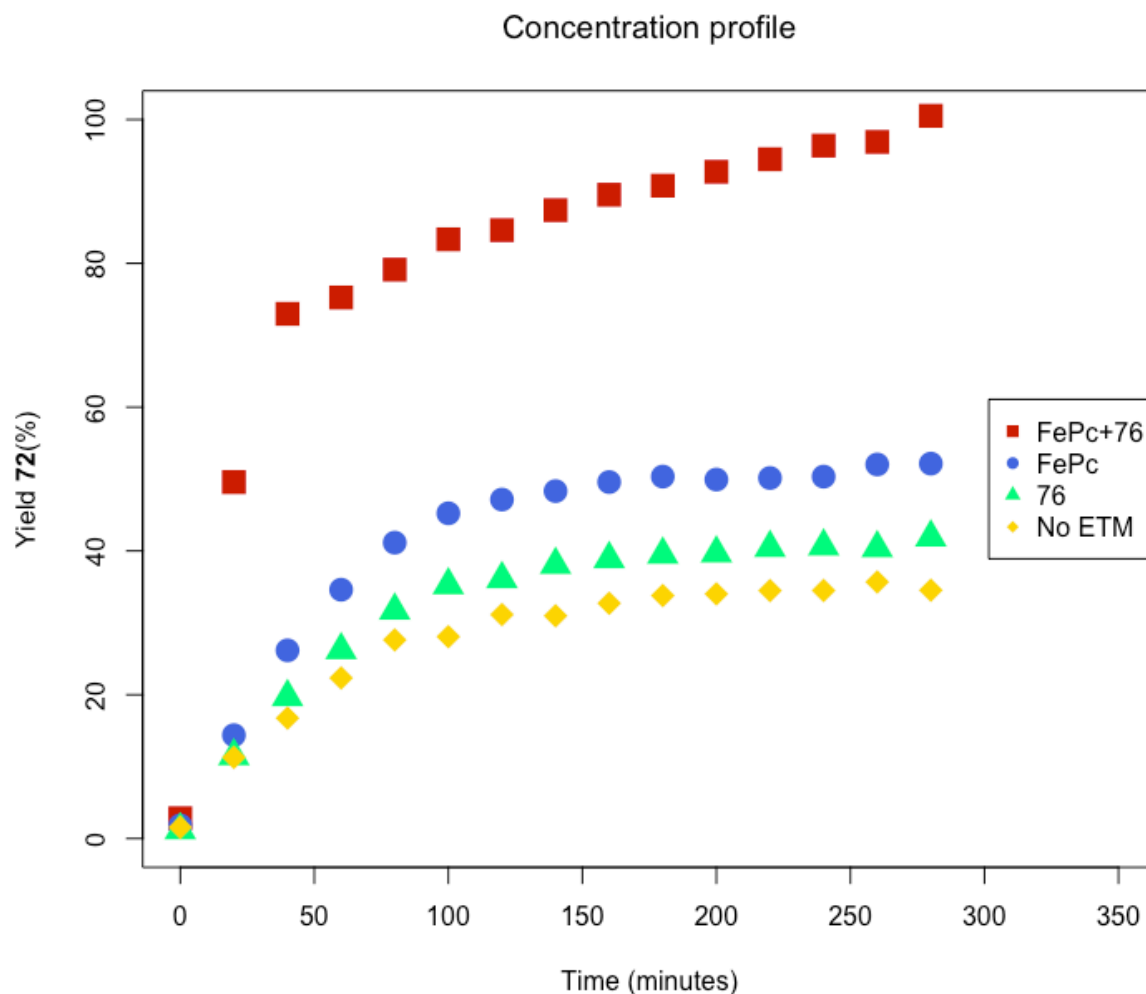
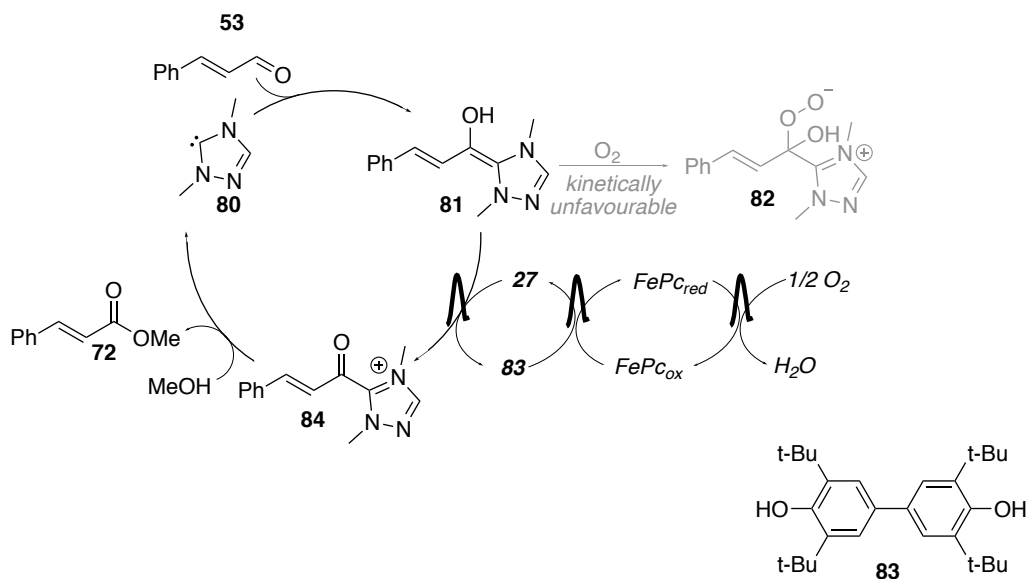


Figure 6. The kinetic profile of the reaction with different ETMs.

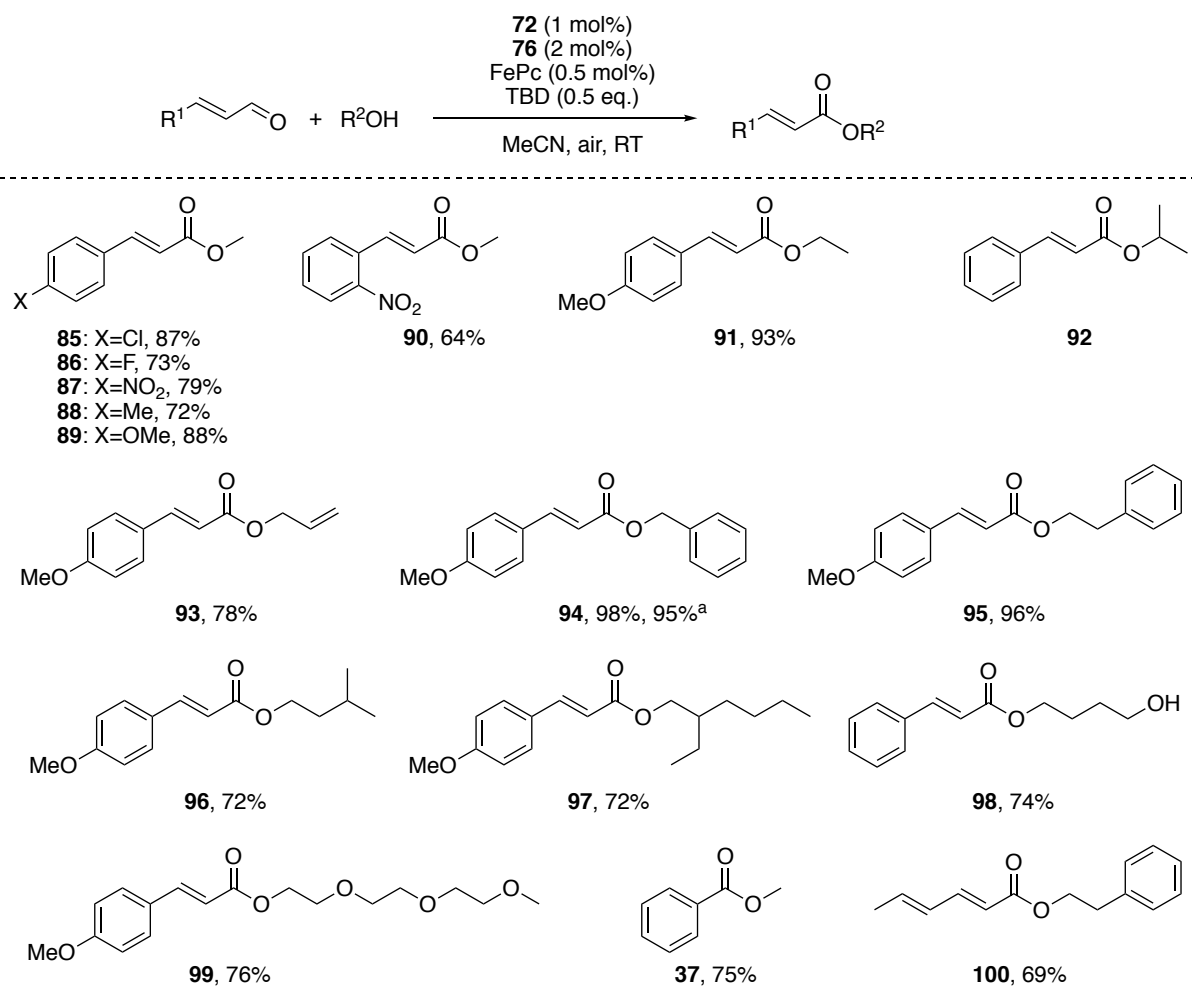
Based on the elimination experiments and the decreasing redox potential of FePc ($E = +0.74$ V *vs.* SCE)^[96] and **27** ($E = -0.52, -0.89$ V *vs.* SCE),^[57] the following mechanism is proposed (Scheme 11). Deprotonation of the triazolium salt yields carbene **80** that through nucleophilic 1,2-addition to cinnamaldehyde yields homoenolate **81**. The homoenolate is then rapidly oxidized by **27** to the α,β -unsaturated acyl azolium **84**, by-passing the oxygenative pathways and the formation of peroxy intermediate **82**. The acyl azolium is intercepted by methanol yielding methyl cinnamate and carbene **80** is regenerated. Compound **83** is then oxidized back to **27** via FePc-catalyzed aerobic oxidation, yielding water as the sole byproduct and completing the catalytic cycle.



Scheme 11. The proposed mechanism of the aerobic esterification of cinnamaldehyde.

Thereafter, the scope of the reaction was evaluated (Scheme 12). Both electron-poor (**85–87**, **90**) and electron-rich (**88–89**) cinnamaldehydes are efficiently transformed into the corresponding methyl esters, for instance methyl 4-chlorocinnamate **85** and methyl 4-methoxycinnamate **89** were isolated in 87% and 88% yield respectively. Subsequently, the scope was extended in regard to the alcohol component (**91–100**). Simple alcohols are well tolerated, and ethanol, isopropanol and benzyl alcohol delivered esters **91**, **92** and **94** in excellent yields. 1,4-Butandiol is also a viable reaction partner yielding monoester **98** in 74% yield. The method also enables efficient gram-scale reactions, and 1.5 grams of **94** was isolated in 95% yield. The gram scale reaction used only 26.7 mg of **76** and 18.9 mg of FePc, while stoichiometric conditions would have required at least 2.48 grams of **27**. Allyl alcohol, which can be sensitive towards oxidative conditions, is unaffected by the developed oxidative system, and ester **93** could be isolated in 78% yield without any sign of over-oxidation.

The 4-methoxycinnamate motif is common in industrially important antioxidants, and commercial sunscreen agents amiloxate (**96**) and octinoxate (**97**) could both be isolated in 72% yield. Aromatic aldehydes could also be employed and methyl benzoate **37** was isolated in 75% yield. Initial attempts with aliphatic enals showed low reactivity and complex reaction mixtures. However, the dienol sorbic aldehyde exhibited good activity and ester **100** was isolated in 69% yield.



Scheme 12. Scope of the NHC-catalyzed aerobic esterification of aldehydes. Aldehyde (1 eq.), alcohol (4 eq.). MeCN (0.2 M). Isolated yields after purification by silica gel chromatography. ^a1.5 grams isolated.

5. Valorization of Glycerol *via* a Dual NHC-Catalyzed Telescoped Reaction (Paper III)

5.1 Chemical Valorization of Biomass

The valorization of biomass into fuels, fine and commodity chemicals is one the great challenges within chemistry and is a prerequisite for sustainable development.^[97] Transesterification of vegetable oils into biodiesel yields glycerol as a byproduct (10 wt%), making it an attractive feedstock for various C₃-chemicals.^[98] Glycerol is currently used as a precursor in the industrial epichlorohydrin synthesis by Solvay,^[97] and glycerol carbonate has gained widespread attention for various uses such as solvent, electrolyte or reagent for both fine chemicals and polymers.^[99]

Valorization of glycerol is typically achieved through transition metal catalysis,^[99a, 100] organocatalytic transformations of glycerol remain much scarcer. Previous reported organocatalytic transformations of glycerol involve transcarbonation with either dialkyl carbonates or urea using NHCs, quaternary ammonium salts or Brønsted bases (Figure 7, A).^[99b, 101] Organocatalytic acylation of glycerol is possible using either superbases, alkali acetates or sulfonic acids as catalysts (Figure 7, B).^[102] Lastly, both homogenous and heterogeneous sulfonic acids have been used to transform glycerol to a variety of different acetals and ethers (Figure 7, C).^[103] Although NHC-catalysis offers several distinct reaction paths, the use of NHC-catalysis in glycerol valorization is currently limited to carbonation reactions. We set out to merge our newly developed system for aerobic NHC catalysis and glycerol upgrading in a telescoped reaction to get access to valuable glycerol derivatives (Figure 7, D).

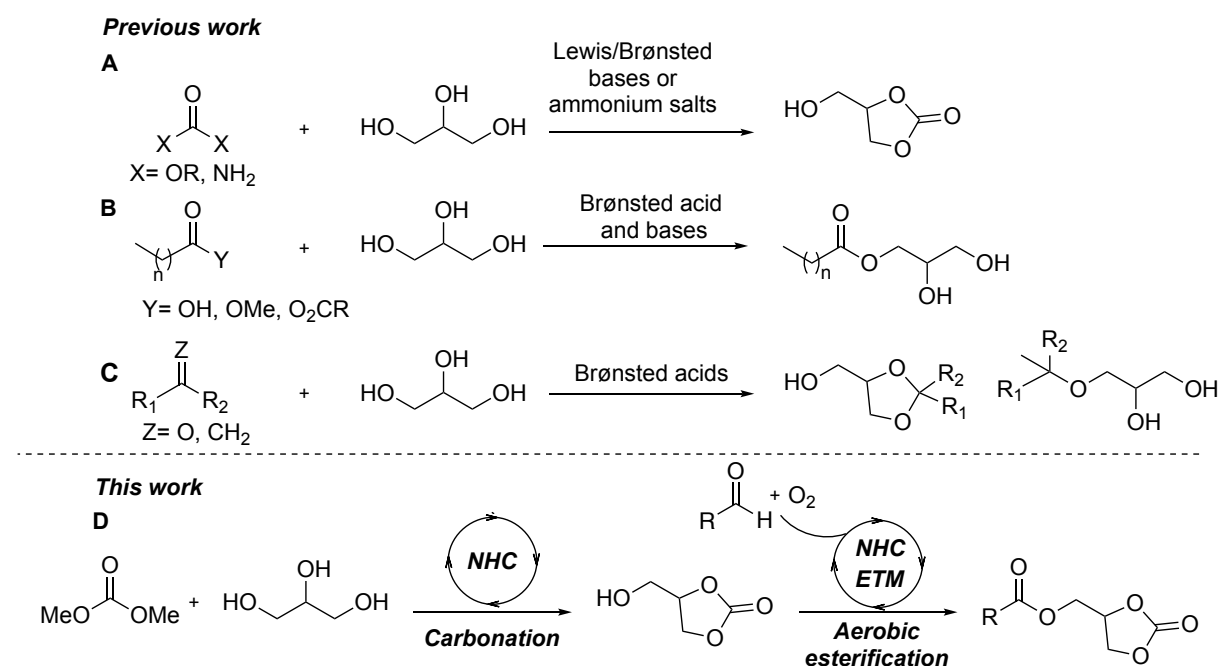


Figure 7. Previous organocatalytic valorizations of glycerol (A-C) and the proposed reaction (D).

6.2 Design of a Telescoped Reaction for Dual Glycerol Functionalization

Formation of unsaturated glycerol carbonate ester **102**, *via* the initial carbonation of glycerol with dimethyl carbonate followed by aerobic acylation using cinnamaldehyde, was chosen as model reaction (Table 3). A successful reaction would offer several advantages such as direct valorization of glycerol, high atom and pot economy^[104] and the incorporation of a carbonate group as a synthetic handle. Moreover, it should be noted that dimethyl carbonate (DMC) is a benign reagent that is non-toxic, biodegradable and is derived from CO₂. The advantages of DMC over other carbonation reagents get especially clear when compared to the highly poisonous phosgene, for instance.^[105]

Promising initial attempts with triazolium salt **73**, TBD and **27**/FePc as ETMs yielded **102** in 89% yield using only 1.1 equivalents of glycerol (entry 1). A scan of different NHC precatalysts showed that thiazolium based catalyst **104** was inactive, while catalysts **19** and **76** gave the product in slightly lower yield (entry 2-4). With bicyclic triazolium **75**, cinnamic acid was obtained as a side product indicating that the oxygenative pathway is active under these conditions, while imidazolium-based catalyst **19** exhibited incomplete consumption of cinnamaldehyde indicating a less robust system as compared to **73**.

Replacement of TBD with either K₂CO₃ or Et₃N resulted in no conversion of cinnamaldehyde (entry 5-6). This effect may be rationalized by that the crucial *in situ* aerobic oxidation of **76** to **27** is base catalyzed, and Et₃N is likely a too weak base while K₂CO₃ suffered from poor solvation, hampering the reaction.^[57] Realizing this, it was possible to reduce the loading of TBD with maintained yield by replacing **76** with **27**, albeit with prolonged reaction time (24h, entry 7, compared to 3h). Performing the reaction under an atmosphere of nitrogen delivered the product in only 5% yield, showing that aerial oxygen truly is the terminal oxidant (entry 8).

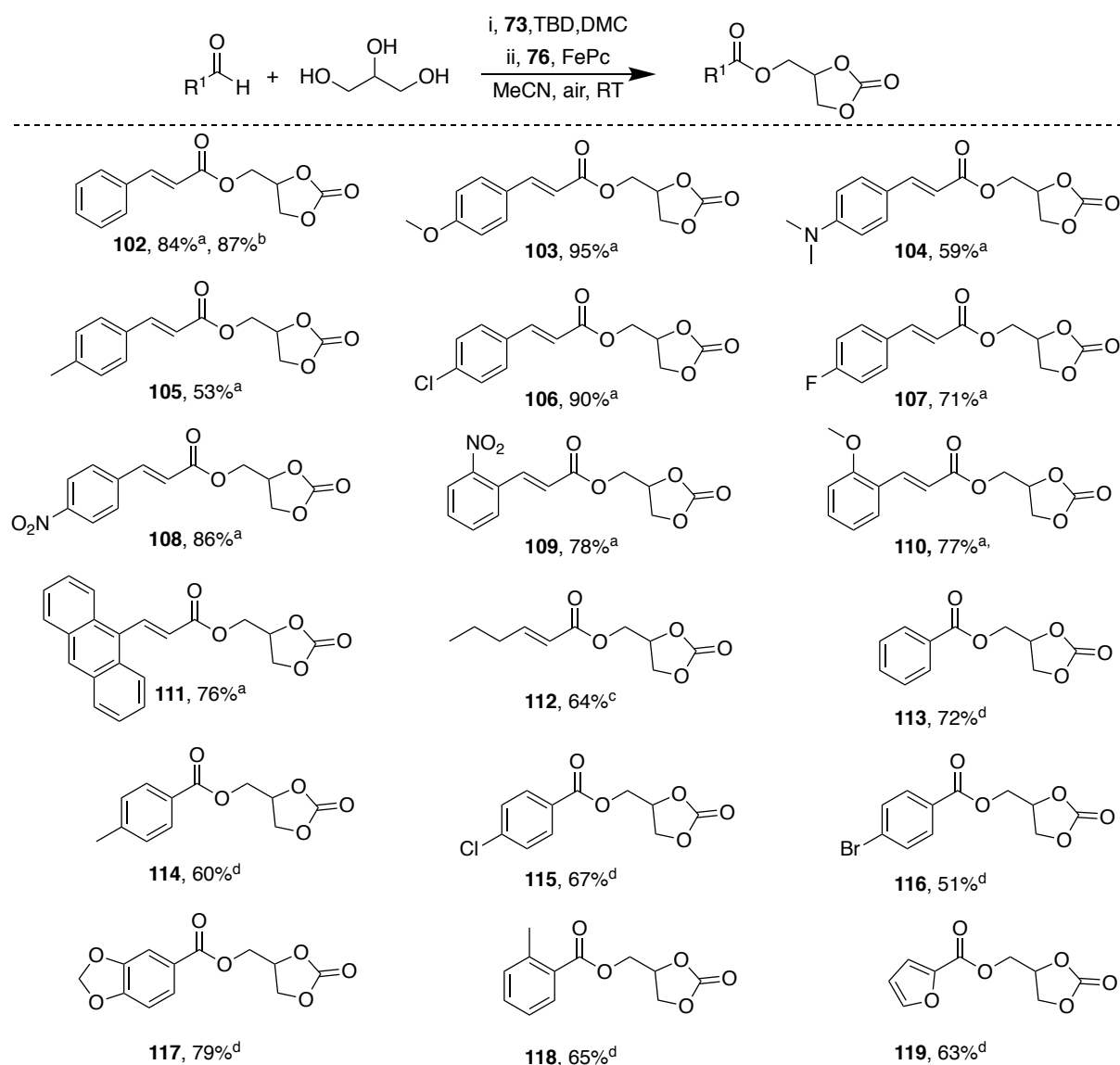
Direct acylation of glycerol yielding ester **103** is also possible (entry 9). However, these reactions yield several undesired side products, mainly the diester and the secondary ester, which cannot effectively be separated from the main product. The amount of side products formed remained stable around 10% regardless of solvent selection and concentration. For instance, when the reaction was performed in acetone, **103** was obtained in 81% yield. In this reaction a competing aldol product, in addition to the secondary ester and the diester, was identified as side products (entry 10). Moreover, when the NHC is excluded from the carbonation step, an incomplete conversion of glycerol with subsequent side product formation (14% by ¹H NMR) is noted, suggesting that the carbonation step also is NHC-catalyzed.

Table 3. Screening of reaction conditions for the telescoped valorization of glycerol.

<div style="display: flex; justify-content: space-around; align-items: flex-end;"> <div style="text-align: center;"> 73 </div> <div style="text-align: center;"> 104 </div> <div style="text-align: center;"> 19 </div> <div style="text-align: center;"> 75 </div> <div style="text-align: center;"> TBD </div> </div> <div style="display: flex; justify-content: space-around; align-items: flex-end; margin-top: 20px;"> <div style="text-align: center;"> 27 </div> <div style="text-align: center;"> 76 </div> <div style="text-align: center;"> FePc </div> </div>							
Entry	Cat	ETM1	ETM2	Base	Solvent	Yield (%) ^a	
						102	103
1. ^b	73	76	FePc	TBD	MeCN	89	
2. ^b	75	76	FePc	TBD	MeCN	86	
3. ^b	104	76	FePc	TBD	MeCN	0	
4. ^b	19	76	FePc	TBD	MeCN	81	
5. ^b	73	76	FePc	K ₂ CO ₃	MeCN	0	
6. ^b	73	76	FePc	Et ₃ N	MeCN	0	
7. ^c	73	27	FePc	TBD	MeCN	88	
8. ^{b,d}	73	76	FePc	TBD	MeCN	5	
9. ^e	73	76	FePc	TBD	MeCN		87
10. ^e	73	76	FePc	TBD	Acetone		81

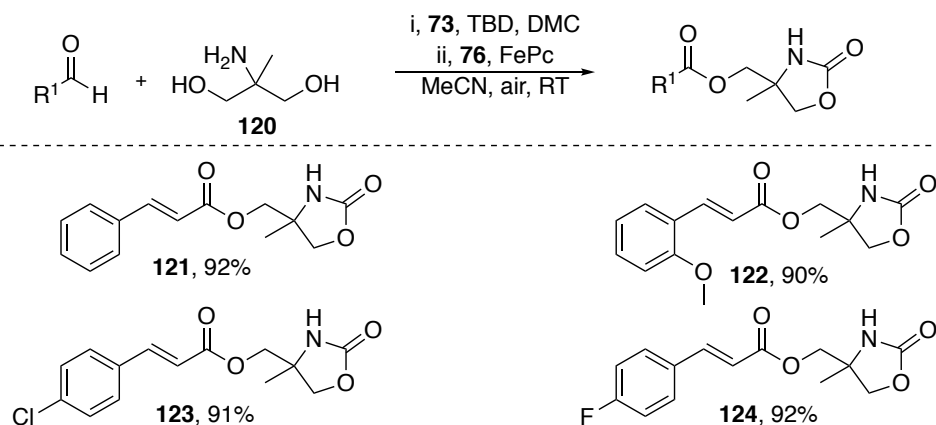
a) Determined by ¹H NMR with durene as internal standard. b) i, Glycerol (1.1 eq.), TBD (0.5 eq), **73** (2 mol%), solvent/dimethyl carbonate 5:2. ii, Cinnamaldehyde (0.5 mmol), FePc (0.5 mol%), **76** (2 mol%). c) As in b), but with 0.2 eq. TBD and 0.01 eq. of **27**. d) Last step performed under a nitrogen atmosphere. e) Glycerol (4 eq.), TBD (0.5 eq.), **73** (2 mol%), cinnamaldehyde (0.5 mmol), FePc (0.5 mol%), **76** (2 mol%).

Having found conditions that enable selective functionalization of glycerol (Table 3, entry 1), the scope of the transformation was investigated (Scheme 13). Both electron donating groups (EDG, **103–105**, **110**) and electron withdrawing groups (EWG, **106–109**) is well tolerated on the cinnamaldehyde scaffold providing glycerol carbonate esters in moderate to excellent yields. For instance, 4-chlorocinnamaldehyde and 2-methoxycinnamaldehyde yielded esters **106** and **110** in 90% and 77% yield respectively. Aliphatic enals initially showed low reactivity, however using 4 mol% of the more active catalyst **75** enabled the formation and isolation of aliphatic ester **112** in 64% yield. Benzaldehydes appear to be less reactive than cinnamaldehydes, requiring 4 mol% of catalyst **73** to be successful. With that modification of the reaction protocol, a range of different aromatic aldehydes was used, delivering the products in moderate to good yields (**113–119**). As an example, piperonal and furfural yielded **117** and **119** in 79% and 63% yield respectively.



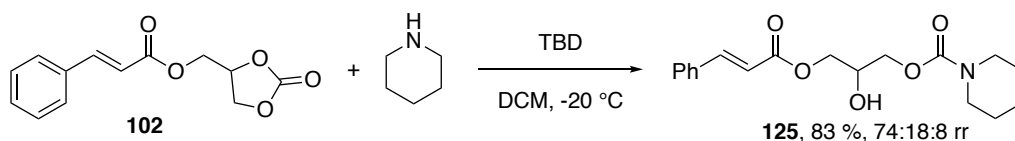
*Scheme 13. The scope of the NHC-catalyzed dual functionalization of glycerol. a) i, Glycerol (1.1 eq.), TBD (0.5 eq.), **73** (0.02 eq.), MeCN/DMC 5:2 (0.8 M). ii, Aldehyde (0.5 mmol), FePc (0.005 eq.), **76** (0.02 eq.) and MeCN (0.2 M). b) 1.6 Grams isolated. c) As in a, but with 4 mol% of catalyst **87** used. d) As in a, but with 4 mol% of catalyst **84** used.*

The above-mentioned protocol could be extended to the synthesis of 2-oxooxazolidine esters by replacing glycerol with aminoalcohol **120** (Scheme 14). As for the reaction with glycerol, the reaction tolerated both electron-rich and electron-poor cinnamaldehydes, delivering the products in excellent yields. 2-Methoxycinnamaldehyde and 4-fluorocinnamaldehyde delivered their corresponding oxooxazolidines in 90% and 92% yield respectively.



Scheme 14. Formation of 2-oxooxazolidine esters via NHC-catalyzed carbonation and aerobic acylation of aminoalcohol **165**. i, **120** (1.0 eq.), **73** (0.02 eq.), TBD (0.5 eq), MeCN/DMC 5:2 (0.8 M). ii, Aldehyde (0.5 mmol), FePc (0.005 eq.), **76** (0.02 eq.), MeCN (0.2 M), isolated yields.

Ring-opening of glycerol carbonates has been used for sustainable synthesis of pharmaceuticals and polymers, and is thus of great interest.^[106] Hence, selective functionalization of the less electrophilic carbonate moiety in presence of the α,β -unsaturated ester function would enable the use of the herein obtained products as sustainable building blocks for further synthesis. Inspired by reports from Kleij *et al.*,^[107] the TBD-catalyzed ring-opening of **102** with piperidine was investigated. At -20 °C, the use of 5 mol% of TBD in dichloromethane (DCM) delivered acyclic carbamate **125** in 83% yield and good regioisomeric ratio (Scheme 15). When higher loadings of TBD or other solvents (THF, MeCN) were used, the amide was formed as a side product. Performing the reaction at ambient temperature resulted in decreased regioselectivity.



Scheme 15. Organocatalytic ring-opening of **102** with piperidine. **102** (0.2 mmol), piperidine (1.2 eq.), TBD (0.05 eq.) DCM (0.8 M), isolated yield, regioisomeric ratio determined by ¹H NMR of crude material, major isomer separable by flash chromatography.

6. *N*-Acylation of Oxazolidinones via Aerobic NHC Catalysis (paper III)

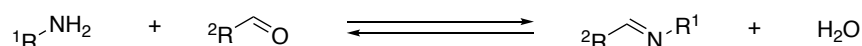
6.1 The Difficulty of Developing NHC-Catalyzed *N*-acylations

As previously mentioned, NHC-catalyzed acylations show a strong preference for *O*-acylations over *N*-acylations.^[56] But why is *N*-acylations so unfavorable? Well, one contributing factor is that the nucleophilic addition of NHCs to imines and even iminium ions are considerably less facile than the addition to aldehydes.^[108] And since most NHC-catalyzed acylations involve an aldehyde, addition of an amine leads to imine formation, which hampers the reaction (Figure 8, A). Drawing inspiration from this difficulty, Fuchter and coworkers developed an NHC-catalyzed amidation based on slow release of the amine, hence inhibiting imine formation.^[109]

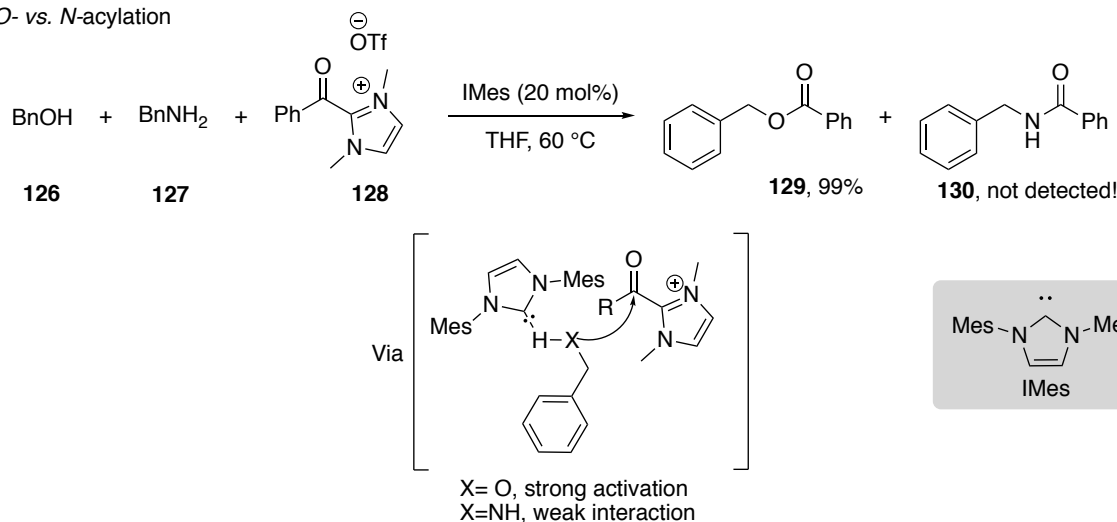
Studer *et al.* have investigated what dictates the selectivity between *O*- and *N*-acylations in great detail.^[110] Reacting preformed acyl azolium **128** with a 1:1 mixture of benzyl alcohol (**126**) and benzyl amine (**127**) in presence of 20 mol% of IMes resulted in complete acylation of benzyl alcohol (Figure 8, B). But if the reaction was performed in absence of IMes, a 3:1 mixture of *O*-acylated and *N*-acylated product was obtained. They also found that benzyl alcohol did not react with **128** without IMes present. However, benzyl amine reacted cleanly with **128** without IMes present, even at room temperature. They attribute this drastic effect to an *in situ* activation of alcohols by hydrogen bonding with the free carbene. Computational investigations corroborate that such an activation is stronger for alcohols than for amines, which seem to explain the observed selectivity.

We imagined that electron poor amines such as oxazolidinone, a five-membered cyclic carbamate, would be able to circumvent both of the earlier mentioned drawbacks. The decreased nucleophilicity means that iminium ion formation would be minimized. Moreover, the pK_a-value of the oxazolidinone proton is much more acidic than ordinary amines, and much closer to that of the alcohol proton, Figure 8, C).^[111] We hoped that this would mean that oxazolidinones could be activated by hydrogen bonding to the NHC in a similar fashion as alcohols. Another possibility would be activation by deprotonation. Moreover, acylated oxazolidinones are both biologically^[112] and synthetically useful,^[113] while their synthesis often is tedious involving sensitive reagents such as acyl chlorides and lithium reagents. Hence, this would be a prime setting for our aerobic methodology.

A, Imine formation



B, O- vs. N-acylation



C, pK_a-values of various O- and N-acids

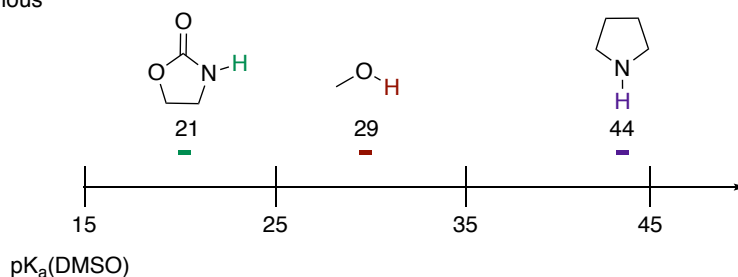


Figure 8. Factors governing the selectivity in O- vs. N-acylations.

6.2 Optimization and Scope

The reaction between cinnamaldehyde (**53**) and oxazolidinone (**131**) to give **132** was chosen as the model reaction for an optimization study (Table 4). Initially, different NHC precatalysts were investigated and it was found that triazolium **73** performed the best, followed by triazolium **75**, imidazolium **19** and lastly thiazolium **133** which did not work at all. A solvent screen showed that dichloromethane, anisole and ethyl methyl ketone gave lower yields than acetonitrile. Ethyl acetate gave **132** in 55% yield, slightly higher than acetonitrile. At this point, the saturated acylated oxazolidinone, butyrolactone and cinnamic acid was identified as the main side products, which indicate an inefficient oxidation of the Breslow intermediate. To accelerate the oxidation, the amount of solvent was reduced to half and DBU was used instead of TBD, which resulted in an isolated yield of 89%.

Next, the effect of the ETMs was evaluated. Using Co-based ETM **134** instead of FePc resulted in a decreased yield of 39%. Exchanging the Karasch oxidant for quinone **134** resulted in a slightly reduced yield of 78%. Performing the reaction under a nitrogen atmosphere resulted in 5% yield, showcasing that aerial oxygen is indeed the terminal oxidant.

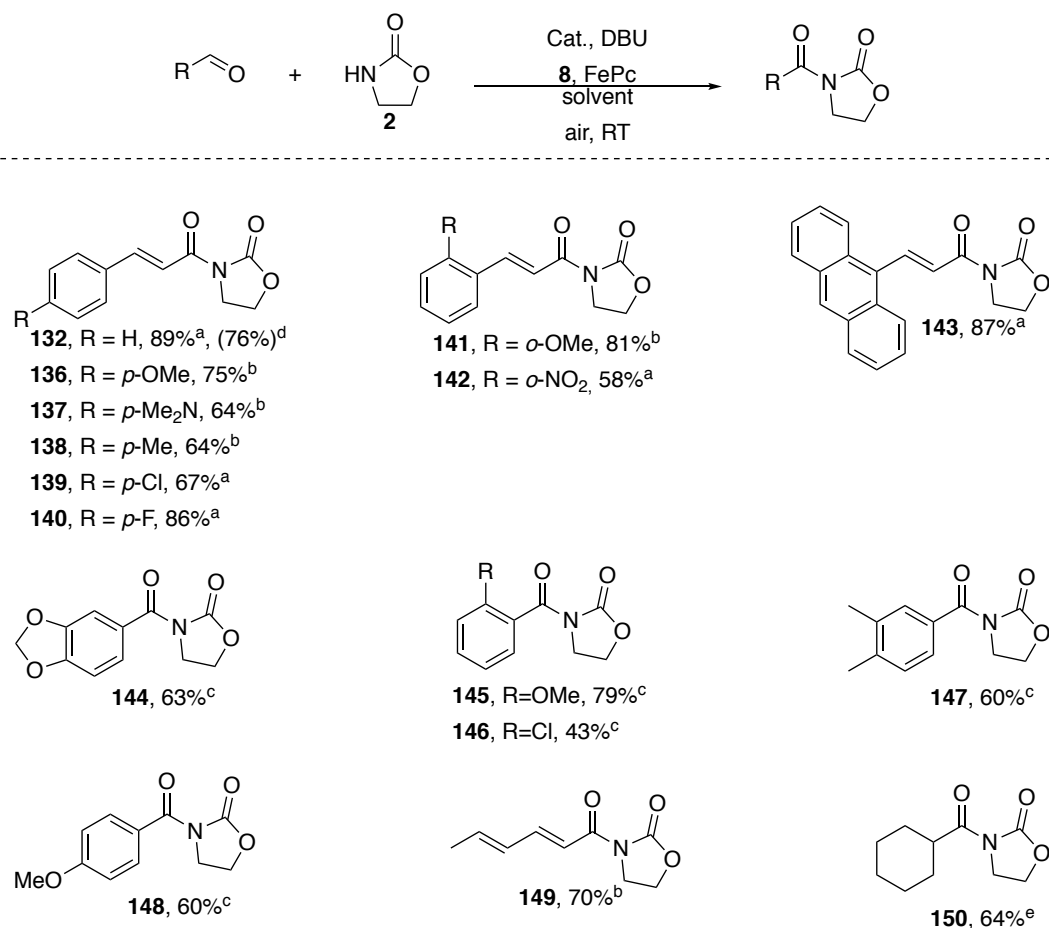
Table 4. Optimization of the aerobic *N*-acylation of oxazolidinone.

Entry	Cat.	Solvent	Base	ETM	ETM'	Yield
1. ^a	75	MeCN	TBD	27	FePc	47
2. ^a	73	MeCN	TBD	27	FePc	53
3. ^a	19	MeCN	TBD	27	FePc	32
4. ^a	133	MeCN	TBD	27	FePc	0
5. ^a	73	Anisole	TBD	27	FePc	24
6. ^a	73	EtOAc	TBD	27	FePc	55
7. ^a	73	DCM	TBD	27	FePc	35
8. ^a	73	MEK	TBD	27	FePc	32
9. ^b	73	EtOAc	DBU	27	FePc	90/89^c
10. ^b	73	EtOAc	DBU	27	135	39
11. ^b	73	EtOAc	DBU	134	FePc	78
12. ^{b, d}	73	EtOAc	DBU	27	FePc	5

Reaction conditions: ^a**53** (1 eq.), **131** (1.5 eq.), cat (5 mol%), base (0.5 eq.), ETM (5 mol%), ETM' (3 mol%), solvent (0.16 M). ^bWith cat (1 mol%), base (0.2 eq.), ETM (3 mol%), ETM' (2 mol%), solvent (0.31 M). ^cIsolated yield, **131** (1.3 eq.). ^dPerformed under N₂.

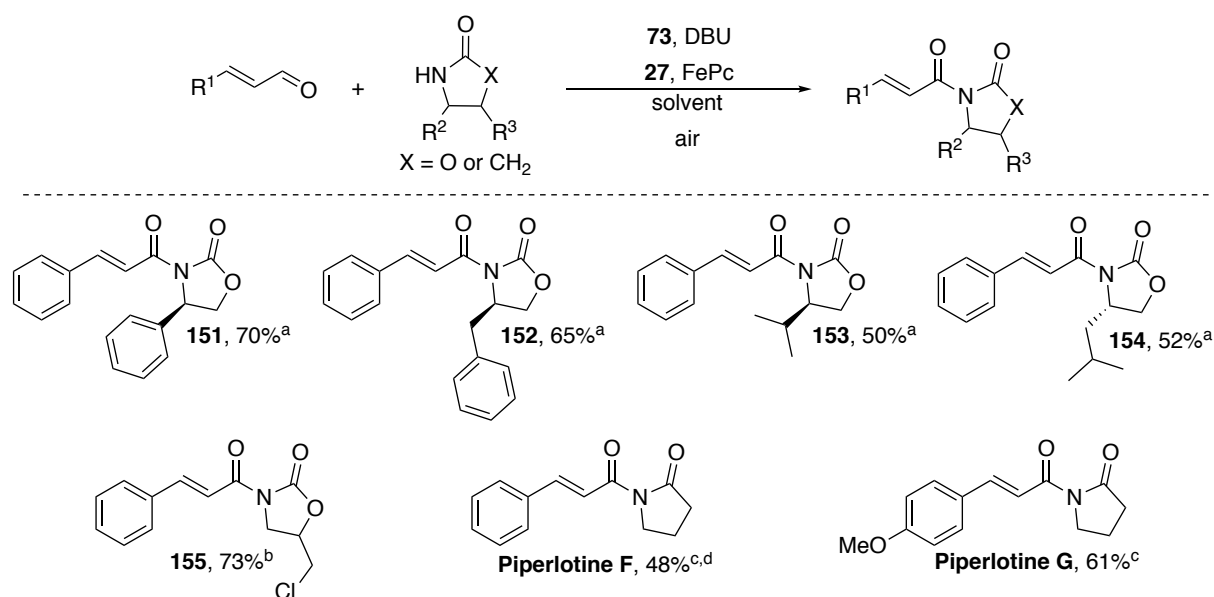
With an optimized procedure in hand, we proceeded to evaluate the scope of the reaction (Scheme 16). Cinnamaldehydes bearing electron donating substituents reacts poorly under the developed reaction conditions. However, by using mesityl-substituted catalyst **75** instead of **73** a high reactivity was obtained. With that modification both electron rich and electron poor aldehydes worked, for instance 2-methoxycinnamaldehyde and 4-fluorocinnamaldehyde delivered the products **141** and **140** in 81% and 86% yield respectively. The effect of the *N*-mesityl group in NHC-catalysts is well-studied, and it is proposed that its success is a result of making the initial 1,2-addition to the aldehyde irreversible.^[114] Invoking such an argument initially seems to make sense, the electron rich aldehyde is a less potent electrophile and making the addition of the NHC to the aldehyde irreversible would likely make the reaction more efficient. However, this does not explain why electron rich aldehydes performs very well in the previously described oxidative esterifications (e.g. **89**, **91**, **93–97** scheme 12). The major change between this system and the previous ones is the change of nucleophile, hence both the nucleophile and the catalyst should be involved in the step that requires the *N*-mesityl substituted NHC. Two such steps exist, either the addition of the nucleophile to the acyl azolium forming a tetrahedral intermediate or the collapse of the tetrahedral intermediate yielding the product and regenerating the carbene. The latter step has been shown to be rate determining for the esterification of alcohols using ynals.^[69b, 115]

Aromatic aldehydes can also be used, however a slightly increased loading of catalyst **73** (4 mol%) was needed for efficient reactions. It was discovered that electron rich benzaldehydes reacted better than electron poor ones, for instance 2-methoxybenzaldehyde and 2-chlorobenzaldehyde gave products **144** and **145** in 79% and 43% yield, respectively. Large amounts of the carboxylic acid were discovered as a side product in the case of electron poor aldehydes, indicating that the oxygenative pathway is active here. Lastly, it was discovered that aliphatic aldehydes also are competent reaction partners, giving products **149** and **150** in 70% and 64% yield.



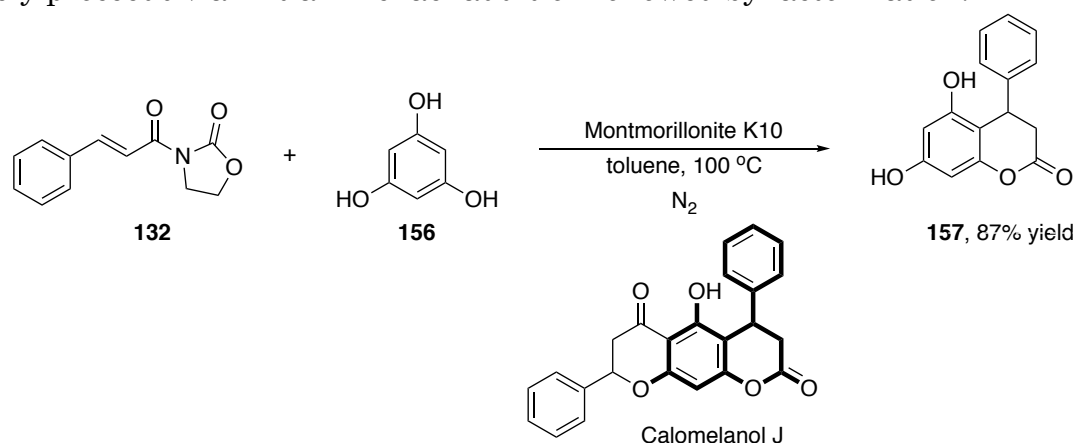
*Scheme 16. The scope of the aldehyde reaction partner in the NHC-catalyzed acylation. a As in table 4 entry 9. b As in table 4 entry 9 but using **75** instead of **73**. c 4 mol% of **73** used. d Gram-scale. e As in table 4 entry 9 but using **75** (5 mol%) instead of **73** and using 0.8 eq. DBU.*

Next, the use of other nucleophiles was investigated (Scheme 17). Chiral oxazolidinones with substituents at the 4-position requires heating to 60 °C and a slight increase of base (40 mol%) to be efficient. This is most likely an effect of increased sterical hindrance in proximity to the nitrogen. With that modification a range of acylated homochiral oxazolidinones could be obtained in moderate to good yields (**151–154**). If the substituent is placed in the 5-position, the reaction proceeds under standard conditions leaving the primary alkyl chloride in **155** untouched. It was found that the lactam 2-pyrrolidine also is a viable nucleophile, which enabled the total synthesis of two natural products, piperlotine F and G.^[116] Acyclic nucleophiles such as acetamide, *N*-methylacetamide, acetanilide, nicotinamide and methyl carbamate are unsuccessful in the reaction.



Scheme 17. The scope of the nucleophile in the NHC-catalyzed acylation. *a* As in table 4 entry 9, but with 40 mol% DBU and performed at 60 °C. *b* As in table 4 entry 9. *c* 73 (1 mol%), DBU (1.5 eq.), 2-pyrrolidine (1.5 eq.), performed at 60 °C. *d* 4 Å MS added (0.2 g).

Lastly, it was discovered that acylated oxazolidinone **132** could be transformed into the 2-chromanone core present in a family of natural products called the calomelanols. By reacting **132** with phloroglucinol using Montmorillonite K10 as a catalyst compound **157** was isolated in 87% yield (Scheme 18).^[117] The reaction likely proceeds via initial Michael addition followed by lactonization.



Scheme 18. Synthesis of compound **157**.

7. Summary of NHC-Catalyzed Aerobic Acylations

A system based on two different ETMs that allows for aerobic acylations have been developed. The use of two ETMs proved pivotal for obtaining a selective oxidation of the Breslow intermediate, as shown in exclusion experiments. Based on the redox potentials and elimination experiments, we suggest a mechanism in which the Breslow intermediate is directly oxidized by the Kharasch oxidant (**27**) yielding the acyl azolium and hydroquinone **83**, which in turn is re-oxidized by a FePc-O₂ specie (Scheme 11). Generally, the reaction is conducted at room temperature using low loadings of both the NHC and the ETMs, highlighting the efficiency of the devised protocol. The system proved sensitive towards both the nature and loading of NHC. An interesting effect was noticed where increased loading of the NHC gave significantly decreased yields. The effect can be attributed to a mismatch in the rates of the NHC-catalyzed cycle and the ETM cycle, leading to an accumulation of the Breslow intermediate which will eventually yield the carboxylic acid *via* the oxygenative pathway.

The system allows for both *O*- and *N*-acylations. In terms of the *O*-acylations the scope is broad, and a range of both primary and secondary alcohols can be successfully acylated. It was also possible to use our aerobic system for a dual functionalization of glycerol, yielding a range of glycerol carbonate esters in a telescoped manner. For the *N*-acylations, only electron poor and cyclic *N*-nucleophiles, such as oxazolidinones and lactams, have proven successful. The need of electron poor nucleophiles has been rationalized by a decreased tendency to form imines with the used aldehydes and with an increased acidity of the *N-H* proton.

With respect to the aldehyde reaction partner, the reactions exhibit a rather broad scope. However, some trends are evident. In general, cinnamaldehydes and other α,β -unsaturated aldehydes give higher yields than aromatic aldehydes which give higher yields than aliphatic aldehydes. Interestingly, the electrophilicity of aldehydes varies in an opposite trend, aliphatic > aromatic > α,β -unsaturated.^[69d] Nonetheless, with slight variations of the reaction protocols a wide range of aldehydes are applicable in the reactions.

8. Aerobic Oxidative NHC-Catalyzed Synthesis of Dihydropyranones (Paper I and IV)

8.1 Natural Occurrence of Dihydropyranones

Dihydropyranones form an intriguing class of compounds and can be found within several natural products and biologically active compounds (Figure 9). For instance, nepetalactone contains a 3,4-dihydropyranone moiety. Nepetalactone is the principal component responsible for the attractive effect of catnip (*Nepeta cataria*) towards cats.^[118] A 3,4-dihydropyranone motif can also be found in Neocucurbitacin A, isolated from the fruits of *Luffa operculata*, a traditional medicinal plant from South America. Neocucurbitacin A inhibits osteogenesis (bone formation) by reducing the amount of polyoma enhancer binding protein 2 α A (PEBPL α A) and osteoclastogenesis inhibitory factor (OCIF) mRNA.^[119] The 5,6-dihydropyranone moiety is also prevalent in nature, for instance in the antibiotic aspyrone and the cytotoxic goniodiol.^[120]

There exists a number of NHC-catalyzed protocols toward the synthesis of the 3,4-dihydropyranone scaffold.^[121] However, most of them suffer from poor atom economy due to the use of stoichiometric amounts of oxidants,^[71] internal leaving groups,^[122] sacrificial reagents^[62] or coupling reagents.^[123] We envisioned that our developed aerobic system could be used to access the dihydropyranone structure.

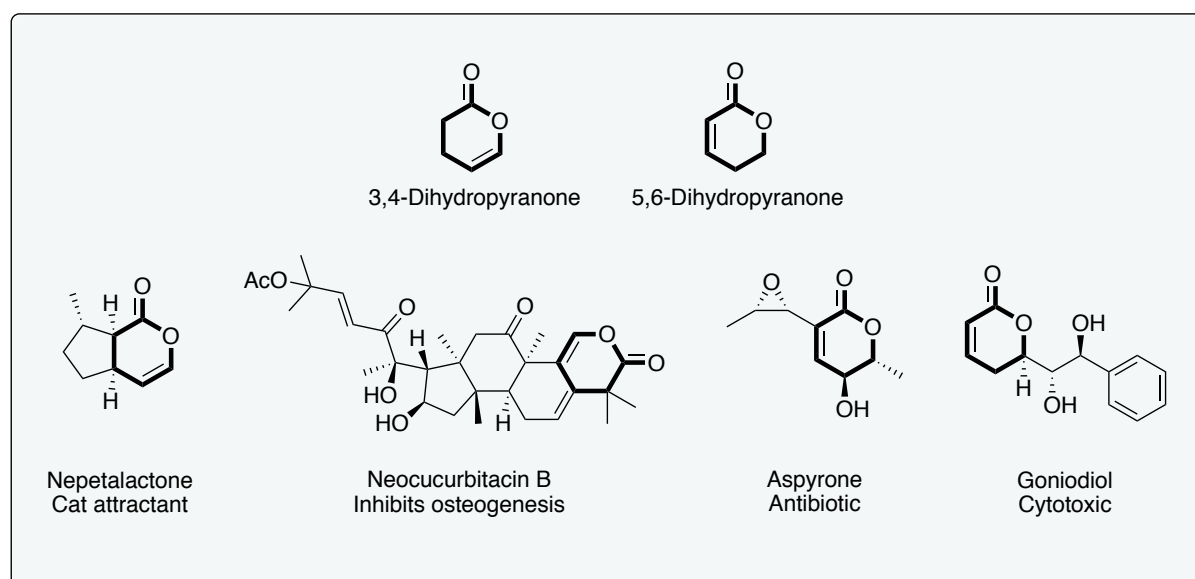
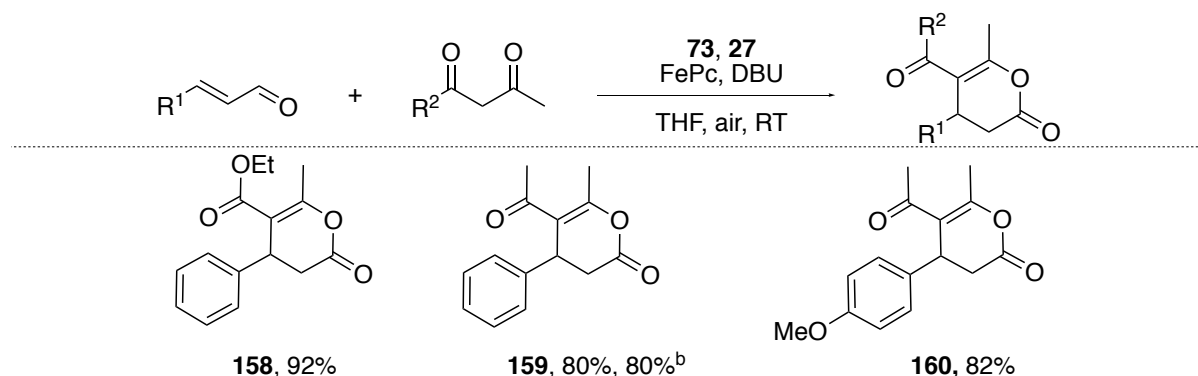


Figure 9. Natural products and biologically relevant compounds containing the dihydropyranone moiety.

8.1 Racemic synthesis of dihydropyranones (paper I)

Taking inspiration Studer's initial report, we quickly found that aerobic synthesis of dihydropyranones is indeed possible. Using catalyst **73** (10 mol%), **27** (5 mol%) and FePc (10 mol%) in THF with DBU (10 mol%) as base, dihydropyranones **158**–**160** could be isolated in good to excellent yields (Scheme 19). The reaction could also be scaled up to 1.4 g, delivering dihydropyranone **159** in 80% yield. The success of this reaction encouraged us to investigate if it is possible to obtain homochiral dihydropyranones using a similar strategy.



*Scheme 19. Aerobic NHC-catalyzed synthesis of dihydropyranones. a) Aldehyde (1 eq.), 1,3-dicarbonyl (1.5 eq.), DBU (0.1 eq.), **73** (0.05 eq.) FePc (0.1 eq.), **27** (0.05 eq.) and THF (0.1 M). Isolated yields after purification by silica gel chromatography. b) 1.4 Grams isolated.*

8.2 Development of an asymmetric synthesis of dihydropyranones (paper IV)

The reaction between cinnamaldehyde **53** and acetylacetone **56** yielding dihydropyranone (*S*)-**57** was chosen as model reaction (Table 5). Initial screening focused on identifying conditions that maintained high efficiency and selectivity when performed in open reaction vessels and using wet solvents, thus stoichiometric amounts of the Kharasch oxidant were used. This preliminary screen indicated that the use of NHC precatalyst **161** and lithium acetate in toluene was crucial for the development of a robust and effective reaction. Thereafter, attempts to enable aerobic oxidation were initiated by introducing different ETMs.

By using a combination of Kharasch oxidant and Co(II) based ETM **162**, dihydropyranone **57** could be isolated in excellent enantiomeric excess (ee), albeit in poor yield (entry 1). Replacing the Kharasch oxidant with quinone **134** resulted in increased yield. Changing to FePc and Kharasch oxidant as the ETM couple resulted in an increased yield and reduced reaction time (entry 4). Running the reaction at higher temperature (40 °C) additionally reduced the reaction time with maintained selectivity (entry 5).

In an attempt to further increase the yield, the reaction was conducted under an atmosphere of oxygen, but, surprisingly, this resulted in no product formation at all (entry 6). It was hypothesized that a catalytically inactive dimeric μ -oxo species, $[\text{FePc}]_2\text{O}$, was formed under the oxygen rich conditions.^[124] This prompted us to

further probe the stability of the ETM couple. Exclusion of either FePc, **27** or both resulted in very low yield (entry 7–9) and performing the reaction under an atmosphere of nitrogen delivered the dihydropyranone in only 17% yield (entry 10). Monitoring the reaction *via* gas chromatography mass spectrometry, GC-MS, showed that **27** is completely converted into its reduced form **83** after 3h. However, upon addition of one additional portion of FePc **83** is quantitatively re-oxidized to **27**. Together these results corroborate that deactivation of FePc is the major inactivation pathway. By adding FePc sequentially, inactivation was circumvented and dihydropyranone **57** was obtained in 79% yield and 94% ee (entry 11).

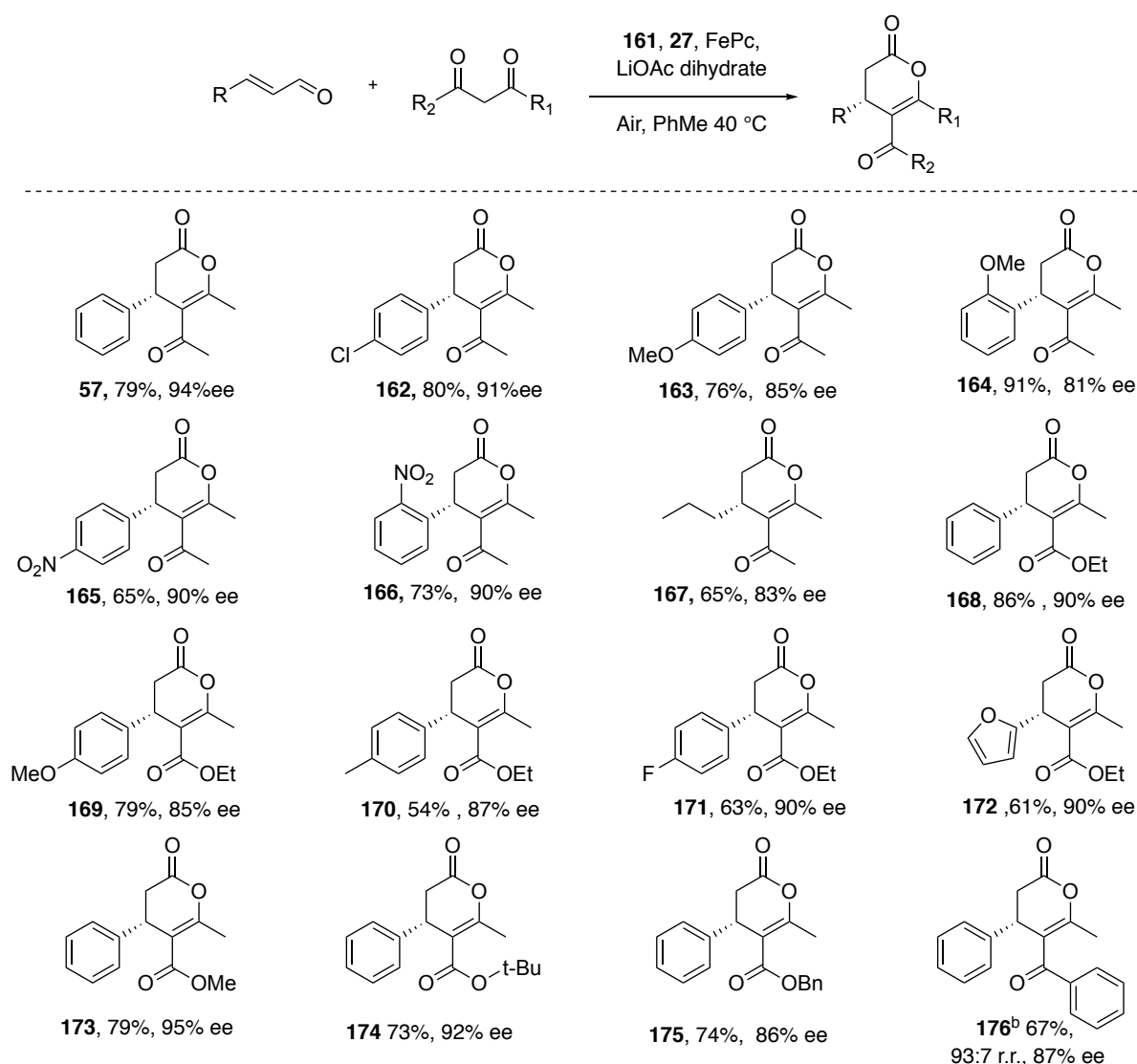
Table 5. Screening of reaction conditions for the asymmetric synthesis of dihydropyranones.

	53	56				
Entry ^a	Temp (°C)	Time (h)	ETM' (eq.)	ETM (eq.)	Yield (%)	ee (%)
1	r.t	46	162 (0.02)	27 (0.1)	29	94
2	r.t	48	162 (0.02)	134 (0.1)	58	ND
3	r.t	72	FePc (0.02)	134 (0.1)	62	95
4	r.t	48	FePc (0.02)	27 (0.1)	62	95
5	40	22	FePc (0.02)	27 (0.1)	69	95
6 ^b	r.t	48	FePc (0.02)	27 (0.1)	0	-
7 ^c	r.t	48	FePc (0.02)	-	6%	ND
8 ^c	r.t	48	-	27 (0.1)	7%	ND
9 ^c	r.t	48	-	-	0	-
10 ^d	r.t	48	FePc (0.02)	27 (0.1)	17	ND
11^e	40	25	FePc (0.06)	27 (0.2)	79	94

134	162	FePc

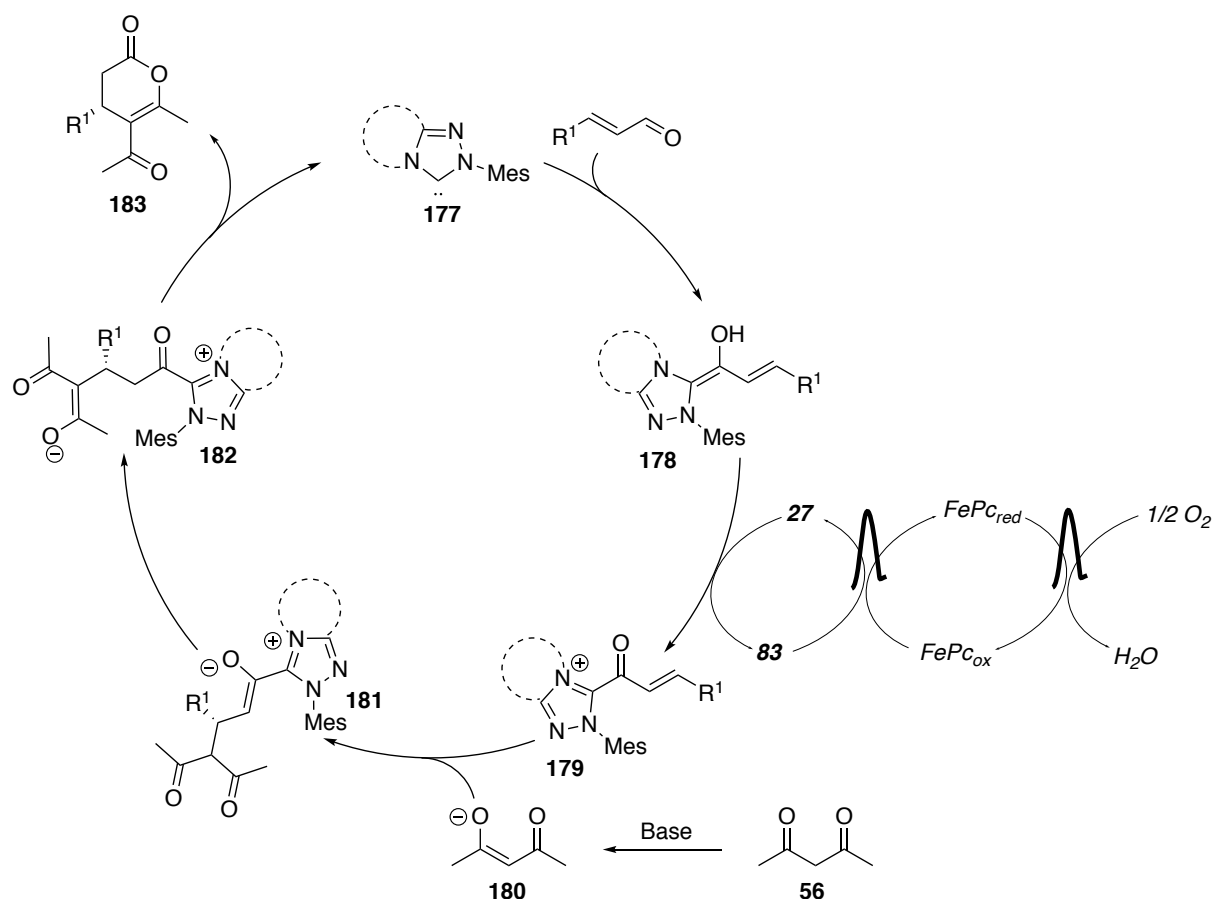
a) The reactions were performed in open reaction vessels at the indicated temperature (see Table) in toluene with cinnamaldehyde **53** (1 eq.), acetylacetone **56** (3 eq.), **161** (0.1 eq.), LiOAc*2H₂O (0.65 eq.) ETM (See Table), ETM' (See Table). b) The reaction was conducted in an atmosphere of pure O₂. c) Yield was determined with NMR against internal standard. d) Reaction conducted under an atmosphere of nitrogen. e) Sequential addition of FePc (3*2 mol%). ND= not determined

With an efficient protocol finalized, the scope of the transformation was examined (Scheme 20). With acetylacetone as the nucleophile several different dihydropyranones could be isolated in good yields and good to excellent ee (**162–167**). For instance, 4-chlorocinnamaldehyde and 2-nitrocinnamaldehyde delivered corresponding dihydropyranones **162** and **165** in 80% yield, 91% ee and 73% yield, 90% ee respectively. Aliphatic enals is also reasonably well tolerated in the reaction and **167** was isolated in 65% yield and 83% ee. 1,3-Ketoesters also proved viable reaction partners and several ester-substituted dihydropyranones was obtained in good yield with full regioselectivity and good to excellent ee (**168–175**). For instance, cinnamaldehyde and methyl acetoacetate yielded dihydropyranone **173** in 79% yield and 95% ee. Asymmetric 1,3-diketones could also be used and compound **176** was obtained in 67% yield, 93:7 r.r. and 87% ee.



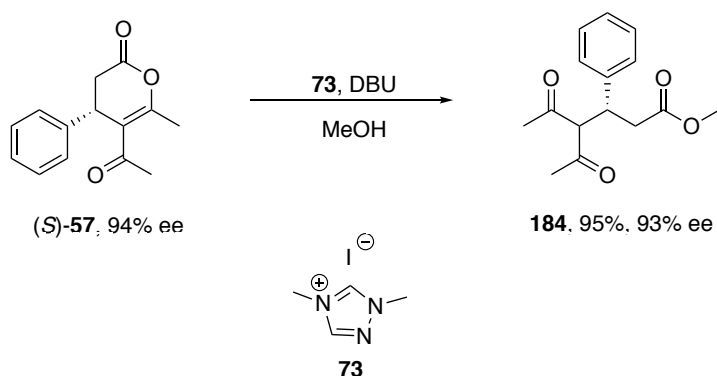
*Scheme 20. The scope of the asymmetric aerobic NHC-catalyzed synthesis of dihydropyranones. a) The reactions were performed in open reaction vessels at 40 °C in toluene (1 mL) with catalyst **161** (0.1 eq.), α,β -unsaturated aldehyde (1 eq.), 1,3-dicarbonyl (3 eq.), LiOAc \cdot 2H₂O (1 eq.) FePc (0.06 eq.) and **27** (0.2 eq.). b) Isolated yields after purification with silica gel chromatography. c) major isomer combined yield r.r. determined by ¹H NMR of the crude reaction mixture.*

The proposed catalytic cycle begins with deprotonation of triazolium salt **161** to form free carbene **177**, which adds in a 1,2-fashion to the enal, forming homoenolate **178** (Scheme 21). The homoenolate is then oxidized by the system of ETMs with oxygen as the terminal oxidant, forming α,β -unsaturated acyl azolium intermediate **179**. Acetylacetone **56** is deprotonated forming enolate **180** that upon asymmetric 1,4-addition to **179** gives chiral enolate **181**. The more stable enolate **182** is formed through proton transfer, which then cyclizes *via* an internal oxa-1,2-addition of the enolate to the acyl azolium, delivering dihydropyranone **183** and regenerating carbene **177**.



Scheme 21. The proposed mechanism for the aerobic NHC-catalyzed synthesis of dihydropyranones.

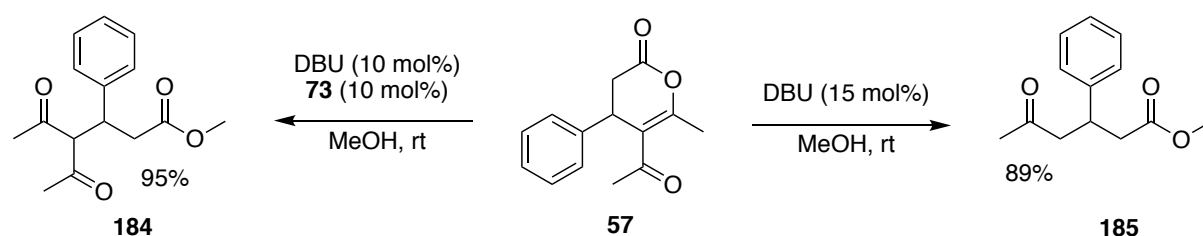
Having identified an aerobic system for the asymmetric synthesis of dihydropyranones, further manipulation of the obtained products was investigated. It was found that treating (*S*)-**57** with equimolar amounts of NHC precursor **73** and DBU in methanol yielded acyclic methyl ester **184** in excellent yield and with minimal loss of optical purity (Scheme 22). The obtained product represents the formal asymmetric Michael addition of acetylacetone to methyl cinnamate, a transformation that is nontrivial due to the low electrophilicity of α,β -unsaturated esters.^[125]



Scheme 22. NHC/base-catalyzed formation of acyclic ester **184** from dihydropyranone **57**. **57** (1 eq.), DBU (0.1 eq.), **73** (0.1 eq.) and MeOH (0.1M). Isolated yields after purification by silica gel chromatography.

9. Formal Addition of Acetone to Unactivated Michael Acceptors *via* Ring-opening and Retro-Claisen Fragmentation of Dihydropyranones (Paper V)

While investigating the ring-opening of dihydropyranones an unexpected side product was identified if NHC precatalyst **73** was omitted. When the loading of DBU was increased to 15 mol%, ketoester **184** was isolated in 89% yield (Scheme 23). A stoichiometric amount of methyl acetate was also formed in the reaction, suggesting that the cleavage of the 1,3-diketone proceeded *via* a retro-Claisen fragmentation.^[126] The isolation of **185** warranted further investigation, since it represents the formal Michael addition of acetone to methyl cinnamate, a reaction that has proven very difficult to achieve. The problem with such a reaction is two-fold; firstly α,β -unsaturated esters suffers from low electrophilicity,^[125, 127] secondly acetone suffers from poor selectivity and the need of activated Michael acceptors such as nitroolefins to react.^[128]

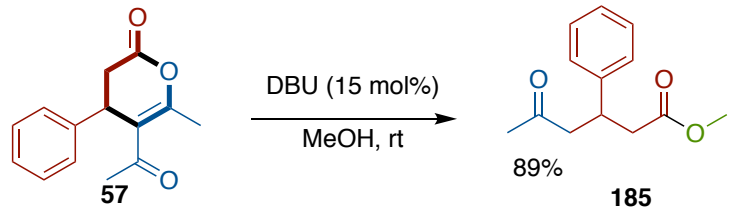
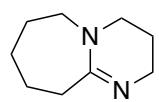
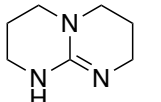
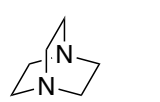
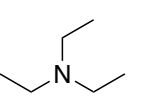


Scheme 23. Discovery of a synthesis of **185**.

Attempts to optimize the ring-opening towards ketoester **185** then commenced. Both the structurally related base TBD and potassium hydroxide were able to mediate the reaction, albeit in slightly lower yield than DBU (Table 6, entry 2, 3). Neither DABCO, triethylamine nor potassium carbonate could promote the retro-Claisen fragmentation, and product **184** was obtained as the sole product (Table 6, entry 4–6).

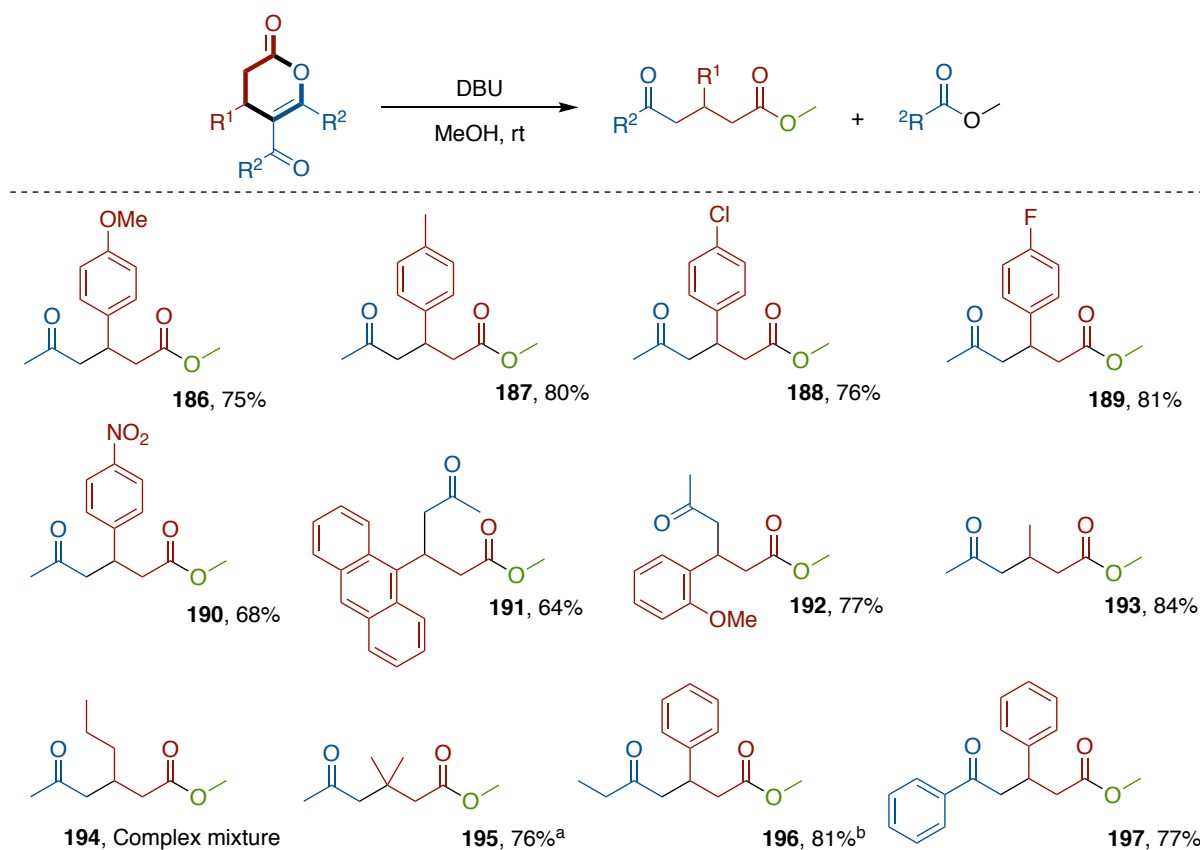
Any attempts to replace methanol as the reaction solvent resulted in drastically reduced yield. Performing the reaction in either acetonitrile or toluene together with five equivalents of methanol resulted in selective formation of **184** over **185**. The retro-Claisen fragmentation was significantly impeded in other nucleophilic protic solvents such as water, isopropanol and ethanol, and the diketoeester was obtained as the main product. For water and isopropanol no **185** was formed, but in ethanol a small amount of the retro-Claisen product could be identified.

Table 6. Optimization of the ring-opening and retro-Claisen fragmentation of dihydropyranones.

			
<div style="display: flex; justify-content: space-around; align-items: center;"> <div style="text-align: center;">  DBU </div> <div style="text-align: center;">  TBD </div> <div style="text-align: center;">  DABCO </div> <div style="text-align: center;">  Et₃N </div> </div>			
Entry	Deviation from standard conditions	Yield (185 , %) ^a	
1.	None	89 ^b	
2.	TBD instead of DBU	83	
3.	KOH instead of DBU	84	
4.	DABCO instead of DBU	0	
5.	Et ₃ N instead of DBU	0	
6.	K ₂ CO ₃ instead of DBU	0	
7. ^c	MeCN instead of MeOH	0	
8. ^c	PhMe instead of MeOH	0	
9. ^d	Water instead of MeOH	0	
10. ^d	IPA instead of MeOH	0	
11. ^d	EtOH instead of MeOH	~10%	

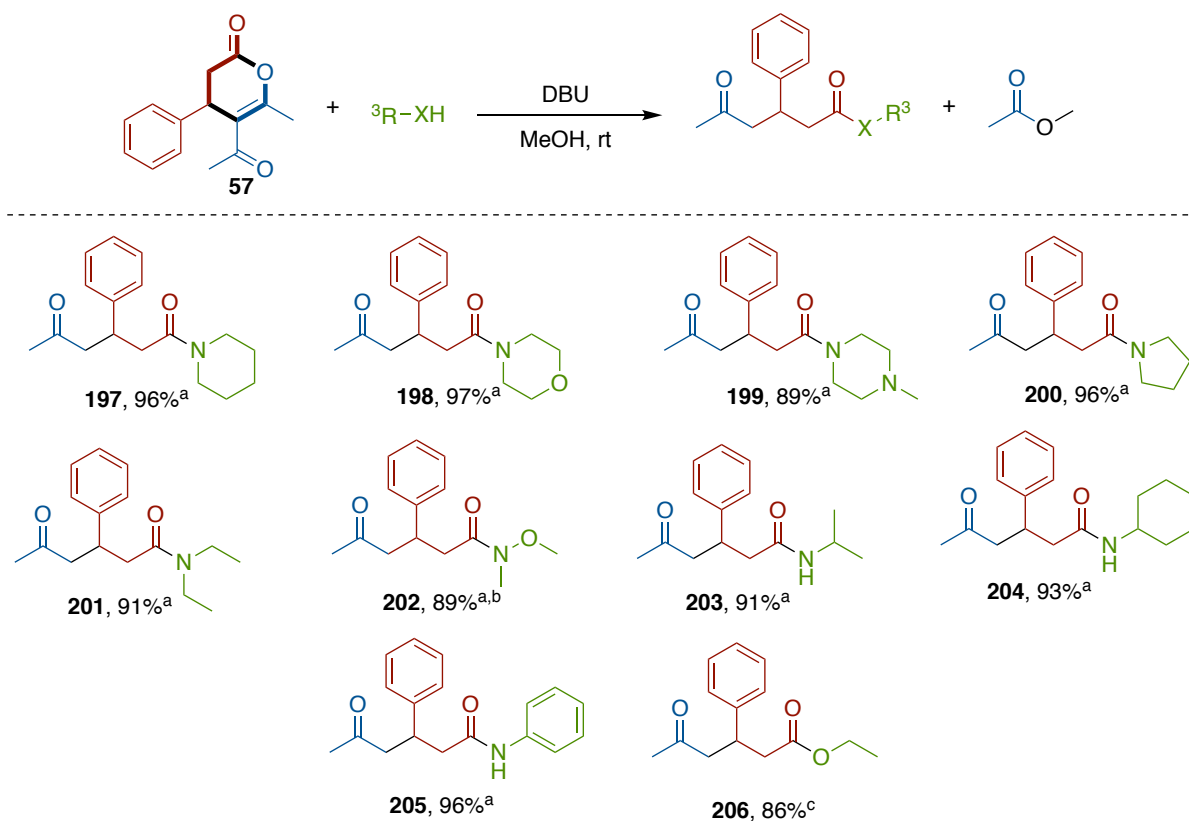
^a **57** (0.12 mmol), base (0.15 eq.) solvent (0.4 mL), stirred at ambient temperature for 24h. Yield determined by ¹H NMR using 1,2,4,5-tetramethylbenzene as internal standard. ^bIsolated yield. ^c5 equivalents of MeOH added. ^dBased on the corresponding carboxylic acid, isopropyl ester or ethyl ester as the product respectively.

After the screening of reaction conditions, the scope with respect to the dihydropyranone was investigated. A wide range of different aryl substituted dihydropyranones reacted well under the developed reaction conditions (scheme 24, **186–192**), for instance fluorinated and anthracenyl-substituted ketoesters **189** and **191** was obtained in 81% and 64% yield respectively. Dihydropyranones with alkyl substituents in the 5-position is also viable substrates for the transformation and methylated substituted product **193** was isolated in 84% yield. The reaction proved sensitive towards the size of alkyl substituents in the 5-position. Longer chains impeded the retro-Claisen fragmentation, for instance a propyl substituted dihydropyranone yielded product **194** together with the diketo-ester as an inseparable mixture. It is possible to use dihydropyranones with a quaternary center at the 5-position in the reaction, albeit with an increased loading of DBU (25 mol%). With that slight modification of the reaction protocol, dimethylated 5-oxohexanoate **195** was obtained 76% yield. Compound **195** represents the formal total synthesis of plant hormone abscisic acid.^[129] Increasing the size of the alkyl substituent in the 4-position resulted in incomplete conversion, however, by running the reaction at 70 °C 5-oxoheptanoate **196** was obtained in 81% yield. Dihydropyranones with aromatic substituents in the 4-position reacts well under the standard reaction conditions, and product **197** was isolated in 77% yield.



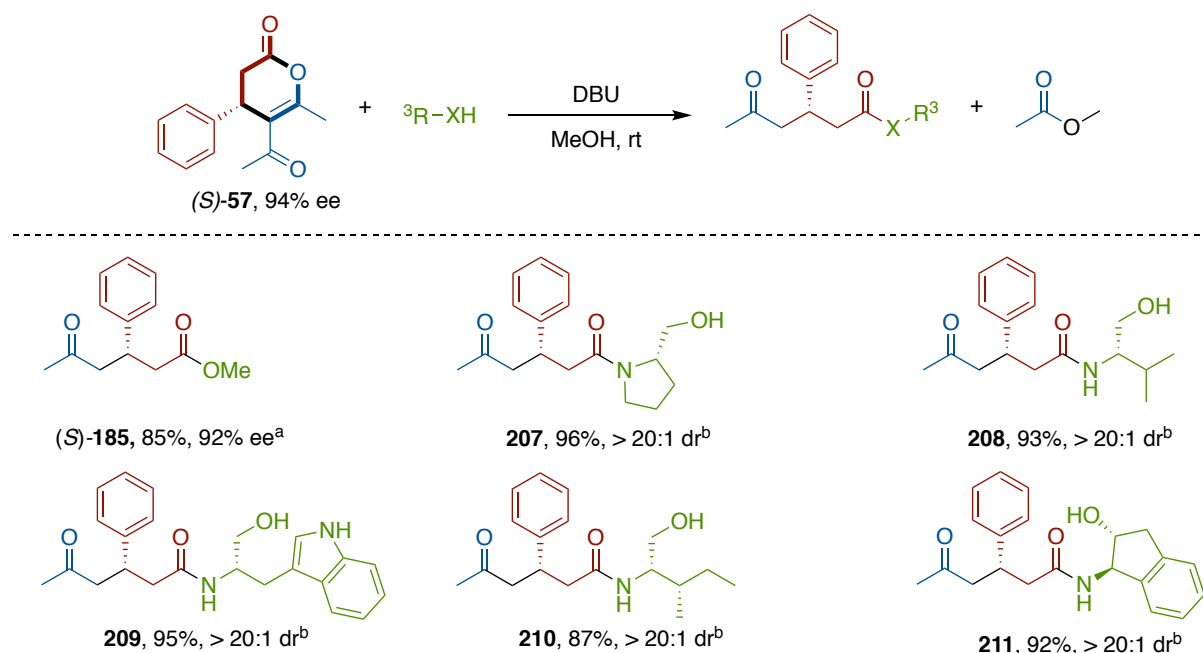
Scheme 24. The scope of the ring-opening and retro-Claisen fragmentation in terms of the dihydropyranone. As in table 6 entry 1, isolated yield. ^a As in table 6 entry 1 but using 25 mol% DBU. ^b As in table 6 entry 1 but performed at 70 °C.

Thereafter, our attention turned to the possibility of performing the initial-ring-opening of the dihydropyranone with other nucleophiles than methanol. As it turns out, it is possible to obtain a wide range of 5-oxohexanamides by reacting the dihydropyranone with an amine, followed by addition of methanol and DBU to initiate the retro-Claisen fragmentation (Scheme 25). Cyclic amines are well suited for the reaction and piperidine, morpholine, *N*-methyl-piperazine and pyrrolidine gave the corresponding 5-oxohexanamides in 89–97% yield (**197–200**). It was also possible to use *N,O*-dimethylamine as the nucleophile in the reaction, yielding Weinreb amine **202** in 89% yield. Primary amines are also viable nucleophiles in the reaction (**203–205**). For instance, cyclohexylamine and aniline gave products **204** and **205** in 93% and 96% yield, respectively. While investigating these amidation reactions, it was discovered that large excess of amine impeded the retro-Claisen fragmentation, possibly via formation of the enaminone from the corresponding diketo-amide. Lastly, it was also discovered that it is possible to obtain the ethyl ester by performing the reaction in ethanol at 70 °C, doing so gave compound **206** in 86% yield. Unfortunately, it is not possible to obtain the corresponding isopropyl- or *tert*-butyl-ester in a similar manner.



Scheme 25. The scope of the ring-opening and retro-Claisen fragmentation in terms of the nucleophile. a 57 (1 eq.) nucleophile (1.1–2.0 eq.), then DBU (15 mol%) and MeOH (0.3 M). Isolated yield. For solid and deactivated nucleophiles DCM (0.6 M) was added in the first step. b The corresponding HCl-salt was used as the nucleophile and was neutralized in situ with DBU. c As in table 6 entry 1 but using ethanol as solvent and running the reaction at 70 °C.

We next sought to investigate if it would be possible to obtain these interesting compounds in an enantioenriched manner. By using our previously developed aerobic method, dihydropyranone (*S*)-**57** could be reliably obtain in gram-scale and in 94% ee. By reacting (*S*)-**57** under the standard condition (*S*)-**185** could be isolated in 85% yield and 92% ee, with only minimal erosion of enantiopurity. (*S*)-**57** reacted with several homochiral aminoalcohols to yield homochiral 5-oxo-hexanamides as a sole diastereomer and with excellent chemoselectivity (Scheme 26, **207–211**). For instance, (*S*)-tryptophanol gave compound **209** in 95% yield, without any trace of competing acylation of the primary alcohol or the indole-nitrogen.

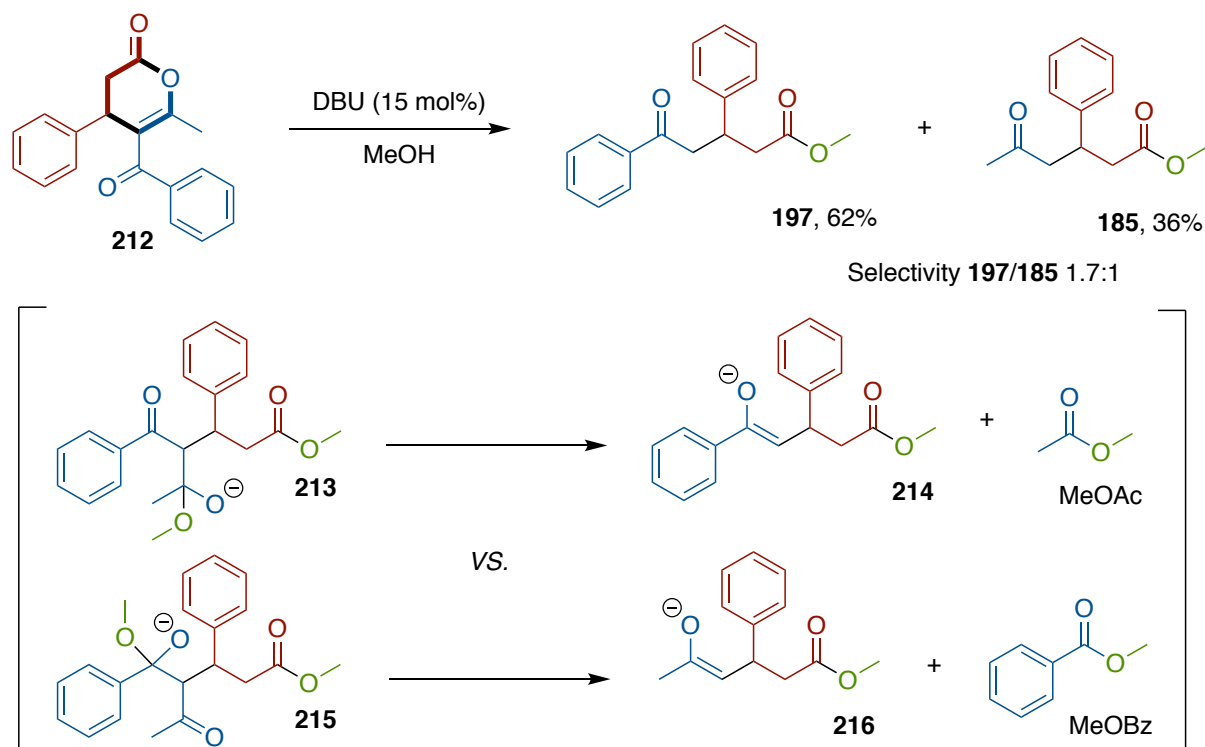


Scheme 26. Synthesis of enantioenriched products. *a* As in table 6 entry 1, isolated yield. *b* (S)-57 (1 eq.) nucleophile (1.1–1.4 eq.) and DCM (0.6 M), then DBU (15 mol%) and MeOH (0.3 M).

9.2 Mechanistic inquiries

Under the developed conditions, ring-opening of the dihydropyranone yields a 1,3-diketone that will react in a retro-Claisen reaction to yield one ketone and one ester. If the produced 1,3-diketone is symmetric, only one set of products can form. However, if the diketone is asymmetric two different pairs of products may form. So far, we have only used dihydropyranones that yield symmetric diketones when ring-opened in the transformation (Scheme 24–26). Use of a dihydropyranone that yields an asymmetric diketone when ring-opened, such as **212** (Scheme 27), might offer some insight into the mechanism of the retro-Claisen fragmentation. The two reaction paths available for **212** is either via anionic hemiacetal **213** to yield enolate **214**, which later gives product **197**, and methyl acetate or via hemiacetal **215** to give enolate **216**, which yields product **185**, and methyl benzoate. When **212** was subjected to the standard reaction conditions, product **197** and **185** was formed in a 1.7:1 ratio.

The low selectivity may seem surprising considering that aromatic ketones generally are more acidic than aliphatic ones. Hence, enolate **214** should be more stable than enolate **216**. One way to approximate their relative stability is to compare the pK_a-values (in DMSO) of two pairs of structurally related ketones: acetone *vs.* acetophenone ($\Delta pK_a=1.8$) and pentan-3-one *vs.* propiophenone ($\Delta pK_a=2.7$). The comparison suggests that **214** should be somewhere in the range of 60 to 500 ($10^{\Delta pK_a}$) times more stable than **216**. The latter value, 500 times more stable, is probably a better estimate since **216** and **214** are structurally more similar pentan-3-one and propiophenone than they are acetone and acetophenone. No matter which value one uses, the selectivity estimated by this approach is considerably bigger than the observed selectivity of 1.7:1. Hence, it seems like the breakage of the C–C bond is not under thermodynamic control.

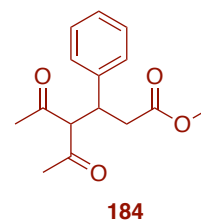
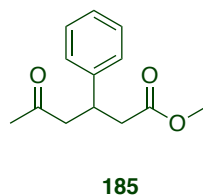
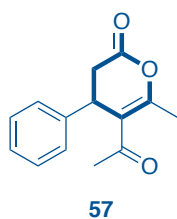


Scheme 27. Reactivity and observed selectivity of asymmetric dihydropyranone **212** under the developed reaction conditions.

Another possible explanation would be that the selectivity is determined by the rate of formation of the anionic hemiacetal, either **213** or **215**. We used the Taft steric parameter to estimate the effect of the methyl/phenyl substituent in the addition of methoxide to the respective ketone to yield either **213** or **215**.^[130] The Taft steric parameter, E_s , is derived from the rate of hydrolysis of substituted esters, and is defined according to equation 1, where k_s is the rate of the acid catalyzed hydrolysis of the ester of interest and k_{Me} the rate of the methyl substituted ester, which is used as a reference. Addition of water to the protonated ester is rate determining in these reactions. Hence, the Taft steric parameter should be a valid descriptor for the difference in rate for the formation of **213** and **215**. The Taft steric parameter for a phenyl group is -2.55 , which means that the formation of **213** should be roughly 350 times faster than formation of **215** ($10^{2.55}$). Clearly, the rate of formation of the anionic hemiacetal is not the determining factor behind the observed selectivity.

$$E_s = \log \frac{k_s}{k_{Me}} \quad (1)$$

To gain further insight into the reaction mechanism the concentration of the reaction was monitored by GC-FID. The concentration profile during the transformation of dihydropyranone **57** to product **185**, using 0.3 eq. DBU to achieve greater conversion, can be seen in figure 10. The initial ring-opening of **57** to yield **184** is very rapid and completes within minutes at room temperature. The transformation of **184** into **185** however, is much slower.



Concentration profile

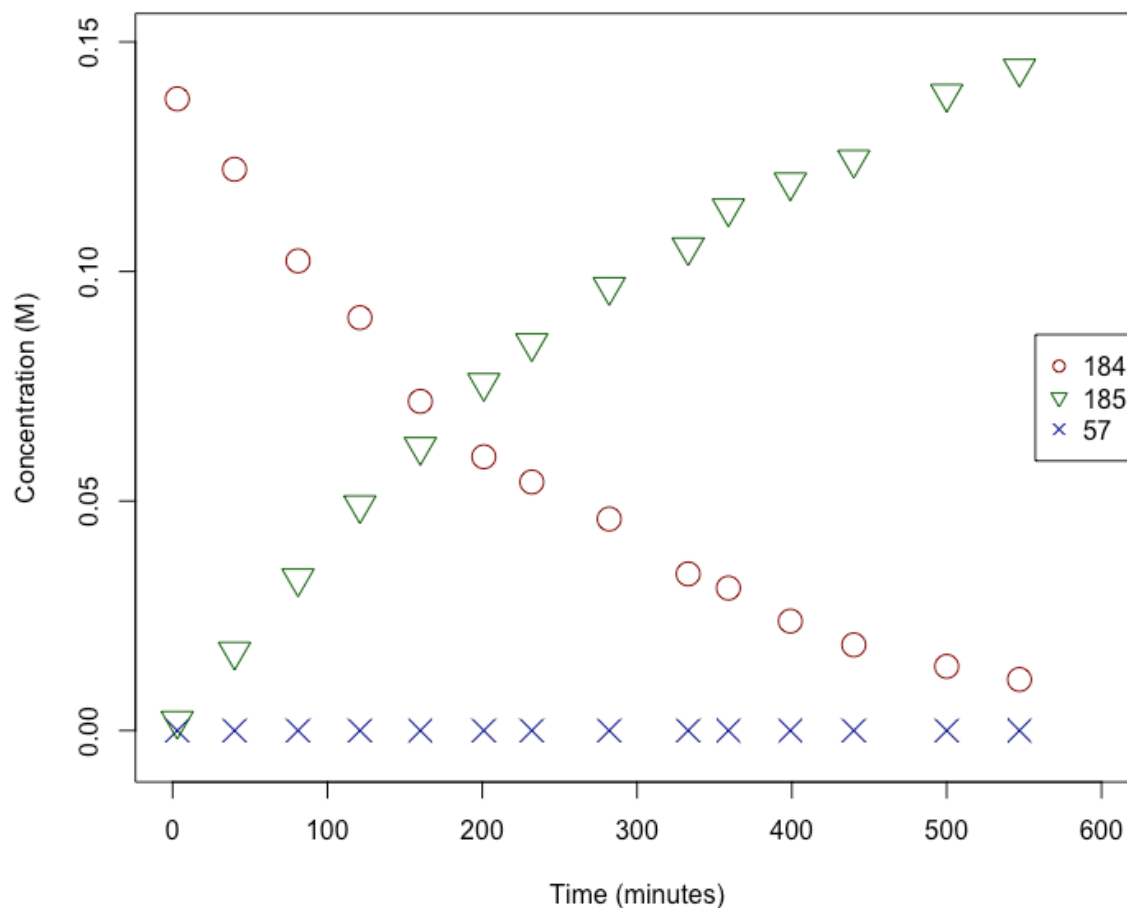


Figure 10. The concentration profile of compounds **57**, **184** and **185** during the reaction of **57** to yield **185**. An increased loading of DBU (0.3 eq.) was used in the reaction to achieve greater conversion during the experiment.

Later, the reaction of preformed **184** to **185** was performed using either 0.15, 0.30 or 0.45 eq. of DBU and the consumption of **184** was monitored over time. Plotting $\ln[\mathbf{184}]$ vs. time gave a straight line for all three loadings of DBU, which shows that the reaction is of the first order with respect to **184** (Figure 11, left graph). The observed overall first order kinetics is not surprising, considering that the reaction is performed under pseudo-first order conditions: $[\mathbf{184}] \ll [\text{MeOH}]$, and the concentration of DBU is constant since it is not consumed in the reaction.

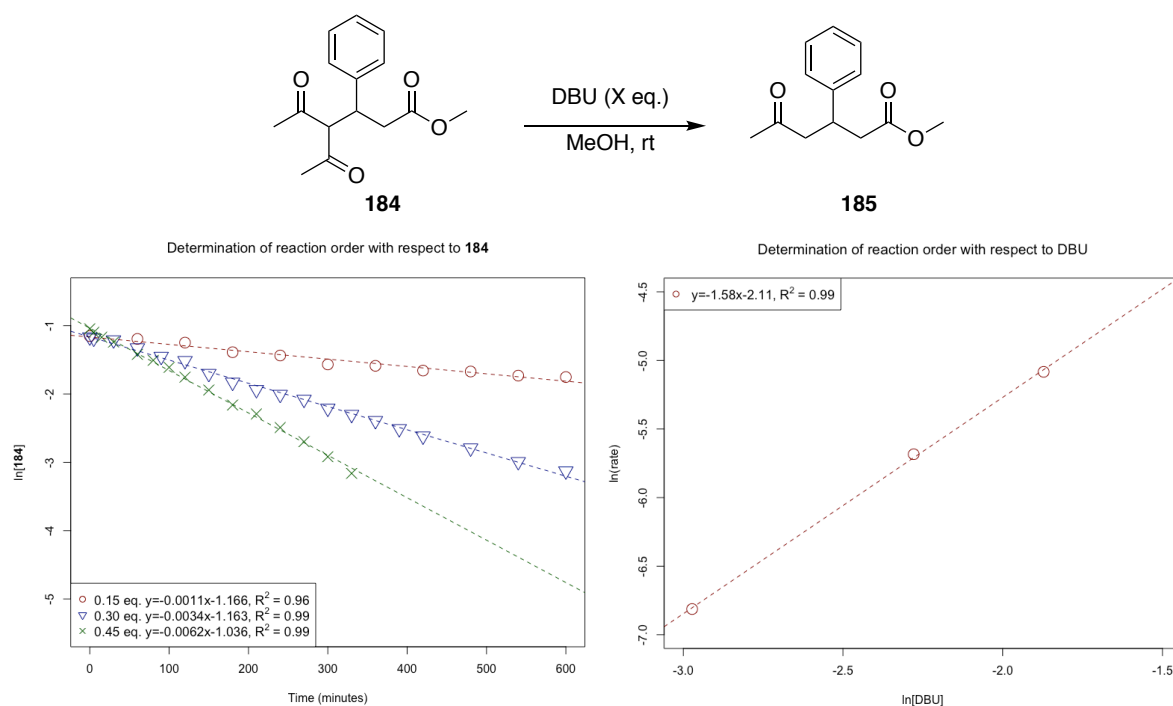


Figure 11. Determination of reaction order in **184** and DBU. Left graph: $\ln[184]$ vs. time, right graph: $\ln(\text{rate})$ vs. $\ln[\text{DBU}]$.

The overall first order kinetics enables one to easily determine the observed rate constant (k_{obs}) for the different reactions, it is simply the slope of the lines in the plot of $\ln[184]$ vs. time. To determine the reaction order in DBU, one plots $\ln(k_{\text{obs}})$ vs. $\ln[\text{DBU}]$, which should yield a straight line where the slope is equal to the reaction order in DBU.^[131] When we applied this method to our system, a reaction order of 1.6 was obtained (Figure 11, right graph).

We then repeated the experiment with five different concentrations of DBU (0.15, 0.30, 0.45, 0.60 and 0.75 eq.). Plotting $\ln[184]$ vs. time gave straight lines once again (Figure 12, left graph). The graph of $\ln(k_{\text{obs}})$ vs. $\ln[\text{DBU}]$, gave a reaction order of 1.2 (Figure 12, right graph, red dashed line) with a lower R^2 -value (0.93) compared to the previous experiment ($R^2=0.99$). However, if one considers only the first three points (0.15, 0.30 and 0.45 eq.) a reaction order of 1.6 ($R^2=0.99$, Figure 12, right graph, green solid line) is obtained. This value agrees well with the result obtained in the previous experiment (1.58 vs. 1.56). It seems that the reaction order of DBU varies with the concentration of DBU. Varying reaction order in catalyst depending on catalyst concentration has been observed earlier, for instance in palladium catalyzed Heck-couplings.^[132] Nonetheless, it seems that the reaction order for DBU is higher than 1 for the studied reaction (for a further discussion, vide infra)

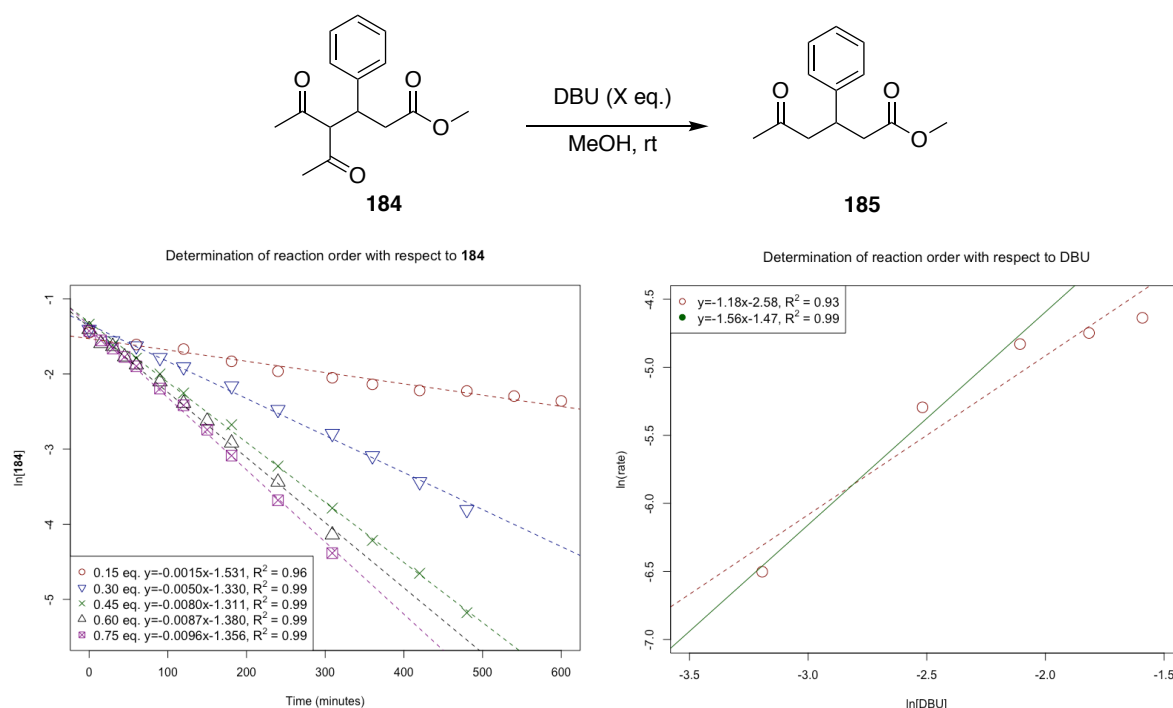
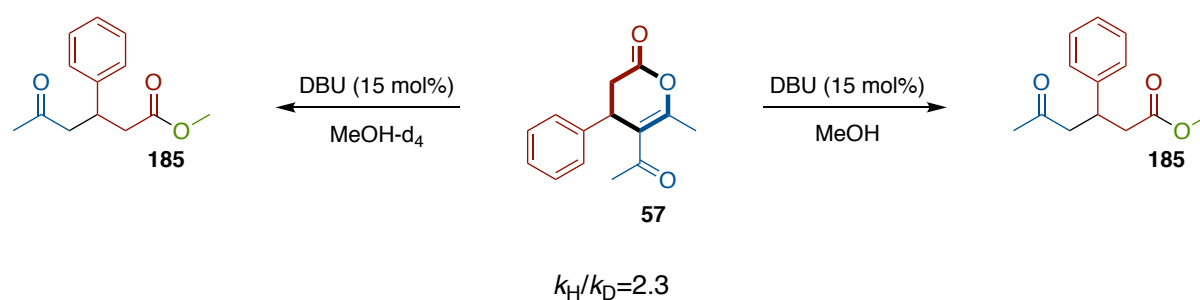


Figure 12. Determination of reaction order in **184** (left graph) and DBU (right graph) using a larger number of different loadings of DBU. Left graph: $\ln[184]$ vs. time, right graph: $\ln(\text{rate})$ vs. $\ln[\text{DBU}]$. The red dashed line in the right graph is based on all five points while the green solid line is based on the three first points.

A normal kinetic isotope effect (KIE, k_H/k_D) of 2.3 was measured by running the reaction in either MeOH or MeOH- d_4 (duplicates, Scheme 28). A KIE of that size suggests a primary effect, meaning that a bond to hydrogen is directly involved in the rate determining step, since the measured value is too large to be the effect of several secondary KIEs.^[133]



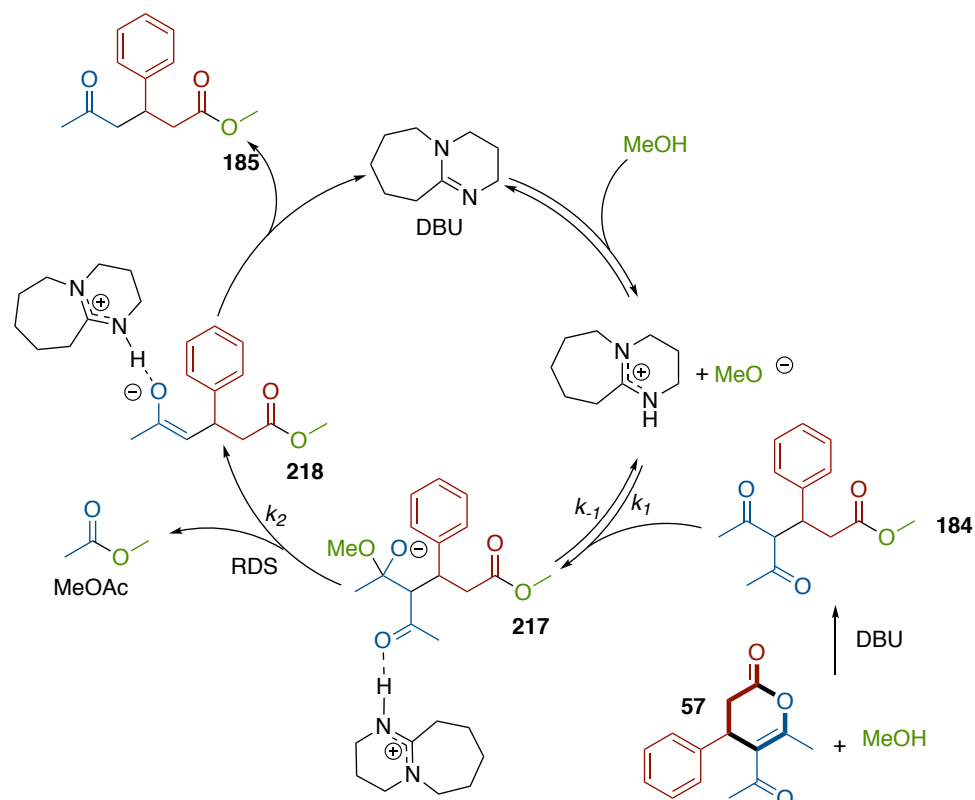
Scheme 28. Determination of the kinetic isotope effect in the transformation of **57** to yield **185**.

We then tried to combine the results from our kinetic experiments to a coherent mechanistic proposal. It is generally accepted that the rate determining step (RDS) for base catalyzed retro-Claisen reactions is the breakage of the C–C bond.^[134] To account for the observed rate law, we imagined that the protonated DBU might coordinate to the anionic hemiacetal during the C–C bond breakage. Protonated amines are known to be potent hydrogen bond donors, and are in fact, much stronger than aliphatic alcohols such as methanol.^[135]

We have envisioned two different mechanism, called path A and path B, that would account for the observed rate law and the observed KIE (Scheme 29). Both reactions begin the same, DBU catalyzes the nucleophilic ring-opening of dihydropyranone **57** to yield **184**. This step is very rapid and completes within minutes at ambient temperature. The mechanism for the retro-Claisen reaction begins with that DBU deprotonates methanol, yielding DBUH⁺ and methoxide. The methoxide adds to the ketone of **184** in a nucleophilic 1,2-addition to yield an anionic hemiacetal, and here is where the two proposed mechanism diverge. In path A, anionic hemiacetal **217** is formed where DBUH⁺ is coordinated to the ketone. In the rate determining step, **217** fragments to yield hydrogen bonded enolate **218** and methyl acetate. Subsequent proton transfer between DBUH⁺ and the enolate yields product **185** and regenerates DBU.

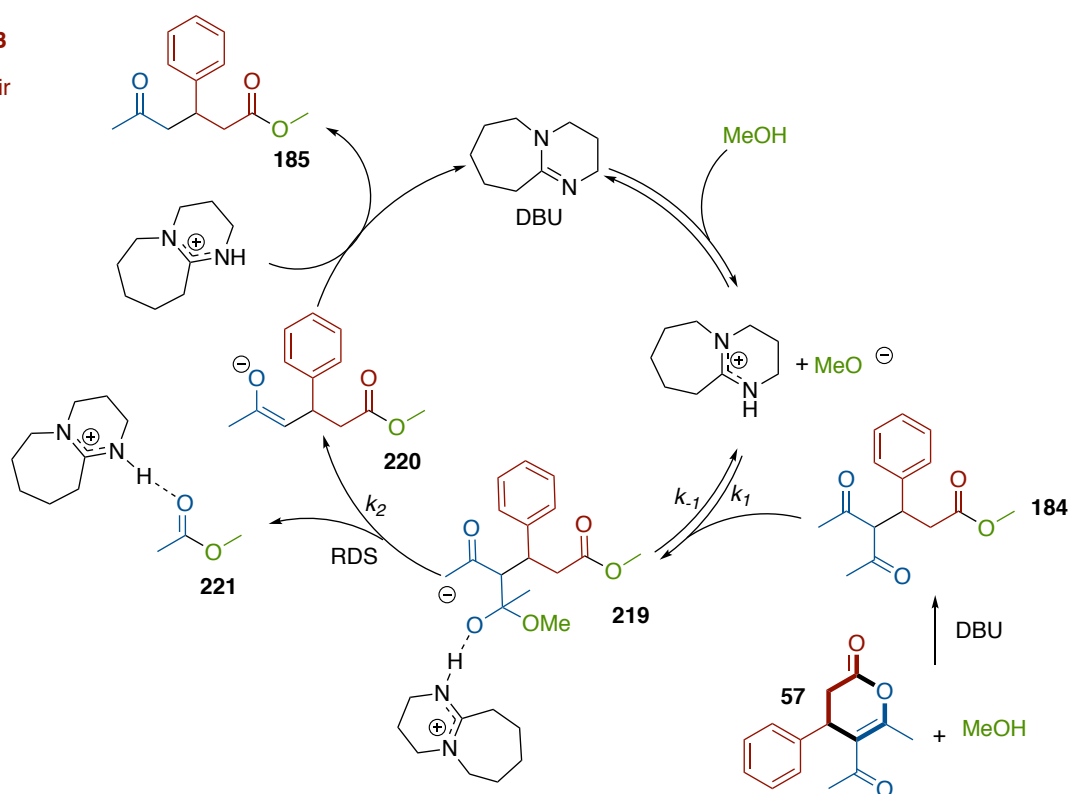
In path B, anionic hemiacetal **219** is instead formed with a hydrogen bond between the anionic hemiacetal and DBUH⁺. In the rate determining C–C bond scission, **219** is transformed into non-coordinated enolate **220** and complex **221** in which DBUH⁺ coordinates to methyl acetate via hydrogen bonding. Complex **41** then dissociates, and proton transfer between enolate **221** and DBUH⁺ regenerates DBU and yield product **185**.

Hydrogen bond



Path B

lon pair



Scheme 29. The two proposed mechanism for the ring-opening and retro-Claisen fragmentation of dihydropyranones. Both options are consistent with the observed rate law.

Both path A and B results in the same rate expression, hence only the derivation of one rate expression is showed (here for path A). Assuming steady state kinetics and that the reaction of **217**→**218** is the RDS, the consumption of **184** is described by equation 2. The concentration of **217** varies with time in accordance to equation 3. The steady state approximation means that the concentration of **217** is constant during the reaction,^[12] which gives equation 4 that can be rearranged to equation 5. Combining equation 2 with equation 5 gives equation 6. Hence, the reaction order in DBU will depend upon how $[MeO^-] \times [DBUH^+]$ varies with the amount of DBU added (here called $[DBU]_0$).

Let's consider two extremes. If DBU is a significantly stronger base than methoxide, DBU will be fully protonated in the solution (eq. 7). Combining eq. 7 and equation 6 yields equation 8, which states that the reaction is of the second order with respect to $[DBU]_0$. If DBU instead is a significantly weaker base than methoxide, equation 9 is valid, where K_b is the base dissociation constant. Combining equation 9 with equation 6 yields equation 10, which states that the reaction is of the first order with respect to $[DBU]_0$. Hence, if DBU is of intermediate basicity compared to methoxide, a reaction order between one and 2 should be expected. The pK_a of DBU in methanol is unknown, but the pK_a of DBU in water has been estimated to 13.5.^[136]

$$-\frac{d[\mathbf{184}]}{dt} = k_2 \times [\mathbf{217}] \quad (2)$$

$$\frac{d[\mathbf{217}]}{dt} = k_1 \times [\mathbf{184}] \times [MeO^-] \times [DBUH^+] - (k_{-1} + k_2)[\mathbf{217}] \quad (3)$$

$$\frac{d[\mathbf{217}]}{dt} = 0 \rightarrow k_1 \times [\mathbf{184}] \times [MeO^-] \times [DBUH^+] = (k_{-1} + k_2)[\mathbf{217}] \quad (4)$$

$$[\mathbf{217}] = \frac{k_1}{(k_{-1} + k_2)} \times [\mathbf{184}] \times [MeO^-] \times [DBUH^+] \quad (5)$$

$$-\frac{d[\mathbf{184}]}{dt} = \frac{k_1 \times k_2}{(k_{-1} + k_2)} \times [\mathbf{184}] \times [MeO^-] \times [DBUH^+] \quad (6)$$

$$[DBU] \approx 0 \rightarrow [DBUH^+] \approx [MeO^-] \approx [DBU]_0 \quad (7)$$

$$-\frac{d[\mathbf{184}]}{dt} \approx \frac{k_1 \times k_2}{(k_{-1} + k_2)} \times [\mathbf{184}] \times [DBU]^2 \quad (8)$$

$$\begin{aligned} [DBUH^+] \approx 0 \rightarrow K_b &= \frac{[DBUH^+] \times [MeO^-]}{[DBU]} \approx \frac{[DBUH^+] \times [MeO^-]}{[DBU]_0} \\ &\rightarrow [DBU]_0 \times K_b \approx [MeO^-] \times [DBUH^+] \end{aligned} \quad (9)$$

$$-\frac{d[\mathbf{184}]}{dt} \approx \frac{k_1 \times k_2}{(k_{-1} + k_2)} \times [\mathbf{184}] \times [DBU]_0 \times K_b \quad (10)$$

9.3 Quantum Chemical investigation of the Reaction Mechanism

Both path A and path B are able to explain the observed rate law, the measured KIE and the sensitivity towards sterical encumbrance in terms of the alcohol partner and in the 4- and 5-position of the dihydropyranone (products **13–15** and **26**). To help differentiate between the two proposed mechanisms, we used density functional theory (DFT) calculations. The calculations were performed using the Gaussian 16 package, revision B.01.^[137] Geometry optimizations and frequency analyses were performed at the ω B97X-D/6-311+G(2d,p) level of theory, and final single point electronic energies were computed using the larger basis set 6-311++G(2df,2pd).^[138] Solvent effects were modeled using the Solvent Modeled based on Density (SMD) method.^[139] The dispersion-corrected and range-separated hybrid functional ω B97X-D has previously been used successfully together with Pople-style basis sets to model organocatalytic reactions where hydrogen bonding is important,^[140] as well as hydrogen bonding between amine superbases such as DBU.^[141]

Three different scenarios were modeled, path A and B as previously described (Scheme 29), and a third option called path C in which DBUH⁺ does not coordinate to the anionic hemiacetal. The transformation of **57** to yield **185** was chosen as the model reaction (Figure 13). The initial ring-opening of **57** to yield **184** is exergonic by -10.3 kcal/mol (ΔG°). Formation of the anionic hemiacetal is strongly endergonic relative **184**. Ion-paired structure **219** calculates as lowest ($\Delta G^\circ=11.2$) kcal/mol, followed by the non-coordinated hemiacetal **217^C** ($\Delta G^\circ=11.9$ kcal/mol) and hydrogen bonded **217** is predicted to lie highest ($\Delta G^\circ=12.6$ kcal/mol).

The subsequent step is the rate determining C–C bond scission. Transition state TS^A, which corresponds to path A, calculates as lowest in free energy at $\Delta G^\ddagger=18.4$ kcal/mol. Transition state TS^B, which corresponds to path B, is predicted to lie 1.7 kcal/mol higher in free energy at $\Delta G^\ddagger=20.1$ kcal/mol. And TS^C, where DBUH⁺ takes no part, calculates as highest with a barrier of $\Delta G^\ddagger=20.6$ kcal/mol. The three transition states are predicted to lie close in energy, in fact close to the estimated accuracy of the used DFT method (estimated as ~ 1.5 kcal/mol).^[138a] However, we expect error cancellation to play an important part in comparing such similar structures. Moreover, similar results were obtained when the transition state energies were re-calculated using the M06-2X-D3 functional.^[142]

Another source of error is the conformational sampling. To mitigate this a large number of possible structures were investigated. Moreover, several additional mechanisms were also explored, such as sequential proton transfer and C–C bond breakage, intramolecular proton transfer of a neutral hemiacetal as described by Singleton,^[143] formation of an acyl ammonium specie in analogy with a process described by Wolf,^[144] and a cyclic transition state as proposed for Lewis acid-catalyzed retro-Claisen reactions.^[145] These alternatives calculate as distinctly higher in free energy, typically $\Delta G^\ddagger>30$ kcal/mol. It is also worth stating that

several of these alternative mechanism does not explain the observed rate law nor the KIE. Lastly, the lowest barrier identified (TS^{A} , $\Delta G^{\ddagger}=18.4$) agrees qualitatively with the observation that the reaction proceed at reasonable rate at room temperature (reaction time $\sim 24\text{h}$).

The scission of the C–C bond is highly exergonic for all three scenarios, but to what extent varies significantly. The hydrogen bonded enolate **218** (path A) calculates as lowest ($\Delta G^{\circ}=-7.6$ kcal/mol), followed by formation of the uncoordinated enolate **220^C** ($\Delta G^{\circ}=-3.1$ kcal/mol) and formation of hydrogen bonded methyl acetate and enolate **220** (path B) is predicted to lie highest at $\Delta G^{\circ}=1.1$ kcal/mol. In the final step of the reaction all three scenarios follow the same mechanism, proton transfer between DBUH^{+} and the enolate yields **185** and DBU. The entire reaction calculates to be exergonic by ~ 25 kcal/mol relative **57**.

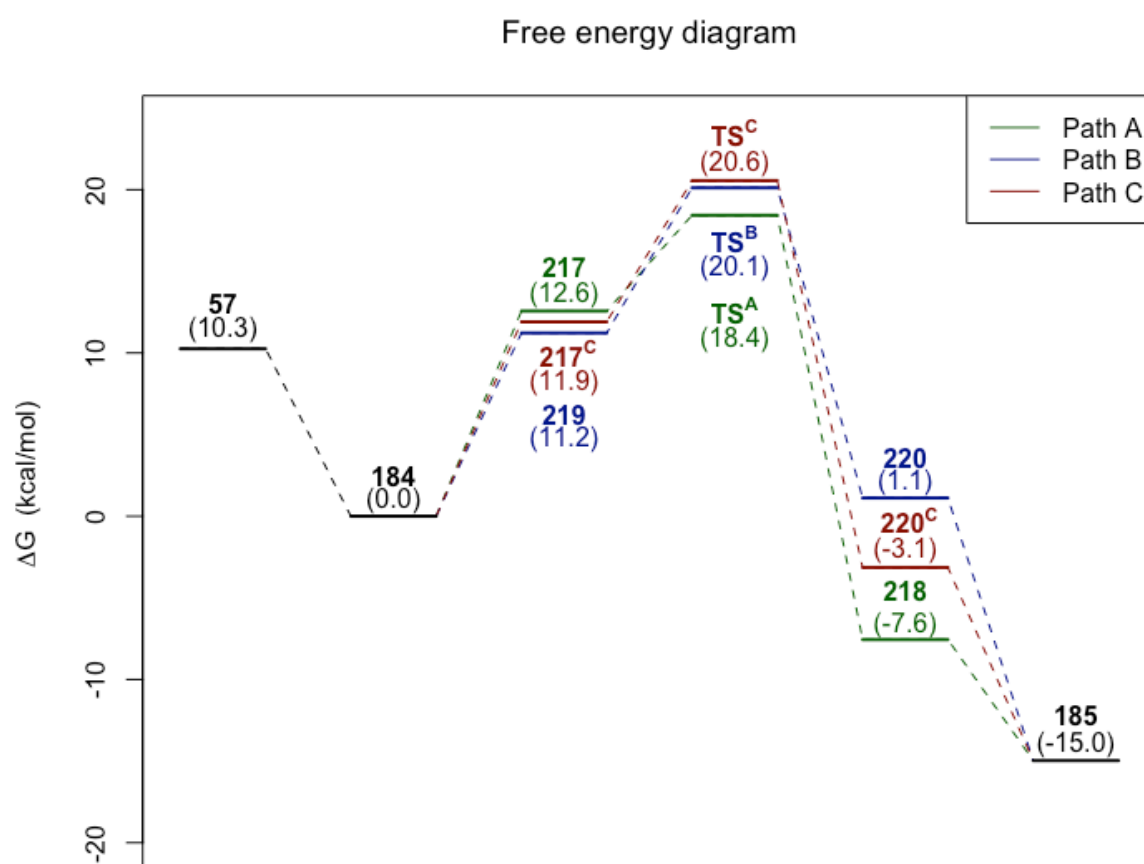


Figure 13. Computed free energy diagram of the transformation of **57** to yield **185** (298.15 K, 1 M) via path A–C. A superscript C denotes the corresponding structure without DBUH^{+} coordination.

Overall, our computational analysis suggest that path A is the most likely mechanism. One way to rationalize this is to analyze what effect coordination of DBUH⁺ has in the step immediately before and after the rate determining transition state. In path A, coordination of DBUH⁺ destabilizes the anionic hemiacetal, but stabilizes the formed enolate in the subsequent step compared to path C. The stabilization of the enolate is significantly greater than the destabilization of the hemiacetal. For path B, the opposite holds true. Coordination of DBUH⁺ stabilizes the anionic hemiacetal marginally, relative path C, while it destabilizes the enolate. Hence, the only strong interaction between DBUH⁺ and the substrate is found in path A.

The structure of TS^A, TS^B and TS^C can be seen in Figure 14. Firstly, we note that the length of the C–C bond being broken varies in accordance with the Hammond postulate, TS^A < TS^C < TS^B.^[146] Moreover, the NH–O distances are very similar in TS^A and TS^B, indicating similar strengths of interaction. However, the hydrogen bond angle is closer to the theoretically optimal 180° for TS^A (177°) than it is for TS^B (163°). One additional difference between TS^A and TS^B, is that in TS^A DBUH⁺ and the phenyl ring adopt a slipped stacked conformation, which is missing in TS^B. This interaction is worth approximately 1.3 kcal/mol, estimated from a TS structure similar to TS^A but without the slipped stacked conformation. Such a conformation is not possible in path B since in that mechanism DBUH⁺ is moving away from the phenyl ring.

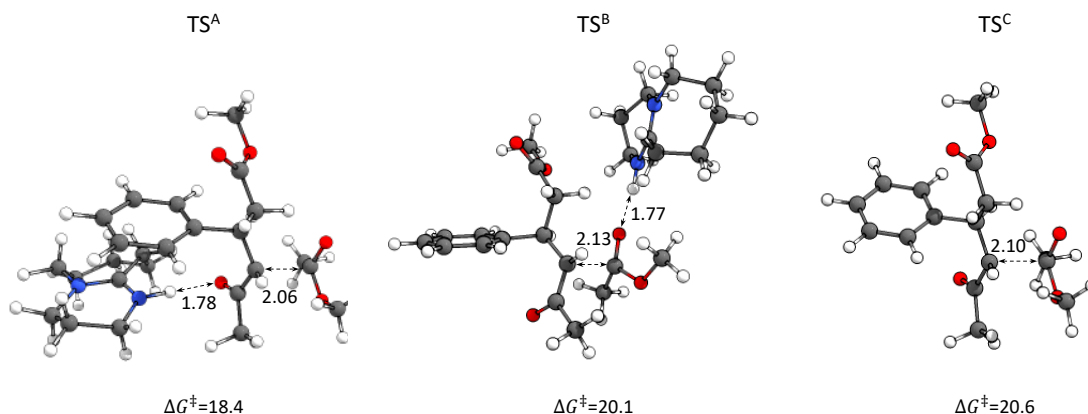


Figure 14. The structures, selected distances and free energies relative **3** TS^A, TS^B and TS^C. Distances are in Angstrom and free energies are in kcal/mol.

10. Summary of Aerobic Synthesis of Dihydropyranones and Their Organocatalytic Ring-Opening and Fragmentation (Paper I, IV and V)

We have shown that it is possible to extend the use of aerobic NHC catalysis to the synthesis of both racemic and homochiral dihydropyranones. Sequential addition of the ETM FePc was crucial for a successful reaction due to deactivation, possibly *via* formation of the dimeric μ -oxo species, $[\text{FePc}]_2\text{O}$. The reaction has a rather broad scope and dihydropyranones are obtained in good yields with good to excellent enantioselectivities. These results show that the developed aerobic system is compatible with the more delicate chemistry available with oxidative NHC catalysis.

An investigation of the ring-opening of dihydropyranones resulted in a method for selective formation of 5-oxohexanoates and 5-oxohexanamides. The reaction proceeds by nucleophilic ring-opening of the dihydropyranone followed by a retro-Claisen fragmentation. The obtained products represent the formal addition of acetone to unactivated Michael acceptors such as α,β -unsaturated esters and amides, a reaction that is very difficult to achieve. The reaction is characterized by a wide substrate scope and was used to obtain a varied range of esters and amides. The mild reaction conditions enable the use of homochiral dihydropyranones with minimal erosion of enantiopurity. The mechanism has been investigated by several kinetic methods and by quantum chemical calculations. Taken together, our results suggest that DBU has a dual role in the reaction, acting both as a Brønsted base and as a hydrogen bond donor.

11. Conclusion and Outlook

Aim 1: Identify a suitable system of ETMs to enable aerobic NHC-catalyzed reactions.

Herein, a strategy for aerobic NHC-catalysis based on a couple of ETMs has been presented. The usage of two ETMs was proven crucial in order to achieve a successful reaction, avoiding formation of kinetic side products. The amount of byproduct formed in the reactions is drastically reduced using aerial oxygen as the terminal oxidant, giving water as the sole byproduct.

Aim 2: Investigate the generality of the develop system compared to traditional oxidative NHC catalysis.

The strategy could successfully be applied to several different acylation reactions. A wide range of different esters could be obtained by aerobic acylations of alcohols, for instance the industrially important antioxidants amiloxate and octinoxate. The aerobic system could also be used in a telescoped NHC-catalyzed valorization of glycerol. The reaction encompasses carbonation of glycerol and subsequent aerobic acylation using aldehydes, delivering the esters in moderate to excellent yields. Successful *N*-acylation of oxazolidinones and lactams by aerobic NHC-catalysis was also demonstrated.

The aerobic system could also be extended to both the racemic and asymmetric synthesis of dihydropyranones. These reactions required higher loadings of both ETMs, and for the asymmetric synthesis a sequential addition of FePc was required to achieve efficient reactions. The need for sequential addition of FePc was attributed to the deactivation of FePc under the reaction conditions, most likely *via* formation of the dimeric μ -oxo species $[\text{FePc}]_2\text{O}$. However, using these modifications of the reaction protocol a wide range of dihydropyranones could be obtained in good yields and in good to excellent ee.

Aim 3: Investigate further use of the developed protocol and the obtained products.

Lastly, a strategy for the formal addition of acetone to unactivated Michael acceptors by ring-opening and retro-Claisen fragmentation of dihydropyranones was developed. The method enables rapid access to a wide range of esters and both secondary, tertiary and Weinreb amides. Homochiral dihydropyranones can be used with minimal erosion of enantiopurity, enabling selective modification of chiral aminoalcohols. The mechanism was investigated by a series of kinetic methods and by DFT calculations. Together, the results suggest a dual role of DBU, acting both as a Brønsted base and as a hydrogen bond donor.

This thesis highlights that the rich chemistry associated with oxidative NHC-catalysis is viable without the use of stoichiometric high molecular weight oxidants. In terms of the ETM system, the Kharasch oxidant **27** has proven an effective and stable ETM, while FePc shows clear signs of degradation during the reaction. Hence, efforts should be directed towards replacing FePc with a more stable ETM.

Strategies to achieve this could potentially be based on disfavoring the oxidative dimerization of FePc by either sterical or electrostatic means. Another approach could be based on immobilization of the ETM on a solid support.

Moreover, future work could be dedicated to the implementation of the developed aerobic system with either α - or γ -activation of aldehydes *via* oxidative NHC catalysis. Mechanistic studies of the ETM system would also be highly useful for future applications. What factors that govern the stability of the system and through what pathway the oxidation of **83** to **27** proceeds, *via* a Fe(III)-superoxide^[147] mechanism in analogy with the Co-catalyzed reaction or by another pathway, remains to be identified.

12. Acknowledgement

The work presented herein would not have been possible without the help and support from numerous people. I would especially like to thank:

My supervisor Henrik Sundén, thank you for showing me the joy of chemical research and for giving me the opportunity to pursue a PhD in your group. These years have been incredibly fun and rewarding, and it would not have been possible without your guidance, knowledge and curiosity. I am genuinely grateful for your enthusiasm and for always taking the time to discuss new ideas.

Linda Ta, thank you for being an awesome friend and co-worker. I could not have wished for a better companion. I am grateful to you for a fantastic collaboration and for the many fun trips, concerts and great meals during these years.

Martin Rahm, thank you for your help and guidance regarding theoretical chemistry, I truly appreciate it.

Nina Kann, thank you for all your help and support and for always taking the time. I have really valued our discussions about chemistry, academia, chili farming and everything in-between.

Jerker Mårtensson and Joakim Andreasson, thank you for your help and interest regarding the kinetic analysis.

I would also like to thank past and present co-workers at floor nine for moral support and for making it fun to go to work.

The research presented herein was founded by the Swedish Research Council (VR and Formas), Magnus Bergvalls stiftelse, Chalmers Area of Advance Nano and C. F. Lundström foundation and is gratefully acknowledged. I would also like to thank stiftelsen Åforsk, Helge Ax:son Johnsons stiftelse and Nils Pihlblads stipendiefond for financial support for conference and summer school attendances.

Lastly, I would like to thank family and friends, my mother and father, my brother, Marie and Stefan, Stefanie and Christine, for infinite encouragement. Lussan, I miss you every day and I so wish you were here. Micaëla, for endless love and support, we made it and I love you.

13. References

- [1] A. Fleming, *Br. J. Exp. Pathol.* **1929**, *10*, 226.
- [2] V. Smil, *Nature* **1999**, *400*, 415.
- [3] J. Rex Whinfield, J. Tennant Dickson, DU PONT, US, **1949**.
- [4] J. I. Jin, *Chem. Eur. J.* **2011**, *17*, 9.
- [5] R. A. Sheldon, *Green Chem.* **2017**, *19*, 18.
- [6] P. T. Anastas, J. C. Warner, *Green Chemistry: Theory and Practice*, Oxford University Press, Oxford, **1998**.
- [7] P. J. Dunn, *Chem. Soc. Rev.* **2012**, *41*, 1452.
- [8] D. J. C. Constable, C. Jimenez-Gonzalez, R. K. Henderson, *Org. Process Res. Dev.* **2007**, *11*, 133.
- [9] a) D. Prat, J. Hayler, A. Wells, *Green Chem.* **2014**, *16*, 4546; b) D. Prat, A. Wells, J. Hayler, H. Sneddon, C. R. McElroy, S. Abou-Shehada, P. J. Dunn, *Green Chem.* **2016**, *18*, 288.
- [10] B. Trost, *Science* **1991**, *254*, 1471.
- [11] R. A. Sheldon, *Green Chem.* **2007**, *9*, 1273.
- [12] (Ed.: A. D. M. a. A. Wilkinson), Blackwell Scientific Publications, Oxford, **1997**.
- [13] C. H. Christensen, J. Rass-Hansen, C. C. Marsden, E. Taarning, K. Egeblad, *ChemSusChem* **2008**, *1*, 283.
- [14] D. R. Dodds, R. A. Gross, *Science* **2007**, *318*, 1250.
- [15] a) F. H. Isikgor, C. R. Becer, *Polym. Chem.* **2015**, *6*, 4497; b) Y. C. Sharma, B. Singh, S. N. Upadhyay, *Fuel* **2008**, *87*, 2355.
- [16] R. M. Heck, R. J. Farrauto, S. T. Gulati, in *Catalytic Air Pollution Control*, John Wiley & Sons, Inc., **2009**, pp. 101.
- [17] a) E. Knoevenagel, *Ber. Dtsch. Chem. Ges.* **1896**, *29*, 172; b) B. List, *Angew. Chem. Inter. Ed.* **2010**, *49*, 1730.
- [18] a) H. D. Dakin, *J. Biol. Chem.* **1909**, *7*, 49; b) R. Kuhn, M. Hoffer, *Berichte der deutschen chemischen Gesellschaft (A and B Series)* **1930**, *63*, 2164; c) F. G. Fischer, A. Marschall, *Berichte der deutschen chemischen Gesellschaft (A and B Series)* **1931**, *64*, 2825.
- [19] a) Z. G. Hajos, D. R. Parrish, *J. Org. Chem.* **1974**, *39*, 1615; b) U. Eder, G. Sauer, R. Wiechert, *Angew. Chem. Inter. Ed.* **1971**, *10*, 496.
- [20] R. B. Woodward, E. Logusch, K. P. Nambiar, K. Sakan, D. E. Ward, B. W. Au-Yeung, P. Balaram, L. J. Browne, P. J. Card, C. H. Chen, *J. Am. Chem. Soc.* **1981**, *103*, 3210.
- [21] B. List, R. A. Lerner, C. F. Barbas, *J. Am. Chem. Soc.* **2000**, *122*, 2395.
- [22] S. Mukherjee, J. W. Yang, S. Hoffmann, B. List, *Chem. Rev.* **2007**, *107*, 5471.
- [23] K. A. Ahrendt, C. J. Borths, D. W. C. MacMillan, *J. Am. Chem. Soc.* **2000**, *122*, 4243.
- [24] A. Erkkilä, I. Majander, P. M. Pihko, *Chem. Rev.* **2007**, *107*, 5416.
- [25] a) P. I. Dalko, *Enantioselective organocatalysis*, WILEY-VCH Verlag GmbH & Co. KGaA, Weinheim, **2007**; b) A. Berkessel, H. Gröger, *Asymmetric Organocatalysis – From Biomimetic Concepts to Applications in Asymmetric Synthesis*, WILEY-VCH Verlag GmbH & Co. KGaA, Weinheim, **2005**; c) J. Aleman, S. Cabrera, *Chem. Soc. Rev.* **2013**, *42*, 774; d) C. A. Busacca, D. R. Fandrick, J. J. Song, C. H. Senanayake, *Adv. Synth. Catal.* **2011**, *353*, 1825.
- [26] D. Parmar, E. Sugiono, S. Raja, M. Rueping, *Chem. Rev.* **2014**, *114*, 9047.
- [27] T. Ishikawa, *Superbases for Organic Synthesis: Guanidines, Amidines, Phosphazenes and Related Organocatalysts*, Wiley, New York, **2009**.
- [28] Z. Zhang, P. R. Schreiner, *Chem. Soc. Rev.* **2009**, *38*, 1187.

- [29] T. Hashimoto, K. Maruoka, *Chem. Rev.* **2007**, *107*, 5656.
- [30] a) H.-J. Federsel, *Nat. Rev. Drug. Discov.* **2005**, *4*, 685; b) M. Breuer, K. Ditrach, T. Habicher, B. Hauer, M. Keßeler, R. Stürmer, T. Zelinski, *Angew. Chem. Inter. Ed.* **2004**, *43*, 788; c) G. Fiorani, W. Guo, A. W. Kleij, *Green Chem.* **2015**, *17*, 1375.
- [31] F. Gomollón-Bel, in *Chemistry International*, Vol. 41, **2019**, p. 12.
- [32] W. A. Herrmann, C. Köcher, *Angew. Chem. Inter. Ed.* **1997**, *36*, 2162.
- [33] A. Igau, H. Grutzmacher, A. Baceiredo, G. Bertrand, *J. Am. Chem. Soc.* **1988**, *110*, 6463.
- [34] A. J. Arduengo, R. L. Harlow, M. Kline, *J. Am. Chem. Soc.* **1991**, *113*, 361.
- [35] M. N. Hopkinson, C. Richter, M. Schedler, F. Glorius, *Nature* **2014**, *510*, 485.
- [36] Z. Li, X. Li, J.-P. Cheng, *J. Org. Chem.* **2017**, *82*, 9675.
- [37] F. G. Bordwell, A. V. Satish, *J. Am. Chem. Soc.* **1991**, *113*, 985.
- [38] a) M. H. Dunn, N. Konstandaras, M. L. Cole, J. B. Harper, *J. Org. Chem.* **2017**, *82*, 7324; b) Y. Chu, H. Deng, J.-P. Cheng, *J. Org. Chem.* **2007**, *72*, 7790.
- [39] I. M. Kolthoff, M. K. Chantooni, S. Bhowmik, *J. Am. Chem. Soc.* **1968**, *90*, 23.
- [40] S. Gehrke, O. Hollóczki, *Angew. Chem. Inter. Ed.* **2017**, *56*, 16395.
- [41] a) H. Mayr, M. Patz, *Angew. Chem. Inter. Ed.* **1994**, *33*, 938; b) B. Maji, M. Breugst, H. Mayr, *Angew. Chem. Inter. Ed.* **2011**, *50*, 6915.
- [42] A. Levens, F. An, M. Breugst, H. Mayr, D. W. Lupton, *Org. Lett.* **2016**, *18*, 3566.
- [43] R. Breslow, *J. Am. Chem. Soc.* **1958**, *80*, 3719.
- [44] T. Ugai, S. Tanaka, S. Dokawa, *J. Pharm. Soc. Jpn* **1943**, *63*, 269.
- [45] H. Stetter, *Angew. Chem. Inter. Ed.* **1976**, *15*, 639.
- [46] G. Wittig, P. Davis, G. Koenig, *Chem. Ber.* **1951**, *84*, 627.
- [47] D. Seebach, *Angew. Chem. Inter. Ed.* **1979**, *18*, 239.
- [48] X. Bugaut, F. Glorius, *Chem. Soc. Rev.* **2012**, *41*, 3511.
- [49] R. Breslow, E. McNelis, *J. Am. Chem. Soc.* **1960**, *82*, 2394.
- [50] F. G. White, L. L. Ingraham, *J. Am. Chem. Soc.* **1960**, *82*, 4114.
- [51] J. Castells, H. Llitjos, M. Moreno-Mañas, *Tetrahedron Lett.* **1977**, *18*, 205.
- [52] L. Jimenez, F. Diederich, *Tetrahedron Lett.* **1989**, *30*, 2759.
- [53] a) H. Inoue, K. Higashiura, *J. Chem. Soc.*, **1980**, 549; b) S. De Sarkar, A. Biswas, R. C. Samanta, A. Studer, *Chem. Eur. J.* **2013**, *19*, 4664.
- [54] Y. Kageyama, S. Murata, *J. Org. Chem.* **2005**, *70*, 3140.
- [55] B. E. Maki, A. Chan, E. M. Phillips, K. A. Scheidt, *Org. Lett.* **2007**, *9*, 371.
- [56] S. D. Sarkar, S. Grimme, A. Studer, *J. Am. Chem. Soc.* **2010**, *132*, 1190.
- [57] M. S. Kharasch, B. S. Joshi, *J. Org. Chem.* **1957**, *22*, 1439.
- [58] L. Ping, J. Bak, Y. Kim, J. Bouffard, *J. Org. Chem.* **2018**, *83*, 9240.
- [59] L. Lin, Y. Li, W. Du, W.-P. Deng, *Tetrahedron Lett.* **2010**, *51*, 3571.
- [60] E. G. Delany, C.-L. Fagan, S. Gundala, A. Mari, T. Broja, K. Zeitler, S. J. Connon, *Chem. Commun.* **2013**, *49*, 6510.
- [61] E. G. Delany, C.-L. Fagan, S. Gundala, K. Zeitler, S. J. Connon, *Chem. Commun.* **2013**, *49*, 6513.
- [62] D. Xie, D. Shen, Q. Chen, J. Zhou, X. Zeng, G. Zhong, *J. Org. Chem.* **2016**, *81*, 6136.
- [63] J. Zhao, C. Mück-Lichtenfeld, A. Studer, *Adv. Synth. Catal.* **2013**, *355*, 1098.
- [64] O. Bortolini, C. Chiappe, M. Fogagnolo, A. Massi, C. S. Pomelli, *J. Org. Chem.* **2016**.
- [65] X. Dong, W. Yang, W. Hu, J. Sun, *Angew. Chem. Inter. Ed.* **2015**, *54*, 660.
- [66] T. Zhu, P. Zheng, C. Mou, S. Yang, B.-A. Song, Y. R. Chi, **2014**, *5*, 5027.
- [67] C. Zhang, J. F. Hooper, D. W. Lupton, *ACS Catal.* **2017**, *7*, 2583.

- [68] CCDC 857879 contains the supplementary crystallographic data for this paper. These data can be obtained free of charge from The Cambridge Crystallographic Data Centre via www.ccdc.cam.ac.uk/data_request/cif.
- [69] a) R. C. Samanta, B. Maji, S. De Sarkar, K. Bergander, R. Fröhlich, C. Mück-Lichtenfeld, H. Mayr, A. Studer, *Angew. Chem. Inter. Ed.* **2012**, *51*, 5234; b) J. Mahatthananchai, P. Zheng, J. W. Bode, *Angew. Chem. Inter. Ed.* **2011**, *50*, 1673; c) S. Vellalath, D. Romo, *Angew. Chem. Inter. Ed.* **2016**, *55*, 13934; d) R. Appel, H. Mayr, *J. Am. Chem. Soc.* **2011**, *133*, 8240.
- [70] For databank for reactivity parameters see: <http://www.cup.lmu.de/oc/mayr/reaktionsdatenbank/>
- [71] S. De Sarkar, A. Studer, *Angew. Chem. Inter. Ed.* **2010**, *49*, 9266.
- [72] X. Wu, B. Liu, Y. Zhang, M. Jeret, H. Wang, P. Zheng, S. Yang, B. A. Song, Y. R. Chi, *Angew. Chem. Inter. Ed.* **2016**, *55*, 12280.
- [73] C. Fang, T. Lu, J. Zhu, K. Sun, D. Du, *Org. Lett.* **2017**.
- [74] J.-E. Bäckvall, *Modern Oxidation Methods*, 2nd ed., Wiley-VCH Verlag GmbH & Co. KGaA, **2010**.
- [75] R. Ciriminna, L. Albanese, F. Meneguzzo, M. Pagliaro, *ChemSusChem* **2016**, *9*, 3374.
- [76] R. A. Sheldon, I. W. C. E. Arends, G.-J. ten Brink, A. Dijkman, *Acc. Chem. Rev.* **2002**, *35*, 774.
- [77] D. S. Lee, Z. Amara, C. A. Clark, Z. Xu, B. Kakimpa, H. P. Morvan, S. J. Pickering, M. Poliakoff, M. W. George, *Org. Process Res. Dev.* **2017**.
- [78] M. Abe, *Chem. Rev.* **2013**, *113*, 7011.
- [79] , Earth System Research Laboratory of NOAA, NASA, U.S., Colorado, United States **2008**.
- [80] P. J. KRUSIC, E. WASSERMAN, P. N. KEIZER, J. R. MORTON, K. F. PRESTON, *Science* **1991**, *254*, 1183.
- [81] P. R. Ogilby, *Chemical Society Reviews* **2010**, *39*, 3181.
- [82] a) W. Adam, S. Grabowski, R. M. Wilson, *Acc. Chem. Rev.* **1990**, *23*, 165; b) J. R. Hurst, J. D. McDonald, G. B. Schuster, *J. Am. Chem. Soc.* **1982**, *104*, 2065.
- [83] a) L. Brewer, *Chem. Rev.* **1953**, *52*, 1; b) J. C. Chaston, *Platinum Metals Rev.* **1964**, *8*, 50.
- [84] K. Schmidt-Rohr, *J. Chem. Ed.* **2015**, *92*, 2094.
- [85] W. T. Borden, R. Hoffmann, T. Stuyver, B. Chen, *J. Am. Chem. Soc.* **2017**, *139*, 9010.
- [86] J. Piera, J.-E. Bäckvall, *Angew. Chem. Inter. Ed.* **2008**, *47*, 3506.
- [87] C. W. Anson, S. Ghosh, S. Hammes-Schiffer, S. S. Stahl, *J. Am. Chem. Soc.* **2016**, *138*, 4186.
- [88] C. E. I. Knappe, A. Imami, A. Jacobi von Wangelin, *ChemCatChem* **2012**, *4*, 937.
- [89] J. Wöltinger, J.-E. Bäckvall, Á. Zsigmond, *Chem. Eur. J.* **1999**, *5*, 1460.
- [90] J.-E. Backvall, R. L. Chowdhury, U. Karlsson, *J. Chem. Soc.*, **1991**, 473.
- [91] J. Piera, K. Närhi, J.-E. Bäckvall, *Angew. Chem. Inter. Ed.* **2006**, *45*, 6914.
- [92] P.-C. Chiang, J. W. Bode, *Org. Lett.* **2011**, *13*, 2422.
- [93] R. S. Reddy, J. N. Rosa, L. F. Veiros, S. Caddick, P. M. P. Gois, *Org. Biomol. Chem.* **2011**, *9*, 3126.
- [94] J.-E. Baeckvall, R. B. Hopkins, H. Grennberg, M. Mader, A. K. Awasthi, *J. Am. Chem. Soc.* **1990**, *112*, 5160.

- [95] Prices from Sigma-Aldrich, accessed 2017-07-11:
<http://www.sigmaaldrich.com/catalog/product/aldrich/d48400?lang=en®ion=SE>
<http://www.sigmaaldrich.com/catalog/product/aldrich/s846511?lang=en®ion=SE>
- [96] O. Yuji, N. Michinori, O. Hiroyuki, T. Eishun, M. Hiro, N. Hachiro, K. Masao, *Bull. Chem. Soc. Jpn.* **1987**, 60, 3731.
- [97] R. A. Sheldon, *Green Chem.* **2014**, 16, 950.
- [98] M. Pagliaro, M. Rossi, *The Future of Glycerol*, 2 ed., Royal Society of Chemistry, Cambridge. U.K, **2010**.
- [99] a) J. Bensemoun, S. Condon, *Green Chem.* **2012**, 14, 2595; b) M. O. Sonnat, S. Amigoni, E. P. Taffin de Givenchy, T. Darmanin, O. Choulet, F. Guittard, *Green Chem.* **2013**, 15, 283.
- [100] C.-H. Zhou, J. N. Beltramini, Y.-X. Fan, G. Q. Lu, *Chem. Soc. Rev.* **2008**, 37, 527.
- [101] a) J. A. Stewart, R. Drexel, B. Arstad, E. Reubsaet, B. M. Weckhuysen, P. C. A. Bruijninx, *Green Chem.* **2016**, 18, 1605; b) H. Mutlu, J. Ruiz, S. C. Solleder, M. A. R. Meier, *Green Chem.* **2012**, 14, 1728; c) J. R. Ochoa-Gomez, O. Gomez-Jimenez-Aberasturi, C. Ramirez-Lopez, B. Maestro-Madurga, *Green Chem.* **2012**, 14, 3368.
- [102] a) F. Jerome, G. Kharchafi, I. Adam, J. Barrault, *Green Chem.* **2004**, 6, 72; b) G. Kharchafi, F. Jerome, J.-P. Douliez, J. Barrault, *Green Chem.* **2006**, 8, 710; c) B. Ren, M. Rahm, X. Zhang, Y. Zhou, H. Dong, *J. Org. Chem.* **2014**, 79, 8134; d) X. Liu, H. Ma, Y. Wu, C. Wang, M. Yang, P. Yan, U. Welz-Biermann, *Green Chem.* **2011**, 13, 697; e) J. n. Pérez-Pariente, I. Díaz, F. Mohino, E. Sastre, *APPL CATAL A-GE* **2003**, 254, 173.
- [103] a) K. Klepáčová, D. Mravec, M. Bajus, *APPL CATAL A-GE* **2005**, 294, 141; b) J. Deutsch, A. Martin, H. Lieske, *J. Catal.* **2007**, 245, 428.
- [104] Y. Hayashi, *Chem. Sci.* **2016**, 7, 866.
- [105] P. Tundo, M. Selva, *Acc. Chem. Rev.* **2002**, 35, 706.
- [106] a) A. M. Truscello, C. Gambarotti, M. Lauria, S. Auricchio, G. Leonardi, S. U. Shisodia, A. Citterio, *Green Chem.* **2013**, 15, 625; b) C. Duval, N. Kébir, R. Jauseau, F. Burel, *J. POLYM. SCI. POL. CHEM.* **2016**, 54, 758; c) G. Rokicki, P. Rakoczy, P. Parzuchowski, M. Sobiecki, *Green Chem.* **2005**, 7, 529.
- [107] a) W. Guo, J. González-Fabra, N. A. G. Bandeira, C. Bo, A. W. Kleij, *Angew. Chem. Inter. Ed.* **2015**, 54, 11686; b) S. Sopeña, V. Laserna, W. Guo, E. Martin, E. C. Escudero-Adán, A. W. Kleij, *Adv. Synth. Catal.* **2016**, 358, 2172.
- [108] A. Patra, S. Mukherjee, T. K. Das, S. Jain, R. G. Gonnade, A. T. Biju, *Angew. Chem. Inter. Ed.* **2017**, 56, 2730.
- [109] R. W. M. Davidson, M. J. Fuchter, *Chem. Commun.* **2016**, 52, 11638.
- [110] R. C. Samanta, S. De Sarkar, R. Frohlich, S. Grimme, A. Studer, *Chem. Sci.* **2013**, 4, 2177.
- [111] a) W. N. Olmstead, Z. Margolin, F. G. Bordwell, *J. Org. Chem.* **1980**, 45, 3295; b) F. G. Bordwell, H. E. Fried, *J. Org. Chem.* **1991**, 56, 4218; c) F. G. Bordwell, G. E. Drucker, H. E. Fried, *J. Org. Chem.* **1981**, 46, 632.
- [112] a) S. Zhu, K. T. Mc Henry, W. S. Lane, G. Fenteany, *Chemistry & Biology* **2005**, 12, 981; b) H.-J. Ha, M. C. Hong, S. W. Ko, Y. W. Kim, W. K. Lee, J. Park, *Bioorg. Med. Chem. Lett.* **2006**, 16, 1880.
- [113] a) D. J. Ager, I. Prakash, D. R. Schaad, *Chem. Rev.* **1996**, 96, 835; b) D. A. Evans, J. Bartoli, T. L. Shih, *J. Am. Chem. Soc.* **1981**, 103, 2127; c) D. A. Evans, M. D. Ennis, D. J. Mathre, *J. Am. Chem. Soc.* **1982**, 104, 1737; d) D. A. Evans, K. T. Chapman, J. Bisaha, *J. Am. Chem. Soc.* **1984**, 106, 4261.

- [114] J. Mahatthananchai, J. W. Bode, *Acc. Chem. Rev.* **2014**, 47, 696.
- [115] K. Zeitler, *Org. Lett.* **2006**, 8, 637.
- [116] a) C.-Y. Li, W.-J. Tsai, A. G. Damu, E. J. Lee, T.-S. Wu, N. X. Dung, T. D. Thang, L. Thanh, *J. Agric. Food Chem.* **2007**, 55, 9436; b) S. Peng, B. Zhang, X. Meng, J. Yao, J. Fang, *J. Med. Chem.* **2015**, 58, 5242.
- [117] M. Iinuma, T. Tanaka, M. Takenaka, M. Mizuno, F. Asai, *Phytochemistry* **1992**, 31, 2487.
- [118] S. M. McElvain, R. D. Bright, P. R. Johnson, *J. Am. Chem. Soc.* **1941**, 63, 1558.
- [119] N. Kawahara, A. Kurata, T. Hakamatsuka, S. Sekita, M. Satake, *Chem. Pharm. Bull.* **2001**, 49, 1377.
- [120] a) T. Sugiyama, T. Murayama, K. Yamashita, T. Oritani, *Biosci. Biotechnol. Biochem.* **1995**, 59, 1921; b) X.-P. Fang, J. E. Anderson, C.-J. Chang, J. L. McLaughlin, P. E. Fanwick, *J. Nat. Prod.*, **1991**, 54, 1034.
- [121] D. C. M. Albanese, N. Gaggero, *Eur. J. Org. Chem.* **2014**, 2014, 5631.
- [122] F. G. Sun, L. H. Sun, S. Ye, *Adv. Synth. Catal.* **2011**, 353, 3134.
- [123] Y. Que, Y. Lu, W. Wang, Y. Wang, H. Wang, C. Yu, T. Li, X.-S. Wang, S. Shen, C. Yao, *Chem. Asian J.* **2016**, 11, 678.
- [124] C. Ercolani, M. Gardini, F. Monacelli, G. Pennesi, G. Rossi, *Inorg. Chem.* **1983**, 22, 2584.
- [125] D. S. Allgäuer, H. Jangra, H. Asahara, Z. Li, Q. Chen, H. Zipse, A. R. Ofial, H. Mayr, *J. Am. Chem. Soc.* **2017**, 139, 13318.
- [126] W. C. Han, K. Takahashi, J. M. Cook, U. Weiss, J. V. Silverton, *J. Am. Chem. Soc.* **1982**, 104, 318.
- [127] J. Yang, A. J. M. Farley, D. J. Dixon, *Chem. Sci.* **2017**, 8, 606.
- [128] a) T. Liu, M. Zhou, T. Yuan, B. Fu, X. Wang, F. Peng, Z. Shao, *Adv. Synth. Catal.* **2017**, 359, 89; b) A. Lu, T. Liu, R. Wu, Y. Wang, G. Wu, Z. Zhou, J. Fang, C. Tang, *J. Org. Chem.* **2011**, 76, 3872; c) S. B. Tsogoeva, S. Wei, *Chem. Commun.* **2006**, 1451.
- [129] a) A. I. Meyers, M. A. Sturgess, *Tetrahedron Lett.* **1989**, 30, 1741; b) D. L. Roberts, R. A. Heckman, B. P. Hege, S. A. Bellin, *J. Org. Chem.* **1968**, 33, 3566.
- [130] a) R. W. Taft, *J. Am. Chem. Soc.* **1952**, 74, 2729; b) R. W. Taft, *J. Am. Chem. Soc.* **1952**, 74, 3120.
- [131] J. P. Birk, *J. Chem. Ed.* **1976**, 53, 704.
- [132] J. Bures, *Angew. Chem. Inter. Ed.* **2016**, 55, 2028.
- [133] a) F. H. Westheimer, *Chem. Rev.* **1961**, 61, 265; b) S. E. Scheppele, *Chem. Rev.* **1972**, 72, 511.
- [134] R. G. Pearson, E. A. Mayerle, *J. Am. Chem. Soc.* **1951**, 73, 926.
- [135] S. J. Pike, E. Lavagnini, L. M. Varley, J. L. Cook, C. A. Hunter, *Chem. Sci.* **2019**, 10, 5943.
- [136] M. S. Miran, M. Hoque, T. Yasuda, S. Tsuzuki, K. Ueno, M. Watanabe, *Phys. Chem. Chem. Phys.* **2019**, 21, 418.

- [137] M. J. Frisch, G. W. Trucks, H. B. Schlegel, G. E. Scuseria, M. A. Robb, J. R. Cheeseman, G. Scalmani, V. Barone, G. A. Petersson, H. Nakatsuji, X. Li, M. Caricato, A. V. Marenich, J. Bloino, B. G. Janesko, R. Gomperts, B. Mennucci, H. P. Hratchian, J. V. Ortiz, A. F. Izmaylov, J. L. Sonnenberg, Williams, F. Ding, F. Lipparini, F. Egidi, J. Goings, B. Peng, A. Petrone, T. Henderson, D. Ranasinghe, V. G. Zakrzewski, J. Gao, N. Rega, G. Zheng, W. Liang, M. Hada, M. Ehara, K. Toyota, R. Fukuda, J. Hasegawa, M. Ishida, T. Nakajima, Y. Honda, O. Kitao, H. Nakai, T. Vreven, K. Throssell, J. A. Montgomery Jr., J. E. Peralta, F. Ogliaro, M. J. Bearpark, J. J. Heyd, E. N. Brothers, K. N. Kudin, V. N. Staroverov, T. A. Keith, R. Kobayashi, J. Normand, K. Raghavachari, A. P. Rendell, J. C. Burant, S. S. Iyengar, J. Tomasi, M. Cossi, J. M. Millam, M. Klene, C. Adamo, R. Cammi, J. W. Ochterski, R. L. Martin, K. Morokuma, O. Farkas, J. B. Foresman, D. J. Fox, Wallingford, CT, **2016**.
- [138] a) J.-D. Chai, M. Head-Gordon, *Phys. Chem. Chem. Phys.* **2008**, *10*, 6615; b) R. Krishnan, J. S. Binkley, R. Seeger, J. A. Pople, *J. Chem. Phys.* **1980**, *72*, 650.
- [139] A. V. Marenich, C. J. Cramer, D. G. Truhlar, *J. Phys. Chem. B* **2009**, *113*, 6378.
- [140] a) Á. Madarász, Z. Dósa, S. Varga, T. Soós, A. Csámpai, I. Pápai, *ACS Catal.* **2016**, *6*, 4379; b) J. V. Alegre-Requena, E. Marqués-López, R. P. Herrera, *Chem. Eur. J.* **2017**, *23*, 15336.
- [141] S. M. Bachrach, *J. Org. Chem.* **2013**, *78*, 10909.
- [142] a) Y. Zhao, D. G. Truhlar, *Theor. Chem. Acc.* **2008**, *120*, 215; b) S. Grimme, J. Antony, S. Ehrlich, H. Krieg, *J. Chem. Phys.* **2010**, *132*, 154104.
- [143] H. R. Aziz, D. A. Singleton, *J. Am. Chem. Soc.* **2017**, *139*, 5965.
- [144] R. Ding, P. R. Bakhshi, C. Wolf, *J. Org. Chem.* **2016**.
- [145] A. Kawata, K. Takata, Y. Kuninobu, K. Takai, *Angew. Chem. Inter. Ed.* **2007**, *46*, 7793.
- [146] G. S. Hammond, *J. Am. Chem. Soc.* **1955**, *77*, 334.
- [147] Such species have been isolated and are believed to have an important role in enzymatic oxygen activation, see C.-W. Chiang, S. T. Kleespies, H. D. Stout, K. K. Meier, P.-Y. Li, E. L. Bominaar, L. Que, E. Münck and W.-Z. Lee, *J. Am. Chem. Soc.*, **2014**, *136*, 10846-10849.